

MECHANISMS OF SYNAPSE DEPRESSION IN RESPONSE TO POSTSYNAPTIC
PATTERNED BURST FIRING

APPROVED BY SUPERVISORY COMMITTEE

Kimberly Huber

Taekyung Kim

Jay Gibson

Todd Roberts

Weichun Lin

DEDICATION

I would like to thank the members of my Graduate Committee, Dr. Kimberly Huber, Dr. Jay Gibson and all present and past members of the Huber lab for their friendship, technical assistance and intellectual inspiration for me. Dr. Huber is an exceptional mentor who has not only boosted me to become a scientist, but also gave me brilliant instruction when I was kind of strayed in my path of life. I would like to express my especial acknowledgement of Julia and Carly's great efforts in helping the progress of my project, and their precise and critical comments on my manuscript and dissertation. I also want to show my gratitude for all my "connections" who deliver your input and form synapses with me.

MECHANISMS OF SYNAPSE DEPRESSION IN RESPONSE TO POSTSYNAPTIC
PATTERNED BURST FIRING

by

CHIA-WEI CHANG

DISSERTATION

Presented to the Faculty of the Graduate School of Biomedical Sciences

The University of Texas Southwestern Medical Center at Dallas

In Partial Fulfillment of the Requirements

For the Degree of

DOCTOR OF PHILOSOPHY

The University of Texas Southwestern Medical Center at Dallas

Dallas, Texas

December, 2016

Copyright

by

CHIA-WEI CHANG, 2016

All Rights Reserved

MECHANISMS OF SYNAPSE DEPRESSION IN RESPONSE TO POSTSYNAPTIC
PATTERNED BURST FIRING

Chia-Wei Chang

The University of Texas Southwestern Medical Center at Dallas, 2016

Kimberly M. Huber, Ph.D.

Neuronal activity and experience stimulate synapse pruning (Zuo et al 2005b) to refine neuronal circuits during early postnatal development (Hua & Smith 2004), and are critical for learning and memory (Fu & Zuo 2011). Previous studies suggest that the

activity-dependent transcription factor Myocyte Enhancer Factor 2 (MEF2) prunes functional and structural excitatory synapses in hippocampal and striatal neurons (Flavell et al 2006, Pulipparacharuvil et al 2008), findings that have been correlated with a role for MEF2 in behaviors, including memory formation (Barbosa et al 2008, Cole et al 2012, Dietrich 2013). Here, I report the use of a physiologically-relevant neuronal activity paradigm to study MEF2 transcriptional activity and function in the hippocampus. Utilizing optogenetics and biolistics, a method to sparsely express genes in neurons, I precisely controlled both activity and gene expression in a single neuron to study the cell-autonomous role of MEF2 in response to specific neuronal firing patterns..

In my study, I demonstrate that postsynaptic burst firing, physiologically-relevant activity commonly observed in hippocampal CA1 pyramidal neurons, stimulates transcriptional activation of endogenous MEF2A and MEF2D transcription factors. I find that burst firing for 1 hr (which I refer to as ‘brief’ stimulation) elicits MEF2-dependent synapse depression. Although we hypothesized that the depression event was the result of synapse elimination, due to MEF2’s known role as a negative regulator of excitatory synapse number (Flavell et al 2006, Pfeiffer et al 2010, Tsai et al 2012), surprisingly, we discovered that depression induced by brief stimulation was caused by silencing of synapses. Among potentially MEF2A/D-regulated genes, *Arc* was robustly induced by brief postsynaptic burst firing via activation of endogenous MEF2A/D. In contrast, chronic (24 hr) postsynaptic burst

firing promotes an elimination of synapses that occurs independently of MEF2A/D. Overall, these results demonstrate the activation of MEF2 in response to physiological patterns of neural activity, and demonstrate that brief and chronic activity stimulate distinct mechanisms of synapse depression – MEF2-dependent synapse silencing, and MEF2-independent synapse elimination.

PRIOR PUBLICATIONS

1. Christina Gross, Chia-Wei Chang, Seth M. Kelly, Aditi Bhattacharya, Sean M.J. McBride, Scott W. Danielson, Michael Q. Jiang, Chi Bun Chan, Keqiang Ye, Jay R. Gibson, Eric Klann, Thomas A. Jongens, Kenneth H. Moberg, Kimberly M. Huber, and Gary J. Bassell *Increased expression of the PI3K enhancer PIKE mediates deficits in synaptic plasticity and behavior in Fragile X syndrome*. Cell Report 2015 May 5;11(5):727-36. doi: 10.1016/j.celrep.2015.03.060. Epub 2015 Apr 23.
2. Zilai Zhang, Mou Cao, Chia-Wei Chang, Cindy Wang, Xuanming Shi, Xiaoming Zhan, Shari G. Birnbaum, Ilya Bezprozvanny, Kimberly M. Huber and Jiang I. Wu *Autism-Associated Chromatin Regulator Brg1/Smrca4 Is Required for Synapse Development and Myocyte Enhancer Factor 2-Mediated Synapse Remodeling* Molecular and Cellular Biology. 2015 Oct 12;36(1):70-83. doi: 10.1128/MCB.00534-15.

LIST OF FIGURES

Figure 1. 1 Categories of different types of dendritic spine based on their morphology	35
Figure 1. 2 Spatial and temporal expression profile of <i>Mef2</i> genes in brain	36
Figure 1. 3 Posttranslational modifications modulate MEF2 activity	37
Figure 2. 1 PPS induced patterned firing activity on neurons transfected with Channelrhodopsin.....	67
Figure 2. 2 Postsynaptic burst firing induces MEF2-dependent transcriptional activity	68
Figure 2. 3 Postsynaptic burst firing-induced MEF2-dependent transcription is blocked by cell autonomous <i>Mef2a/d</i> deletion	69
Figure 2. 4 Chr2H134R expression is not altered by the genotype of transfected cell and does not change basal neuronal transmission.	70
Figure 2. 5 Brief postsynaptic burst firing activates MEF2-dependent synapse depression ...	71
Figure 2. 6 Chronic postsynaptic burst firing induces synapse depression that does not rely on cell autonomous MEF2A and MEF2D	72
Figure 2. 7 Brief activity induce synapse silencing rather than synapse elimination.....	73
Figure 2. 8 Synapse depression generated by brief postsynaptic burst firing are caused by synapse silencing rather than partial recovery of eliminated synapses	74
Figure 2. 9 Dendritic spine elimination is observed in response to chronic, but not brief, postsynaptic burst firing	75
Figure 2. 11 Brief postsynaptic burst firing-induced synapse depression requires <i>de novo</i> transcription.....	77
Figure 2. 12 Brief postsynaptic burst firing specifically activates MEF2-dependent <i>Arc</i> expression.....	78
Figure 2. 13 Activity-driven expression of <i>Arc</i> is required for brief postsynaptic burst firing induced synapse depression.....	79
Figure 2. 14 Chronic postsynaptic burst firing-induced synapse depression exhibits partial <i>Arc</i> dependence	80
Figure 2. 15 Comparison of postsynaptic burst firing observed <i>in vivo</i> and induced <i>ex vivo</i> by PPS	81
Figure 2. 16 Model of postsynaptic burst firing-induced synapse plasticity	82
Figure 3. 1 <i>Brg1</i> deletion causes reduction of functional synapses.....	93
Figure 4. 1 PIKE functional knockdown rescues cortical hyperexcitability in <i>Fmr1</i> KO mice	102
Figure 4. 2 Acute inhibition of PI3K does not mitigate prolonged UP-states in <i>Fmr1</i> KO mice	103
Figure 4. 3 PIKE functional knockdown attenuates seizure behavior in <i>Fmr1</i> KO mice	104
Figure 5. 1 Calcineurin inhibition may attenuate chronic postsynaptic burst firing induced	

MEF2-dependent transcription.....	116
Figure 5. 2 CaMKK inhibition does not significantly affect chronic postsynaptic burst firing induced MEF2-dependent transcription	117
Figure 5. 3 Dendritic spine density and mEPSC acquired from neurons subjected to PPS and filled with biocytin	118
Figure 5. 4 Chronic (24 hour) PPS activates MEF2-dependent transcriptional activity	119
Figure 5. 5 Chronic postsynaptic burst firing-induced synapse depression is blocked by embryonic knockout of MEF2A and MEF2D	120
Figure 5. 6 FMRP is not required for postsynaptic burst firing induced synapse depression	121
Figure 5. 7 mGluR5 is partially involved in brief postsynaptic burst firing induced-synapse plasticity	122

LIST OF TABLES

Table 2. 1 Raw electrophysiological measurements in untransfected (U) or transfected (T) hippocampal CA1 neurons in from WT and <i>Mef2a</i> ^{d^{fl/fl}} mice	83
Table 2. 2 Raw electrophysiological measurements in untransfected (U) or transfected (T) hippocampal CA1 neurons in OHSC treated with vehicle or nifedipine.....	85
Table 2. 3 Raw electrophysiological measurements in untransfected (U) or transfected (T) hippocampal CA1 neurons from WT or <i>Arc</i> KO mice.....	86
Table 4. 1 Animal performance in audiogenic seizure	105
Table 4. 2 Fisher's exact test of seizure behavior	106

LIST OF DEFINITIONS

AChR - Acetylcholine receptor

ActD - Actinomycin D

AMPA - AMPA receptor

ASD - Autism spectrum disorder

Arc - Activity regulated cytoskeletal-associated Protein

cAMP - cyclic Adenosine monophosphate

CaMK - Calcium/calmodulin-dependent protein kinase

Centg1 - The gene of PIKE

CF - Climbing fiber

ChR2 - Channelrhodopsin 2

CNS - Central nervous system

CNQX - 6-Cyano-7-nitroquinoxaline-2,3-dione

CREB - cAMP response element binding protein

cv - Coefficient of variation

DG - Dentate gyrus

DHPG - Dihydroxyphenylglycine

DRB - 5,6-Dichloro-1-beta-D-ribofuranosylbenzimidazole

EC - Entorhinal cortex

eEPSC - Evoked excitatory postsynaptic current

Fmr1 - The gene of FMRP

FMRP - Fragile X mental retardation protein

FXS – Fragile X Syndrome

GluA - Iontropic glutamate receptor AMPA subtype

GluN - Iontropic glutamate receptor NMDA subtype

HDAC – Histone deacetylase

LGN - Lateral geniculate neuron

LTD - Long term depression

LTP - Long term potentiation

mGluR - Metabotropic glutamate receptor

MADS – Minichromosome maintenance 1-agamous-deficiens response factor

MDM2 - Mouse double minute 2 homolog

Mdm2 - The gene of MDM2

MEF2 - Myocyte enhancer factor 2

Mef2 - The gene of MEF2

MPEP - 2-Methyl-6-(phenylethynyl)pyridine

mEPSC - Miniature excitatory postsynaptic current

MRE - MEF2 response element

mRNA - Messenger ribonucleotide

NFAT - Nuclear factor of activated T-cells

MSN – Medium spiny neuron

nAChR - Nicotinic acetylcholine receptor

NEDD4 - neural precursor cell expressed developmentally down-regulated protein 4

Nr4a1 - The gene of Nr4a1/NUR77

Nr4a1/NUR77 - Nerve growth factor IB

PSD - Postsynaptic density

NMDAR - NMDA receptor

OHSC - Organotypic hippocampal slice culture

PC - Purkinje cell

PCDH10 - Protocadherin 10

RGS2 - Regulator of G-protein signaling 2

PI3K - Phosphoinositide-3-kinase

PIKE - PI3K enhancer

PPS - Patterned photostimulation

PSD-95 - Postsynaptic density protein 95

SAPAP3 - SAP90/PSD-95-associated protein 3

Stim - Patterned photostimulation

TTX - Tetrodotoxin

qPCR - Quantitative polymerase chain reaction

SRF - Serum response factor

VGCC - Voltage-gated calcium channel

WT - Wild type

TABLE OF CONTENTS

PRIOR PUBLICATIONS	V
LIST OF FIGURES	VI
LIST OF TABLES	VIII
LIST OF DEFINITIONS	IX
TABLE OF CONTENTS	XIII
CHAPTER ONE	1
INTRODUCTION	1
<i>Synapse Elimination</i>	<i>1</i>
Characterization of Synapse Elimination.....	1
Synapse Elimination in Hippocampus	4
Neuronal Activity, Sensory Experience and Synapse Elimination	5
Synapse Elimination and Fragile X Syndrome and Autism	9
<i>Silent Synapses and Their Role in Synapse Elimination</i>	<i>12</i>
Concept for Silent Synapses.....	12
Detection of Silent Synapses.....	14
From Silent Synapse to Long Term Depression and Synapse Elimination.....	16
Unsilencing the Silent Synapse and Synapse Stabilization.....	18
Silent Synapses during Development and Addiction.....	20
<i>Activity-Dependent Regulation and Myocyte Enhancer Factor 2</i>	<i>20</i>
From Activity to Transcription	20
Characterization of Myocyte Enhancer Factor 2 (MEF2).....	21
MEF2 Expression and Transcriptional Regulation.....	22
MEF2-VP16	26
MEF2, synapse elimination and <i>Fmr1</i>	26
<i>Optogenetics and Neuronal Activity Manipulation</i>	<i>28</i>
Traditional Methods.....	28
Channelrhodopsins as a Tool for Introducing Activity	31
Application of Channelrhodopsins	32
<i>Motivation and Rational for the Study</i>	<i>33</i>
CHAPTER TWO	38
BRIEF POSTSYNAPTIC BURST FIRING PROMOTES SYNAPSE SILENCING VIA SELECTIVE ACTIVATION OF MEF2-REGULATED GENE EXPRESSION	38
<i>Introduction</i>	<i>38</i>
<i>Materials and methods</i>	<i>39</i>

Hippocampal Slice Cultures and Transfection	39
Patterned Photostimulation and Drug Treatment.....	40
Imaging of MRE-GFP, the MEF2 transcriptional activity reporter	40
Electrophysiology.....	41
Dendritic Spine Imaging	43
Dissociated Primary Culture	44
Virus preparation	45
RNA extraction and qPCR	45
Statistics	46
<i>Results</i>	47
Brief (1 hour) Postsynaptic Bursts of Action Potentials Activate MEF2A/D-mediated Transcription	47
Brief and Chronic Bursts of Postsynaptic Action Potentials Induce Depression of Excitatory Synaptic Transmission that Differentially Rely on MEF2A/D.....	48
Brief Periods of Postsynaptic Bursting Functionally Silences Excitatory Synapses, whereas Chronic Bursting Causes Synapse Elimination	50
PPS-induced Synapse Silencing Requires Activation of L-type Voltage-Gated Ca ²⁺ channels and <i>de novo</i> Transcription.....	53
Brief Postsynaptic Burst Firing Selectively Activates MEF2-dependent <i>Arc</i> Transcription, which is Required for Synapse Silencing	54
<i>Discussion</i>	57
From Indiscriminative Stimulation to Precise Cell Autonomous Stimulation	57
PPS-induced Physiologically Relevant Neuronal Activity	58
Differential Activity Patterns Lead to Different Types of Synapse Depression	61
Endogenous MEF2 and Activity-Driven Transcriptional Regulation.....	61
Involvement of <i>Arc</i> in Brief PPS-Induced Synapse Silencing	63
Implication of Partial <i>Arc</i> -Dependence in Chronic PPS-Induced Synapse Elimination	64
CHAPTER THREE.....	87
<i>BRG1</i> IS INVOLVED IN FUNCTIONAL EXCITATORY SYNAPSE DEVELOPMENT	87
<i>Introduction</i>	87
<i>Materials and methods</i>	89
Animals.....	89
Hippocampal Slice Cultures and Transfection	89
Electrophysiology:.....	90
<i>Results and Discussion</i>	91
<i>Brg1</i> deletion results in functional synapse loss.....	91

CHAPTER FOUR.....	94
PHOSPHOINOSITIDE-3-KINASE ENHANCER IS ASSOCIATED WITH CORTICAL HYPEREXCITABILITY AND EPILEPSY IN FRAGILE X SYNDROME MOUSE	
MODEL.....	94
<i>Introduction</i>	94
<i>Materials and Methods</i>	95
Animals.....	96
Slice preparation.....	96
UP-state recording.....	97
Audiogenic Seizure test.....	98
<i>Results and Discussion</i>	98
PIKE functional knockdown rescues prolonged UP-states in Fragile X syndrome mouse model.....	98
PIKE functional knockdown attenuates epileptic behavior associated with <i>Fmr1</i> deficiency.....	100
CHAPTER FIVE.....	107
ADDITIONAL STUDIES OF ACTIVITY-DEPENDENT SYNAPTIC DEPRESSION..	107
<i>Summary</i>	107
<i>Materials and methods</i>	107
Dendritic Spine Imaging by Cell Filling.....	107
<i>Results & Discussion</i>	108
Calcineurin inhibition exhibits trends of attenuating chronic postsynaptic burst firing induced MEF2-dependent transcription.....	108
CaMKK is not required for chronic postsynaptic burst firing-induced MEF2-dependent transcription.....	110
Analysis of dendritic spine density in neurons subjected to PPS with biocytin filling	110
Chronic (24 hour) neuronal activity stimulates transcription of the MRE-GFP reporter, and is blocked by embryonic MEF2A/D deletion.....	111
Chronic postsynaptic burst firing induces synapse depression, which is blocked by embryonic MEF2 deletion.....	113
FMRP is not implicated in postsynaptic burst firing-induced synapse depression ...	114
The involvement of mGluR5 in brief activity-induced synapse depression.....	115
CHAPTER SIX.....	123
DISCUSSION AND IMPLICATION.....	123
<i>Transcription Regulation in Chronic Postsynaptic Burst Firing-induced Synapse Depression</i>	123

<i>Determinants that Decide which Synapses to be Silenced/Eliminated</i>	127
<i>Biological Roles of Postsynaptic Burst Firing-induced Synapse silencing/Elimination</i>	129
<i>Fmr1 and MEF2-dependent Synapse Elimination</i>	133
BIBLIOGRAPHY	135

CHAPTER ONE

INTRODUCTION

Synapse Elimination

Characterization of Synapse Elimination

The establishment of a proper-functioning neuronal network relies on adequate synapse formation and elimination (Hua & Smith 2004). During early postnatal development, the rate of synapse formation exceeds that of synapse pruning, creating an environment with an overabundance of excitatory synapses. Subsequent synapse elimination processes then prompt the removal of excessive synapses from the network, resulting in fewer synapses at the adult stage (Rakic et al 1986).

The understanding of activity-driven synapse elimination starts from the study of the neuromuscular junction. At birth, dye labeling showed that each muscle fiber possesses a “junction,” a site characterized by a high density of acetylcholine receptors (AChRs) where multiple axons converge (Balice-Gordon et al 1993, Lichtman & Colman 2000). During the first few postnatal weeks, axons innervating the junction site are gradually eliminated, until there is only one axon remaining. The elimination process is comprised of two steps: (1) loss of AChRs at the focal area where an axon is innervating, and (2) axon retraction. Loss of the focal AChR-rich area precedes the retraction of the corresponding innervating axon (Balice-Gordon & Lichtman 1993), suggesting a stepwise mechanism of synapse elimination.

Moreover, in addition to removal of “losing” connections, the “winning” connections also exhibited enhanced presynaptic release probability (Bennett & Pettigrew 1975).

Synapse elimination also occurs in the central nervous system (CNS), and studies of climbing fibers (CF) innervating Purkinje cells (PCs) in cerebellum provide the first insight into the prevalence of synapse elimination in the CNS. In mice, PCs are innervated by multiple CFs during the early postnatal period. Following a massive elimination of excessive CFs, most PCs are mono-innervated by a single CF at the end of the third postnatal week, (Crepel et al 1980). Similar to the case in the neuromuscular junction, the elimination process of CFs from the innervated PC is also accompanied by changes in individual synaptic strength of each CF. Whole cell recordings of PCs from mouse cerebellar slices showed that responses elicited by stimulation of different CFs were similar in slices prepared from postnatal day 2-3 (p2-3) mice, but difference in the strength of multiple CFs becomes increasingly larger throughout the early postnatal days (from p2 to p27) (Hashimoto & Kano 2003). However, unlike the scenario in the neuromuscular junction, synapse elimination of the CF-PC connection does not involve postsynaptic receptor changes, since there was no difference in quantal amplitude between stronger and weaker CFs. Instead, during the developmental stage the presynaptic multi-vesicular release rate changed, and synapses with lower presynaptic multi-vesicular release rate were subsequently eliminated (Hashimoto & Kano 2003).

Studies of synapse elimination on neuromuscular junction and CF-PC connections

suggest two aspects of synapse elimination: (1) structural elimination, with axon withdrawal for eliminated connections, and (2) functional elimination, with changes in postsynaptic receptor or presynaptic vesicle release rate. Synapse elimination in the cerebrum also shares the same feature. Electron microscopy studies showed that synapse density in the human cortex is reduced during late childhood and adolescence (Huttenlocher 1979, Huttenlocher et al 1982), suggesting the progression of cortical structural synapse elimination during this developmental period. Extensive studies of visual cortical connections also reveal the prevalence of synapse elimination during cerebral development. In the visual pathway, lateral geniculate neurons (LGN) receive ~20 inputs from retinal ganglion cells before eye opening, as estimated by the ratio of total current elicited by a strong stimulus over the current elicited by stimulating a single fiber; however, two weeks after eye opening there are only 1-3 dominant retinal ganglion inputs onto the remaining LGN. (Chen & Regehr 2000, Tavazoie & Reid 2000) . Moreover, the retained retinal ganglion input exhibits a stronger single fiber response compared to the response acquired before eye opening, suggesting the strengthening of the surviving connection --- this feature resembles what is observed in synapse elimination of the neuromuscular junction and CF-PC connection.

The dynamic process of synapse elimination was also demonstrated via *in vivo* and *ex vivo* imaging of dendritic spines, the site at which a vast majority of excitatory synapses are formed (Hering & Sheng 2001). *In vivo* transcranial two-photon imaging of dendritic spines

in numerous cortical areas showed that there were multiple dendritic spines formed and eliminated throughout a one month experimental session (Zuo et al 2005a). The formation and elimination rate of dendritic spines was more prominent in adolescent mice (1 month old), where around 13 – 20% of dendritic spines were eliminated and 5 - 8% of dendritic spines were formed. On the other hand, in adult mice (4 month old), only 3 – 5% dendritic spines were eliminated and formed during the one month experimental session. Note that, in adolescent mice the dendritic spine elimination rate was larger than the dendritic spine formation rate, while the dendritic spine elimination and formation rates achieved balance in adult mice. This corresponds to what is observed in human studies, in which there are more synapses in cortex at early childhood stages (Huttenlocher 1979, Huttenlocher et al 1982).

Synapse Elimination in Hippocampus

Studies in dissociated mouse hippocampal cultures equivalent to the 3 week age also suggest ongoing synapse elimination and formation. At DIV 19, time-lapse imaging of GFP-tagged PSD-95 protein, a core component of the postsynaptic structure in dendritic spines (Ziff 1997), exhibited dynamic turnover of PSD-95 clusters. During the 24 hour experimental session, there were existing PSD-95 clusters that disappeared, as well as new PSD-95 clusters that emerged from places where there were no previous PSD-95 clusters, suggesting the dynamic elimination/formation of dendritic spines/excitatory synapses (Okabe

et al 1999).

Dendritic spines in hippocampus also exhibited the developmental trend that more synapses are formed during early postnatal age and more synapses eliminated during later postnatal stages. The density of dendritic spines were assessed in dissociated rat hippocampal culture from the first postnatal week to the fourth postnatal week with either DiI labeling (Papa et al 1995) or Golgi-Cox staining (Zhao et al 2013). During the first three postnatal weeks, dendritic spine density continued increasing, but in the fourth postnatal week, dendritic spine density shifted to a trend of decreasing. Moreover, the proportion of spines with a “head” increased during the developmental stages (Papa et al 1995), suggesting that the dynamic formation/elimination of dendritic spines/excitatory synapses was accompanied with the formation of more stable spines.

Neuronal Activity, Sensory Experience and Synapse Elimination

Numerous studies suggest that synapse elimination is an activity-dependent process. In neuromuscular junction, saturating a focal region with α -bungarotoxin, an irreversible competitive antagonist for a subtype of AChRs, nicotinic acetylcholine receptor (nAChR), promoted the removal of AChRs from that region and subsequent elimination of the overlying axonal terminal (Balice-Gordon & Lichtman 1994). On the contrary, when the whole neuromuscular junction was saturated with α -bungarotoxin, no loss was observed, suggesting

that synapse elimination at the neuromuscular junction depends on competition of activity between each innervating axon.

The activity-dependency of synapse elimination is also observed in the CNS. *In vivo*, neuronal activity is triggered by experience, such as sensory input through visual or touch stimuli. Monocular deprivation of kittens by suturing one eyelid caused rapid rearrangement of geniculocortical arbors (Antonini & Stryker 1993). Brief monocular deprivation (6 - 7 days) was sufficient to cause axon retraction from the deprived eye, and chronic monocular deprivation (33 days) would further promote geniculocortical overgrowth in the non-deprived eye. This observation not only suggests a similarity in synapse elimination processes between the neuromuscular junction and geniculocortical projections, in which the stronger connection prevails and the weaker connection is eliminated, but also the idea that synapse elimination is dictated by activity.

LGN receives input from both eyes (Williams et al 2002), and hence monocular deprivation would enhance the contrast of different input activity (inputs from contralateral eye and ipsilateral eye) onto LGN, but binocular deprivation would deplete the contrast. Monocular deprivation, as described earlier, promoted elimination of geniculocortical connections serving the deprived eye (Antonini & Stryker 1993), but binocular deprivation caused no effect on axonal/synapse elimination for neither connection (Haruta & Hata 2007); these suggest activity competition is also crucial for axonal/synapse elimination of

geniculocortical arbor.

Sensory deprivation introduced by whisker trimming provides more evidence for the role of experience and activity in synapse elimination. As described earlier, *in vivo* transcranial two-photon imaging was used to reveal the dynamic process of synapse elimination in various cortical areas (Zuo et al 2005a), and the same approach was also used to investigate how experience and activity is involved in synapse elimination. In the study, authors found that trimming whiskers of young mice (1 month old) for two weeks attenuated elimination of dendritic spines in layer I barrel cortex originating from layer V pyramidal neurons in contralateral barrel cortex (Zuo et al 2005b).

On the other hand, dendritic spine density in barrel cortex ipsilateral to the trimmed side was not different from dendritic spine density in barrel cortex of mice without whisker trimming, suggesting that experience and activity specifically regulate synapse elimination in neurons that receive input. Interestingly, synapse formation was not altered by whisker trimming, indicating experience and activity exclusively regulate synapse elimination in the dynamic of synapse formation/elimination. Moreover, dendritic spine elimination in adult mice (> 4 month old) was susceptible to whisker trimming as well, but with less sensitivity --- daily whisker trimming for 2 months was required for significant mitigation of dendritic spine elimination rate. In young mice, restoring sensory experience input by cessation of whisker trimming not only restored dendritic spine elimination, but accelerated the dendritic spine

elimination rate. Intraperitoneal injection of a non-competitive use-dependent NMDA antagonist, MK-801, attenuated the dendritic spine elimination rate but did not affect dendritic spine formation, corresponding to the results observed in the whisker trimming experiment. This result further confirms the requirement of activity in synapse elimination and suggests the involvement of NMDA receptor-mediated activity.

Moreover, although complete removal of sensory input by whisker trimming strongly attenuates synapse elimination rate (Zuo et al 2005b), partial deprivation by chessboard whisker trimming, which removes whiskers intermittently in a pattern like a chessboard, did not affect synapse elimination rate (Pan et al 2010). This result suggests another example for the importance of activity competition in synapse elimination.

Synapse elimination in the hippocampus also requires activity. Dynamic removal of PSD-95 clusters was blocked by the voltage gated sodium channel blocker tetrodotoxin (TTX) and the competitive AMPA/kainate receptor antagonist 6-cyano-7-nitroquinoxaline-2,3-dione (CNQX), but was not affected by application of the competitive NMDA receptor antagonist 2-amino-5-phosphonopentanoic acid (APV) alone, suggesting the involvement of activity via AMPA receptor-mediated transmission in hippocampal synapse elimination (Okabe et al 1999). Pathway-specific inhibition of axonal transmission using partial regional expression of tetanus toxin light chain demonstrated that activity-dependent competition drives hippocampal synapse elimination *in vivo* (Yasuda et al 2011). Upon expression, tetanus toxin

light chain cleaves a synaptic vesicle protein VAMP2/synaptobrevin2 and thus inhibits presynaptic vesicle release (Yamamoto et al 2003). Transgenic expression of tetanus toxin light chain in a subset of presynaptic neuron from either entorhinal cortex (EC) or dentate gyrus (DG) promoted elimination of respective inactivated EC-DG or DG-CA3 connections, assessed by immunocytochemical labeling of axons in brain sections isolated from p12 – p30 mice and field EPSC recording in brain slices prepared from p11- p17 mice. When mice received a hippocampal injection of TTX once a day from p9 to globally suppress neuronal activity, the elimination of inactive axons was significantly suppressed, suggesting it is the competition of activity between nearby axons that drives the elimination of inactive synapses; on the contrary, inactivity of axons does not cause synapse elimination itself.

Synapse Elimination and Fragile X Syndrome and Autism

Synapse elimination is critical during development to trim excessive connections for refinement and maturation of neuronal circuits. Hence, deficits in synapse elimination result in improper pruning and eventually lead to an overly connected neuronal network, which has been hypothesized to underlie some neurodevelopmental disorders.

Fragile X syndrome (FXS) is a neurodevelopmental disorder characterized by synapse pruning deficits and hyperconnectivity. The molecular cause for FXS arises from loss-of-function mutations in a single gene, *FMRI*. In most cases, the mutation is an

expansion of CGG trinucleotide repeats (from normal 5-50 repeats to over 200 repeats) in the promoter region of *FMRI*. The CGG repeat expansion causes hypermethylation of the promoter and eventually leads to silencing of the *FMRI* gene and loss of its protein product Fragile X mental retardation protein (FMRP) (Pfeiffer & Huber 2009). In addition to the commonly observed CGG repeat expansion, intragenic loss-of-function point mutation or deletion could also lead to FXS (Lugenbeel et al 1995). FMRP is a RNA-binding protein that interacts with RNA through motifs including KH1, KH2, RGG box, and NDF (Pfeiffer & Huber 2009). While bound to RNA, FMRP is associated with translating polyribosomes and is implicated in translational control of its bound transcripts (Kanai et al 2004). Disruption of FMRP's association with its target transcripts leads to FXS (Antar et al 2004).

Evidence suggesting that FXS patients are deficient in synapse elimination comes from anatomical studies of human subjects. Postmortem cortical sections from FXS patients revealed excessive dendritic spines and filopodia-like dendritic spines, suggesting FXS patients possess an increased number of excitatory synapses, which may contribute to an increased propensity to epilepsy in FXS patients (Hinton et al 1991, Rudelli et al 1985). FXS is linked to autism spectrum disorder (ASD) (Hagerman et al 2005). Moreover, postmortem brain tissues from temporal lobes of adult ASD patients exhibited increased dendritic spine density compared with non-ASD persons at similar age, while neurons from temporal lobes of childhood ASD patients did not show difference in terms of dendritic spine density compared

to non-ASD children (Tang et al 2014), suggesting the role of synapse elimination deficiency in the development of ASD.

In a mouse model of FXS, the expression *Fmr1* gene, which encodes fragile X mental retardation protein (FMRP), has been disrupted. Neurons from the neocortex of adult FXS mouse model recapitulated the phenotype observed in human FXS patients; those neurons displayed higher dendritic spine density (Galvez & Greenough 2005, McKinney et al 2005). In contrast to what observed in neocortex, mature hippocampal CA1 neurons from FXS mouse model showed a similar dendritic spine density compared to neurons from wild type mice; however, in terms of dendritic spine morphology (Cheng et al 2014) (Figure 1.1), hippocampal CA1 neurons from FXS mouse model exhibited a higher density of stubby dendritic spines, which have large heads and are associated with increased synaptic strength (Grossman et al 2006). Moreover, developing hippocampal *Fmr1* KO dissociated neuron culture displayed increased synapses as assessed by immunocytochemical markers, and acute postsynaptic expression of FMRP in either WT or *Fmr1* KO neurons negatively regulated functional and structural synapse number (Pfeiffer & Huber 2007). Further support for a role of *Fmr1* in synaptic pruning comes from a mosaic FXS mouse model, which has both WT and *Fmr1* KO neurons. Simultaneous recordings from layer 5A pyramidal neurons in somatosensory cortex demonstrated that neurons with postsynaptic deletion of *Fmr1* failed to prune synaptic connections, unlike WT neurons within the same brain region (Patel et al

2014).

Interestingly, both *in vivo* synapse formation and elimination rates were increased in the FXS mouse model. However, a sensory-deprivation induced enhancement of synapse elimination rate was absent in the FXS mouse model, suggesting that the FXS mouse model is less sensitive to modulation by experience and activity (Pan et al 2010).

Silent Synapses and Their Role in Synapse Elimination

Concept for Silent Synapses

Loss of connectivity can be achieved not only by synapse elimination, but also by the formation of silent synapses. Silent synapses can be generated *de novo*, such as those present during the first postnatal week in hippocampus (Isaac et al 1995, Liao et al 1995), or by removing AMPA receptors from existing synapses, such as pyramidal neurons in layer I/II that contain functional synapses at birth which become silent over time (Rumpel et al 2004). The concept of silent synapses emerged from structurally present synapses that did not demonstrate synaptic transmission (Atwood & Wojtowicz 1999). Silent synapses were proposed when researchers observed some “ineffective synapses” that presynaptic stimuli were not able to elicit postsynaptic firing from in spinal cord neurons (Merrill & Wall 1972); However, those “ineffective synapses” could reliably transduce signals by deafferentation (cutting the connection of axons and soma) of a subset of presynaptic fibers (Wall 1977).

For excitatory synapses, silent synapses can be categorized into two types: presynaptically silent or postsynaptically silent. Presynaptically silent synapses do not release neurotransmitter in response to low frequency action potential firing, but many presynaptic silent synapses can be unsilenced when exposed to high frequency presynaptic action potentials (Cabezas & Buno 2011). A postsynaptically silent synapse is a synapse that does not respond to presynaptic neurotransmitter release. A postsynaptically silent synapse lacks functional AMPA receptors but still has NMDA receptors. Since only AMPA receptors can mediate signal transmission at resting membrane potential, the synapse is silent unless the postsynaptic site was depolarized by other means, such as the back-propagating potential when the neuron fires in response to other non-silent inputs. Thus, an AMPA-lacking synapse with NMDA receptors is an “AMPA silent synapse” (Kerchner & Nicoll 2009). In addition, there is also evidence suggesting a model in which some postsynaptically silent synapses are caused by low glutamate concentration in their synaptic cleft (Choi et al 2000).

AMPA silent synapses were first identified in the developing brain and reported to be implicated in developmental plasticity (Hanse et al 2013). Although silent synapses are present in adult brains, they are less well-characterized. Glutamate binding to AMPA receptors and postsynaptic calcium influx are required for the generation of silent synapses (Wasling et al 2012, Xiao et al 2004). Silent synapses can be generated via either metabotropic glutamate receptor (mGluR) or NMDAR-associated pathways and are

implicated in long term depression (LTD) (Hanse et al 2013). The process of silencing a synapse is mediated by AMPA receptor-endocytosis; because AMPA receptors tend to traffic in clusters (Hanse et al 2013), when AMPA receptor endocytosis occurs in an individual synapse, all AMPA receptors on that synapse tend to be endocytosed together to generate a silent synapse without AMPA receptor, rather than a weakened synapse with reduced surface AMPA receptor expression.

Detection of Silent Synapses

There are various ways to detect the presence of silent synapses. Comparing the coefficient of variation (cv) of AMPA and NMDA eEPSC amplitude was used to examine the existence of silent synapses (Kullmann 1994). This method is based on the theory that quantal content (m) is proportional to $1/cv^2$; their relationship can be expressed by the equation:

$$m \sim 1/cv^2$$

However, quantal content (m) equals the number of presynaptic release sites (n) times the release probability (p), which can be expressed as the following equation,

$$m = n * p$$

Hence, the fidelity of this method is based on the presumption of uniform p and large number of n . Therefore, data obtained by this method would be difficult to interpret if the experiment was performed in a brain area that does not fit the criteria (Faber & Korn 1991).

Failure rates at hyperpolarized membrane potential (AMPA-mediated response) and depolarized membrane potential (NMDAR-mediated response) were used to assess the presence of silent synapses as well (Funahashi et al 2013). By applying minimum presynaptic stimulation, the failure rates of eliciting a response in the recorded postsynaptic neurons were assessed. Higher failure rate at hyperpolarized membrane potential indicates the presence of silent synapses.

For AMPA-silent synapses, which lack AMPA receptors but still possess NMDA receptors, measurement of the ratio of AMPA to NMDA evoked EPSC amplitude provides a crude estimation for the prevalence of silent synapses (Beique et al 2006). However, this method assumes that the NMDAR-mediated component is not changed on the synapses of interest and additional assessment of the NMDAR-mediated component is required if the researcher wants to use AMPA/NMDA eEPSC amplitude ratio to address the presence of silent synapses.

As described above, a silent synapse is a synapse that is structurally present but does not respond to presynaptic glutamate release. Thus, with the combination of spatial resolution microscopic imaging and whole cell patch clamp recording, the presence of silent synapses can be determined at the resolution of a single dendritic spine. After the identification of a dendritic spine, which is the presumed site for a synapse, exogenous glutamate could be delivered to the dendritic spine either via puffing (Renger et al 2001) or uncaging caged

glutamate (Beique et al 2006), and AMPAR- and NMDA-mediated responses caused by single dendritic spine activation could be measured to determine if the targeted dendritic spine represents a silent synapse. Notably, unlike other electrophysiological methods described above, which measure responses elicited by evoking endogenous (synaptic) glutamate release, this method employs exogenous glutamate to trigger responses. As such, the concentration of exogenous glutamate should be carefully considered in designing experiments utilizing this method.

The presence of AMPA-silent synapses can also be detected morphologically. Immunocytochemistry with antibodies against pre- and post-synaptic markers (*e.g.* synapsin, synaptophysin), along with AMPA receptors and NMDA receptors to assess synaptic co-clusters could be used to determine sites where silent synapses are present (Gomperts et al 1998). Moreover, immunogold labeling and electron microscopy can also be used to locate synapses without postsynaptic AMPA receptors (Petralia et al 1999).

From Silent Synapse to Long Term Depression and Synapse Elimination

Generation of silent synapses, specifically AMPA silent synapses, involves production of synapses without the capability of AMPAR-mediated transmission. Long term depression (LTD) and synapse elimination also involve mitigation of AMPA-mediated transmission, and hence it is an intriguing idea to try to link silent synapse with LTD and synapse elimination.

Long term depression is an activity-dependent process that attenuates synapse transmission for hours. In hippocampus and cortex, LTD can be induced by pathways involving NMDA receptors, metabotropic glutamate receptors or endocannabinoids. It has been reported that NMDAR-dependent LTD is associated with a change of $1/cv^2$ in AMPAR-mediated response but no change in NMDAR-mediated response (Selig et al 1995), suggesting the involvement of silent synapses in NMDAR-dependent LTD. Dihydroxyphenylglycine (DHPG)-induced group I mGluR-dependent LTD involves endocytosis of ionotropic glutamate receptor AMPA subtype 2 (GluA2) (Sanderson et al 2011), implying the formation of silent synapses. Moreover, deletion of *Sapap3*, which encodes a scaffold protein unique for excitatory synapses - SAP90/PSD-95-associated protein 3 (SAPAP3) (Welch et al 2004), results in synapse silencing, and the synapse silencing cause by *Sapap3* deletion is blocked by treatment with a non-competitive mGluR5 antagonist, 2-Methyl-6-(phenylethynyl)pyridine (MPEP) (Wan et al 2011), further supporting the involvement of silent synapse/synapse silencing in mGluRs-dependent LTD.

Silencing of existing synapses is facilitated by AMPA receptor removal from the synapse, a process that also occurs in synapse elimination (Wilkerson et al 2014). Could synapse silencing precede synapse elimination? In rat organotypic slices, optogenetic induction of NMDAR-dependent LTD in CA3-CA1 pathway weakened synapses, as assessed by postsynaptic calcium transients. Furthermore, 50% of those weakened synapses were

eliminated 7 days after LTD induction (Wiegert & Oertner 2013), suggesting that LTD can lead to synapse elimination, and that synapse silencing may precede the occurrence of synapse elimination.

If synapse silencing takes place before the occurrence of synapse elimination, how would silent synapses be eliminated when AMPAR-mediated transmission is absent? LTD of AMPAR eEPSC and NMDAR eEPSC are triggered and proceed through distinct mechanisms; LTD of AMPAR eEPSC requires calcineurin activity and endocytosis, while LTD of NMDAR eEPSC is unaffected by inhibition of calcineurin activity and endocytosis but requires actin depolymerization (Morishita et al 2005). Moreover, while the removal of AMPA receptors is more often an all-or-none occurrence, depression of NMDAR-mediated response tends to take place gradually (Selig et al 1995). These data indicate the presence of a mechanism that can eliminate silent synapses independent of AMPAR-mediated transmission.

Unsilencing the Silent Synapse and Synapse Stabilization

In contrast to being eliminated, a silent synapse can also be unsilenced. In the developing brain (postnatal week 1-3), silent synapse unsilencing can be triggered when there is no activity for several minutes --- in other words, in the absence of presynaptic release (Abrahamsson et al 2007). However, the unsilenced synapse could be reversed to silent synapse by AMPAR-mediated activity (Wasling et al 2012). Unsilencing a silent synapse can

also be achieved by paired presynaptic and postsynaptic activity; such as pairing low-frequency stimulation with prolonged postsynaptic depolarization (Chancey et al 2013, Isaac et al 1995). In adult-born dentate granule cells, GABA-mediated depolarization is required for unsilencing (Chancey et al 2013), providing *in vivo* evidence that paired presynaptic and postsynaptic activity can promote unsilencing. Moreover, whisker trimming during the first postnatal week resulted in increased AMPA silent synapses in neurons from layer IV barrel cortex (Ashby & Isaac 2011), suggesting that silent synapse unsilencing is an experience-dependent process.

However, simply unsilencing a silent synapse does not guarantee a stable connection. In the developing brain, unsilenced synapses are labile and can be reverted back to silent synapses via AMPA receptor activation (Wasling et al 2012). Further stabilization is required to make a stable synapse. The process of stabilizing unsilenced synapses involves changing synapse-specific structural components. This transition includes (Hanse et al 2013) recruitment of GluA2-containing AMPA receptors and a switch from GluN2A-only NMDA receptors to GluN2A/2B tri-heteromeric NMDA receptors, which have lower surface mobility and less incidence of endocytosis. Within the postsynaptic density, there is a decreased expression of SAP102, a PSD scaffold protein with high mobility (Zheng et al 2010), and increased expression of PSD-95, PSD-93 and SAP97.

Silent Synapses during Development and Addiction

Although studies investigating silent synapses are mostly done in developing brain, evidence also indicates the presence of silent synapses in the adult brain. For example, silent synapses may be generated in response to exposure to drugs of abuse (Huang et al 2009). Medium spiny neurons (MSN) in the nucleus accumbens of cocaine-treated rats exhibited more silent synapses relative to control animals. Interestingly, these silent synapses were created by *de novo* insertion of GluN2B into the plasma membrane, rather than silencing existing synapses. By recruiting calcium-permeable AMPA receptors, these newly formed silent synapses established new connections that contributed to cocaine craving (Ma et al 2016), suggesting a post-developmental plasticity that utilizes silent synapses to remodel neuronal circuitry.

Interestingly, it was reported that *in vivo* expression of CaMKIV or CREB in hippocampi of p21 – p30 rats was sufficient to induce *de novo* generation of silent synapses (Brown et al 2011, Marie et al 2005), as assessed by AMPA/NMDA eEPSC amplitude ratio and NMDA eEPSC amplitude. These data also supports the role of silent synapses after early postnatal development.

Activity-Dependent Regulation and Myocyte Enhancer Factor 2

From Activity to Transcription

Cells can alter their physiology via regulation of gene transcription. Activity-dependent transcription factors are proteins that respond to changes in neuronal activity by driving specific target genes that will, in turn, modulate cellular physiology. When a neuron fires or is depolarized, voltage-gated calcium channels allow calcium influx, activating calcium-dependent kinases and/or phosphatases that may in turn phosphorylate/dephosphorylate target transcriptional factors, such as CREB to modulate transcriptional regulation.

Characterization of Myocyte Enhancer Factor 2 (MEF2)

Myocytes Enhancer Factor 2 belongs to the minichromosome maintenance 1-agamous-deficiens-serum response factor (MADS) box family of transcription factors. MEF2 was originally identified for its role in muscle differentiation and was later found to be expressed in a variety of tissues. Its protein expression is most abundant in muscle, brain and lymphocytes. In vertebrates, there are 4 identified MEF2 genes (MEF2A, MEF2B, MEF2C and MEF2D) and all are composed of 3 domains: (1) MADS box, a 57-amino acid motif located at the extreme N-terminus and serving as a minimum DNA binding domain, (2) MEF2 domain, a 29-amino acid extension located next to the MADS box on the C-terminus side which cooperates with the MADS box to provide high affinity DNA binding and homo-/heterodimerization, and (3) the transactivation domain, which is located at the

C-terminus side and serves as the site for transcriptional activity. The MADS box, in addition to DNA binding, also mediates dimerization of MADS box proteins, however, MEF2 cannot dimerize with other MADS box proteins due to its MEF2 domain, which is unique to the MEF2 family (Black & Olson 1998).

Sequences in MADS box and MEF2 domains shares high (~ 95%) similarity among all 4 MEF2 genes, while the sequences in the transactivation domain are more diverse between the 4 MEF2 genes (McKinsey et al 2002b, Potthoff & Olson 2007). MADS box proteins generally bind A/T-rich DNA sequences, and with the cooperation between the MADS box and MEF2 domain, the MEF2 family binds a unique sequence YTA(A/T)₄TAR, which is found in the regulatory region of MEF2 transcriptional target genes and termed the MEF2 response element (MRE) (Gossett et al 1989). Researchers have taken advantage of this unique sequence recognized by MEF2 to generate MEF2 transcriptional reporters (Flavell et al 2006, Pfeiffer et al 2010).

MEF2 Expression and Transcriptional Regulation

MEF2 expression varies with cell type and developmental stage (Figure 1.2). For example, *in situ* hybridization of mouse hippocampus suggests (Lyons et al 1995) that MEF2C starts to significantly express from embryonic day 14.5, while MEF2A and MEF2D expression is marginal. As development progresses, MEF2C expression gradually dwindles

while MEF2A/D expression rises, such that at postnatal day 14 (p14) MEF2A/D is strongly expressed while MEF2C expression has decreased. MEF2B expression in the hippocampus is marginal across developmental time points to p14. From p14 into adulthood, MEF2A, C, D maintain the same level of expression, with MEF2B expression decreasing to minimal detectable levels.

Although MEF2C is strongly expressed in the hippocampal CA1 region, its expression is more prevalent in inhibitory neurons, as neurons with high MEF2C mRNA are mostly parvalbumin-positive (Kamme et al 2003, Speliotes et al 1996). Thus, in hippocampal CA1 pyramidal neurons, MEF2A and MEF2D are the predominantly-expressed MEF2 genes.

MEF2 transcriptional activity is controlled by several mechanisms, including interactions with co-activators and -repressors. As a transcription factor, MEF2 generally acts as an enhancer, but depending on the stimulus and which co-factors MEF2 is associated with, MEF2 can act as a bidirectional regulator. In the absence of transactivating stimuli, targets of MEF2 exist in a repressed state due to association with class IIa histone deacetylases (HDACs), which bind to the MADS box/MEF2 domain of MEF2 via the N-terminal domain. The C-terminus of class IIa HDACs possess deacetylase activity that can catalyze the removal of acetyl groups from histones to silence and repress target genes. However, class IIa HDACs repress MEF2 targets independently of deacetylase activity by recruiting additional co-repressors through the N-terminal region. Moreover, class IIa HDACs promote

SUMOylation of the transactivation domain of MEF2D, which in turn represses the transcriptional activity of MEF2D (Shalizi & Bonni 2005).

In the presence of transactivating stimuli, class IIa HDACs are phosphorylated and exported from the nucleus, allowing for association of MEF2 with transcriptional coactivators, including CREB binding protein (CBP) and p300, which are histone acetyl transferases. Histone acetyl transferases catalyze the addition of acetyl groups to histone to relax chromatin structure and enhance gene expression (McKinsey et al 2002b).

As an activity-dependent transcription factor, MEF2 can translate neuronal activity into transcriptional activity. Depolarization promotes postsynaptic calcium flux via activation of voltage-gated calcium channels, which in turn triggers CaMK signaling and calcineurin signaling (McKinsey et al 2002b). CaMK phosphorylates class IIa HDACs, creating a docking site for a chaperone protein 14-3-3; upon binding of 14-3-3, HDACs are released from MEF2. Nuclear expulsion of HDACs allows p300 to bind, which in turn acetylates histones to promote expression of MEF2-bound target genes.

Calcium influx also triggers a calcineurin (protein phosphatases 2B)-mediated pathway. In the absence of calcium signaling, calcineurin is an inactive dimer, with its catalytic A chain being bound and repressed by its inhibitory B chain. Upon calcium influx, calcium-bound calmodulin binds to the A chain and hence disrupts the association between the A chain and B chains, allowing the A chain to exert its phosphatase activity. Calcineurin

dephosphorylates nuclear factor of activated T-cells (NFAT), allowing NFAT to translocate into the nucleus to bind and recruit p300 to MEF2. Calcineurin also facilitates MEF2-dependent transcription by dephosphorylating MEF2; phosphorylated MEF2 is targeted by caspases for cleavage, resulting in the removal of the transactivation domain. Without the transactivation domain, MEF2 is unable to transactivate its targets even though it can still dimerize and bind DNA. Thus, MEF2 dephosphorylation by calcineurin prevents MEF2 degradation (Anderson et al 2004, McKinsey et al 2002a).

The MEF2 transcriptional activity can be modulated by post-translational modifications, including phosphorylation and sumoylation. Phosphorylation of the MEF2 MADS box increases the affinity of MEF2 for its target genes, and phosphorylation of the transactivation domain and domain-connecting coils of MEF2 can modulate its stability and transcriptional activity (Rashid et al 2014) (Figure 1.3). Although the transactivation domain sequence of the MEF2 family diverges, putative phosphorylation sites involving proline-directed serine are conserved among MEF2A, MEF2C and MEF2D. Kinases that target MEF2A/C for phosphorylation include p38MAPK and ERK5, and ERK5 also phosphorylates MEF2D (Shalizi & Bonni 2005).

Sumoylation of the MEF2 family has been reported for MEF2A, C and D (Gregoire & Yang 2005, Kang et al 2006, Riquelme et al 2006). Sumoylation of MEF2 protein attenuates its transcriptional activity. Sumoylation of MEF2A and MEF2C can be facilitated by

preceding phosphorylation (Kang et al 2006, Lu et al 2014), indicating cooperative post-translational modifications to repress MEF2 transcriptional activity.

MEF2-VP16

In order to study the transactivation ability of MEF2, a constitutively active artificial MEF2 was generated by fusing the MADS box/MEF2 domain from MEF2C with herpes simplex virus type 1 VP16 (Barbosa et al 2008, Wu et al 1994). VP16 is from Herpes Simplex virus and is an essential tegument protein involved in the transcriptional activation of viral immediate early promoters during the lytic phase of viral infection. VP16 can be fused to cellular transcription factors to enhance transcription rates, including the general transcription factor TFIIB and the transcriptional coactivator PC4. The N-terminal residues of VP16 provide specificity for the immediate early genes, while the C-terminal residues take place in transcriptional activation. Within the C-terminal region there are two activation regions that can activate transcription independently and cooperatively.

MEF2, synapse elimination and *Fmr1*

Previous reports describe roles for MEF2A and MEF2D in regulation of synapse elimination (Flavell et al 2006). Knockdown of MEF2A/D increased the density of PSD95/synapsin 1 co-clusters and enhanced mEPSC frequency in dissociated hippocampal cultures. Furthermore, the *Mef2a/d* deletion-induced enhancement of structural/functional

synapses was blocked by inhibition of calcineurin or activity. Transfection of MEF2-VP16, a constitutively active MEF2 protein, attenuated eEPSC amplitude/ mEPSC frequency. These data suggest that MEF2A/D mediates activity-dependent synapse elimination in hippocampus (Pfeiffer et al 2010). Interestingly, increasing the activity of dissociated hippocampal cultures through application of a high concentration of potassium ions into the extracellular media did not cause a reduction in structural and functional synapses (personal communication with the author of (Flavell et al 2006)), despite the fact that the same condition was able to activate MEF2A/D-dependent transcription (Flavell et al 2008).

As described previously, Fragile X Syndrome (FXS) is associated with deficits in experience and activity-dependent synapse pruning, and raises the possibility that *Fmr1* might be related to MEF2-mediated synapse elimination. Indeed, MEF2-VP16-mediated reductions in hippocampal eEPSC amplitude/mEPSC frequency and dendritic spine density were absent in FXS mice (Pfeiffer et al 2010), suggesting the involvement of *Fmr1* in MEF2-VP16 driven synapse elimination.

MEF2-mediated dendritic spine plasticity plays a role in modulating cocaine sensitivity (Pulipparacharuvil et al 2008). Cocaine administration in mice promoted phosphorylation of MEF2A at serine 408/444, which inhibits MEF2A transcriptional activity. MEF2A/D knockdown by shRNA in nucleus accumbens increased dendritic spine density, similar to observations in dissociated hippocampal culture (Flavell et al 2006). Cocaine

administration increased dendritic spine density in nucleus accumbens that could be reversed by MEF2-VP16 expression, but interestingly, MEF2-VP16 administration alone did not affect dendritic spine density. Notably, MEF2-VP16 expression in the nucleus accumbens sensitized the response of mice toward cocaine administration, as mice administered with cocaine spent more time in the cocaine-paired area during the conditional place preference test. These results suggest that MEF2-mediated synapse elimination can modulate behaviors associated with addiction to drugs of abuse.

Optogenetics and Neuronal Activity Manipulation

Traditional Methods

In molecular biology, one approach to study the function of a particular gene/protein is to artificially express it and study the impact from the gain of function of the interested gene/protein. For studies about activity-driven biological events, researchers also utilized similar approaches by raising activity levels via artificial means.

Many activity-driven neuronal events are caused by depolarization, such as the opening of voltage-gated channels. Hence, a straight forward way to trigger activity-dependent neuronal events is to continuously depolarize neurons by adding a high concentration of potassium into the extracellular environment (Flavell et al 2008). Since membrane potential is maintained by the differential ion concentration between the

intracellular and extracellular environments, increasing the extracellular potassium concentration would abolish the potassium concentration gradient and cause tonic depolarization. However, this approach depolarizes all neurons in the culture, making it difficult to study cell autonomous or pathway-specific events. Moreover, increasing extracellular potassium simply makes the affected neuron tonically depolarized, which is a status obviously aberrant from physiological condition (Kandel & Spencer 1961, Nakashiba et al 2008, Thompson & Best 1989).

Another way to increase neuronal circuit activity is to inhibit GABAergic transmission (Guo et al 2016). GABAergic inhibition removes the hyperpolarizing input from the inhibitory interneuron and thus globally raises activity in the treated neuronal culture. However, this approach shares similar concerns with increasing extracellular potassium concentration; it affects all neurons in the circuit and thus cell autonomous or pathway-specific events are difficult to study. In addition, this approach simply raises circuit activity; researchers cannot specifically apply an activity pattern to a single neuron.

A common method used to investigate transcription factor function is the construction and use of constitutively active proteins that can be expressed in neurons (Barbosa et al 2008). This approach allows the investigation of cell autonomous events. Nevertheless, when researchers are using constitutively active transcription factors for their experimental design, a take-home message that should be kept in mind is that the transactivation driven by

constitutively active transcriptional factors is not resulted from the natural transactivation process by the non-artificial transcriptional factors. Furthermore, although the constitutively active transcription factor is supposed to drive an activity-dependent process, the resultant transactivation occurs in a condition where no actual activity is applied.

In order to study pathway-specific events, researchers developed a system able to inhibit the presynaptic input from a specific pathway. (Nakashiba et al 2008, Yamamoto et al 2003, Yasuda et al 2011). In this system, transgenic animals were generated to express two genes/proteins: a tetracycline-controlled transactivator under the control of a presynaptic site-specific promoter, and tetanus toxin light chain under the control of a tetracycline operator. Tetanus toxin light chain cleaves a synaptic vesicle protein, VAMP2/synaptobrevin2, and thus inhibits presynaptic vesicle release when expressed (Yamamoto et al 2003). The tetracycline-controlled transactivator can bind the tetracycline operator and drive tetanus toxin light chain expression only if it is bound by tetracycline or doxycycline. Hence, in this system, a specific presynaptic input can be inhibited by using an appropriate mouse line to drive a tetracycline-controlled transactivator in the desired area. The timing of presynaptic inhibition can also be controlled by manipulating the time at which animals are fed tetracycline or doxycycline. This approach allows studies regarding the impact of loss-of-activity from a particular input.

Channelrhodopsins as a Tool for Introducing Activity

Traditional methods used to introduce neuronal activity share the same caveat: the pattern and timing of activity are unable to be controlled in a cell-specific manner. The development of channelrhodopsins removes this handicap and refines experiments to study activity-dependent biological processes.

Channelrhodopsins are light-activated channels that were discovered in algae. Since its discovery, channelrhodopsin 2 (ChR2) quickly became the favorite tool for neuroscientist to study activity-dependent processes. Channelrhodopsins are permeable to cations, and non-selective for protons, sodium, potassium and calcium ions. Channelrhodopsins have a reversal potential close to 0 mV at physiological pH, and elicit maximum response when exposed to blue spectral range light (~470 nm), although particular channelrhodopsin variants have been engineered with shifted spectral responsiveness. When exposed to a continuous light source, photocurrents caused by channelrhodopsin activation would peak quickly, then dwindle to steady state status due to desensitization (Lin 2011).

Much effort has been put into engineering channelrhodopsins to create more efficient and versatile proteins. For example, the mutation H134R (ChR2H134R) has less desensitization and increased light sensitivity compared with the original ChR2, but with slower channel closing which makes it less temporally precise. (Lin 2011).

Application of Channelrhodopsins

Goold et al (Goold & Nicoll 2010) expressed ChR2H134R in CA1 pyramidal neurons in rat organotypic slice culture and induced postsynaptic bursts with patterned photostimulation of 3 Hz 50 ms pulse for 24 hours. They observed that this specific protocol was able to induce functional and structural synapse elimination via a mechanism requiring L-type voltage gated-calcium channels, similar to what is observed by driving MEF2 activity in a similar preparation (Flavell et al 2006, Pfeiffer & Huber 2009). Interestingly, the 24 hour postsynaptic bursts-induced synapse elimination occurred independently of presynaptic activity, NMDAR-mediated activity, and calcineurin activity. Furthermore, the authors demonstrated that this plasticity required the presence of GluA2 receptors.

Channelrhodopsins have also been used to elicit presynaptic release. Simon et al (Wiegert & Oertner 2013) expressed ChR2-E123T-T159C in the hippocampal CA3 region and used blue light to elicit synaptic responses in CA1 neurons as assessed by calcium transients imaging in the CA1 region. The authors then utilized a LTD-induction protocol to induce synapse weakening with blue light stimulation; 7 days after the LTD-induction protocol they observed that ~ 50% of the synapses weakened by the LTD protocol were eliminated.

Channelrhodopsins have also been used *in vivo* and for behavioral experiments. Liu et al (Ramirez et al 2013) expressed ChR2 in hippocampal neurons that were activated during a

fear conditioning task. Specifically, expression of ChR2 in neurons activated in the fear conditioning task occurred by the tetracycline-controlled transactivator/tetracycline operon system described earlier. The authors were able to induce a “false” fear memory in those mice by activating ChR2 with blue light, even if the mice were not in the room where they received the electrical shock.

Motivation and Rational for the Study

Previous evidence indicates a critical role of MEF2 in the control of activity-dependent synapse pruning and circuit refinement. However, these studies utilized conventional approaches such as tonic elevation of neuronal activity via high potassium treatment or the constitutively active construct MEF2-VP16 (Flavell et al 2006, Flavell et al 2008). Although these conventional approaches can effectively elevate neuronal circuit activity or activate MEF2-regulated gene expression, their robust effects make it difficult to understand how MEF2 is regulated by physiological neuronal activity and how endogenous MEF2 activity contributes to synapse pruning in response to activity elevation. While one study recapitulates activity-induced MEF2-dependent synapse depression in inhibitory neurons using corticostriatal co-culture (Tian et al 2010), evidence for its role in cortical and hippocampal excitatory neurons is still unclear.

The use of optogenetics allows deliberate control of neuronal activity, permitting an

examination of the effects of physiologically-relevant frequencies and durations. This technique offers an opportunity to further refine the role of MEF2 in activity-dependent plasticity. Cell autonomous increases in activity introduced by optogenetics (Goold & Nicoll 2010), which raised the firing rate of individual neurons to 1.5~2 fold of their average spontaneous firing rate (Nakashiba et al 2008, Thompson & Best 1989), promoted functional and structural synapse depression/pruning in affected neurons. Interestingly, the chronic activity elevation-induced synapse depression depends on activation of L-type voltage-gated calcium channel and *de novo* transcription, resembling the features of MEF2 activation (Flavell et al 2006). This suggests not only that MEF2 may be involved in this type of plasticity, but also hints at how MEF2 can be regulated by physiologically-relevant neuronal activity to drive activity-dependent synapse depression/pruning.

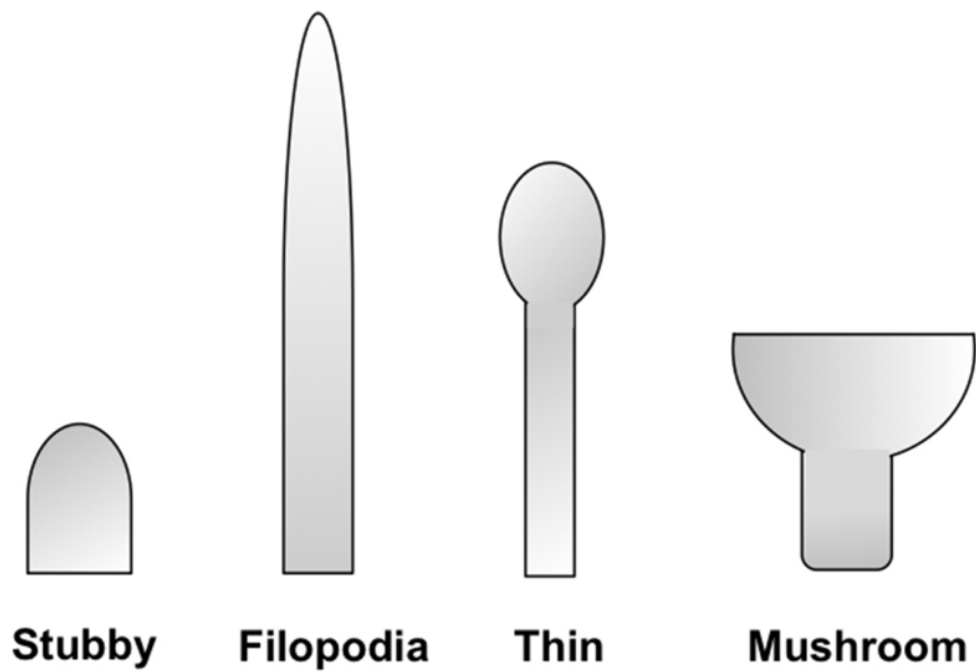


Figure 1. 1 Categories of different types of dendritic spine based on their morphology
Illustration of different types of dendritic spine based on their morphology. Picture was excerpted from (Cheng et al 2014).

Table 1. Relative levels of *Mef2* gene expression in developing brain

		Days postcoitum					
		12.5	14.5	16.5	Nn	2 week	Adult
Olfactory bulb	2A	-	+	+	+	+	+
	2B	-	+	+	++	++	+++
	2C	-	++	++	+++	+++	+++
	2D	+	++	++	++	++	++
Amygdala	2A	-	-	-	-	+	+
	2B	-	-	+/-	-	-	-
	2C	+	+++	+++	+	-	++
	2D	+/-	++	++	+	+	++
Cerebral cortex	2A	-	-	+	+	+	+
	2B	+	++	++	+++	++	+++
	2C	++	+++	+++	+++	+++	+++
	2D	+	+	++	++	++	++
Hippocampus	2A	nd	-	-	+	+++	+++
	2B	nd	+	+	+	+	+/-
	2C	nd	+++	+++	++	++	++
	2D	nd	+	+	+	+++	+++
Thalamus	2A	++	++	+++	+++	+++	+++
	2B	-	+	+	+	++	-
	2C	+	+	+	+	+	++
	2D	+	+	+	++	+	++
Midbrain/colliculus	2A	-	+	+	+	+	-
	2B	-	-	-	+	++	++
	2C	-	++	++	++	++	+++
	2D	-	++	++	++	++	++
Cerebellum	2A	nd	-	-	+	+	+
	2B	nd	-	-	++	+	-
	2C	nd	+	++	++	++	+
	2D	nd	+	+	+	++	++
Pontine nuclei	2A	nd	nd	++	++	-	+
	2B	nd	nd	+/-	+	++	++
	2C	nd	nd	++	++	++	+++
	2D	nd	nd	+	+	+	++
Medulla	2A	+/-	+	+	+	nd	nd
	2B	-	-	+	+	nd	nd
	2C	-	+	+	+	nd	nd
	2D	+	+	+	+	nd	nd

nd, not determined; Nn, neonatal.

Figure 1. 2 Spatial and temporal expression profile of *Mef2* genes in brain RNA expression for each MEF2 genes in different developmental stages and brain regions was assessed by *in situ* hybridization. Table is excerpted from Lyons's work (Lyons et al 1995).

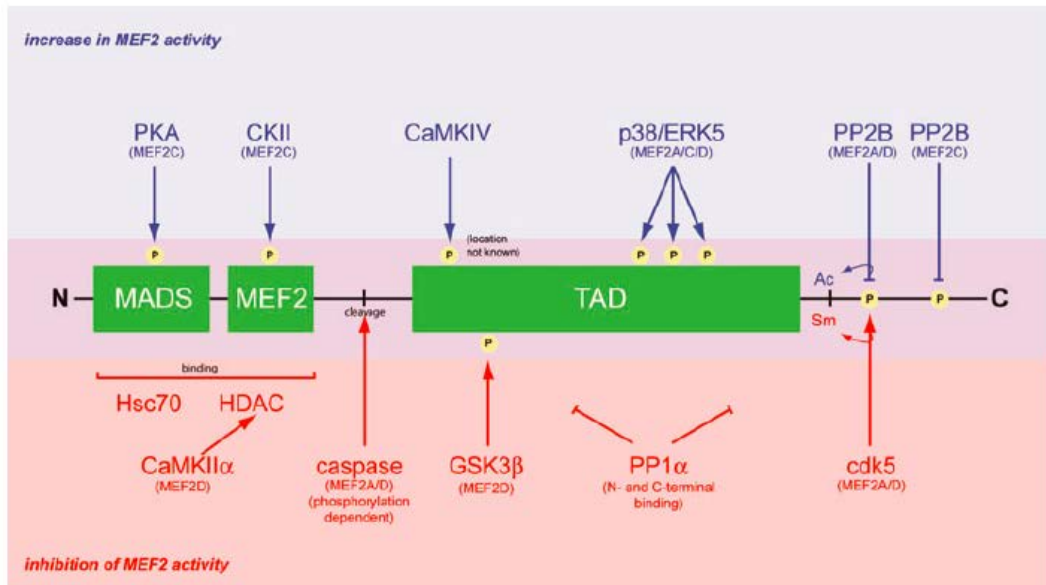


Figure 1. 3 Posttranslational modifications modulate MEF2 activity

Schematic illustration of posttranslational modifications that modulate MEF2 activity and enzymes responsible for each posttranslational modification. Pathways in blue color represent posttranslational modifications that enhance MEF2 activity, and pathways in blue color represent posttranslational modifications that decrease MEF2 activity. Picture was excerpted from (Rashid et al 2014).

CHAPTER TWO

BRIEF POSTSYNAPTIC BURST FIRING PROMOTES SYNAPSE SILENCING VIA SELECTIVE ACTIVATION OF MEF2-REGULATED GENE EXPRESSION

Introduction

Experience and activity-dependent synapse elimination plays an important role in the refinement of neuronal circuits during early postnatal development and is implicated in learning and memory (Fu & Zuo 2011, Hua & Smith 2004, Zuo et al 2005b). Myocyte Enhancer Factor 2 (MEF2), a transcription factor that is activated by neuronal depolarization and Ca²⁺ influx, is implicated in pruning and depression of excitatory synapses and dendritic spines onto cortical neurons (Flavell et al 2006, McKinsey et al 2002b). However, the physiological patterns of neural activity that activate MEF2 and lead to MEF2-dependent synapse pruning or depression are unknown.

To address this question, I examined the role of *Mef2* genes in activity-dependent synapse depression in organotypic hippocampal slice cultures. To control and drive action potential firing in individual neurons, I biolistically transfected channelrhodopsin 2 (ChR2) into CA1 neurons in slice culture and induced firing with a patterned photostimulation (PPS) protocol (50ms pulses of blue light at 3 Hz) for either 1 (brief) or 24 hour (chronic), which resulted in respective elevation of neuronal activity. Both brief and chronic elevation of neuronal activity activate MEF2-dependent transcriptional activity in CA1 neurons, as measured by the transcriptional reporter, MRE-GFP, and caused functional synapse

depression as measured by decreases in evoked (e) EPSCs and miniature (m) EPSC frequency 24 hour after PPS onset. Interestingly, postsynaptic deletion of *Mef2a* and *Mef2d*, the major MEF2 family members expressed in CA1, blocked functional synapse depression induced by brief, but not chronic elevation of neuronal activity. Moreover, brief elevation of activity promoted synapse silencing primarily by AMPA receptor removal from synapses, while chronic elevation of activity gave rise to the elimination of dendritic spine structure. Deletion of *Arc*, which is a MEF2 transcriptional target and specifically induced in response to briefly increased neuronal activity, abolished functional synapse depression induced by brief elevation of activity but only partially attenuated the synaptic effect induced by chronic elevation of activity.

Materials and methods

Hippocampal Slice Cultures and Transfection

Organotypic hippocampal slice cultures were prepared from postnatal day (P) 6-7 mice of C57BL/6 mouse strain using previously published protocols (Pfeiffer et al 2010, Stoppini et al 1991). Cultures were biolistically transfected at 3 DIV. Biolistic transfection and gold bullet preparation were performed with the Helios Gene Gun system (BioRad) according to the manufacturer's protocols (McAllister, 2004).

Patterned Photostimulation and Drug Treatment

8-13 days after transfection, 6-8 hippocampal slice cultures consolidated on a culture plate insert in a 6-well plate were flashed by a collimated blue LED (470 nm) from Thorlabs (M470L3-C1 or M470L3-C5) inside a 35°C, 5% CO₂ humidified incubator. The duration of blue light flashing and post-flashing incubation time are indicated in text. The collimated light density at the location where slices were flashed was calibrated to 35 mW/mm², measured by Fieldmax Top photometer. LED are driven by a T-Cube LED Driver, 1200 mA Max Drive Current (Thorlabs), and the pattern (50 ms for each pulse at 3 Hz) of LED flashing was controlled by a PC using custom software (Labview; National Instruments, Austin, TX). Slice culture media was changed fresh prior to photostimulation, and if drug treatment was required in the experiments, drugs were added to slice culture media and equilibrated to the incubator 20 minutes to 1 hour before the onset of photostimulation.

Imaging of MRE-GFP, the MEF2 transcriptional activity reporter

Transfected organotypic slice cultures were subjected to photostimulation with indicated drug treatment. Treated slice cultures were placed in a Warner chamber filled with warm Tyrode's solution containing (in mM): 150 NaCl, 4 KCl, 2 CaCl₂, 2 MgCl₂, 10 glucose, 10 HEPES. Single plane images (1024x1024 pixel resolution) were acquired using a Plan-Neofluar 63X/1.3 or 40X/1.3 oil immersion objectives mounted on a Zeiss LSM 510 inverted confocal microscope. Quantification of green (MRE-GFP) and red (ChR2- or

cre-mCherry) soma fluorescence was performed using ImageJ software as previously described (Pfeiffer et al 2010, Pulipparacharuvil et al 2008). MRE-GFP expression profile was determined by normalizing GFP fluorescence intensity over background fluorescence intensity, and the resultant value was normalized to the average value from control group with 0 hour PPS. Background fluorescence was determined by a region (equal to the region area of the analyzed neuron) in the field of view adjacent to the neuron. Two to three independent slice cultures (litters) were used in each imaging study. Statistical significance between groups was determined with a two-factor ANOVA (factor 1= photostimulation, factor 2 = genotype or drug treatment) with Tukey's multiple comparison test.

Electrophysiology

Simultaneous whole-cell recordings were obtained from CA1 pyramidal neurons in slice cultures visualized using IR-DIC and GFP fluorescence to identify transfected and untransfected neurons (Pfeiffer et al 2010). Recordings were made at 32°C in a submersion chamber perfused at 3 ml/min with artificial cerebrospinal fluid (ACSF) containing (in mM): 119 NaCl, 2.5 KCl, 26 NaHCO₃, 1 NaH₂PO₄, 11 D-Glucose, 4 CaCl₂, 4 MgCl₂, 0.1 picrotoxin, 0.002 2-chloro-adenosine; 0.1% DMSO pH 7.28, 305 mOsm and saturated with 95% O₂/5%CO₂. For evoked EPSC (eEPSC) and mEPSC recordings, neurons were voltage clamped at -60mV through whole cell recording pipettes (~4.5-7 MΩ) filled with an internal

solution containing (in mM): 0.2 EGTA, 130 K-Gluconate, 6 KCl, 3 NaCl, 10 HEPES, 2 QX-314, 4 ATP-Mg, 0.4 GTP-Na, 14 phosphocreatine-Tris, pH7.2 adjusted by KOH, 295 mOsm. To obtain isolated NMDAR mediated eEPSCs, the ASCF was supplemented with 20 μ M DNQX and 20 μ M glycine and the neuron was clamped at +40 mV. The internal pipette solution for NMDAR eEPSCs contained (in mM) 2.5 EGTA, 125 Cs-Gluconate, 6 CsCl, 3 NaCl, 10 HEPES, 10 sucrose, 10 TEA-Cl, 2 QX-314, 4 ATP-Mg, 0.4 GTP-Na, 14 phosphocreatine-Tris, pH7.2 adjusted by CsOH, 295 mOsm; for AMPAR eEPSCs acquired prior to NMDAR eEPSCs, the same internal solution was used, but ACSF was not supplemented with DNQX nor glycine. For mEPSC measurements, the ACSF was supplemented with 1 μ M TTX. Synaptic responses were evoked by single bipolar electrode or 2-conductor cluster electrode placed in stratum radiatum of area CA1 (along the Schaffer collaterals) 20-100 μ m from the recorded neurons with monophasic current pulses (10-300 μ A, 0.2-1 ms). Series and input resistance were measured in voltage clamp with a 400-ms, -10 mV step from a -60 mV holding potential (filtered at 30 kHz, sampled at 50 kHz). Cells were only used for analysis if the series resistance was less than 31 M Ω . Input resistance ranged from 75-600 M Ω . Data were not corrected for junction potential. No significant difference was observed between transfected and untransfected neurons in input resistance, indicating that overall neuronal health and subthreshold membrane conductance were unaffected by biolistic transfection. Synaptic currents were filtered at 2 kHz, acquired

and digitized at 10 kHz on a PC using custom software (Labview; National Instruments, Austin, TX). mEPSCs were detected off-line using an automatic detection program (MiniAnalysis; Synaptosoft Inc, Decatur, Ga.) with a detection threshold set at a value greater than at least 5 S.D. of the noise values, followed by a subsequent round of visual confirmation. The detection threshold remained constant for the duration of each experiment. For eEPSCs shown in figures the stimulation artifact has been digitally removed for clarity. Significance of differences between transfected and untransfected neurons was determined using a paired t-test, and non-parametric analysis was used when data was not normally distributed.

Dendritic Spine Imaging

At 3 DIV, Organotypic hippocampal slice culture were biolistically transfected with PA1-GFP, which expresses a myristoylated form of GFP to enhance filling of dendritic spines, and/or ChR2H134R-mCherry. At 8-13 d post-transfection (11-16 DIV), slices were subjected to photostimulation as indicated in the text. Slices were fixed in 2.5% PFA/4% sucrose for 1.5 hr, followed by permeabilization in 0.5% Triton X-100/10% normal donkey serum for 2 hr. Slices were incubated with 1° anti-GFP antibody (Aves Labs) at 4°C overnight, followed by incubation with 2° anti-chicken Alexa Fluor 488 antibody (Life Technologies) for 4 hr at room temperature. Secondary apical dendrites (150-200 μ M from soma) of transfected CA1 neurons were imaged using a Zeiss LSM 780 2-photon laser scanning microscope. Images

were obtained using an excitation wavelength of 920 nm and a 40X 1.4 NA oil immersion objective. An interval of 0.3 μM and pixel resolution of 2048 \times 2048 was used to acquire Z-stacks, generating images with pixel dimensions of 0.07 \times 0.07 \times 0.3 μm . For each neuron, 1-2 regions of interest were acquired. Imaging experiments were performed blind to treatment.

Dissociated Primary Culture

Dissociated CA3-CA1 hippocampal cultures (dentate gyrus was discarded) were prepared from P0 mice using modified, previously published protocols (Waung et al 2008). Briefly, dissected hippocampi from P0 mice were trypsinized for 10 min, and dissociated by trituration. After centrifugation, neurons were plated in Neurobasal A medium (Invitrogen) supplemented with B27 (2%; Invitrogen), 0.5 μM glutamine, and 1% fetal bovine serum (FBS) at a density of 450 neurons/ mm^2 on 35 mm dishes coated overnight with 50 $\mu\text{g}/\text{ml}$ poly-D-lysine. Cultures were fed at 1 day *in vitro* (DIV) and every 5 days afterwards by replacing half the media with serum-free glial-conditioned Neurobasal A media (containing B27, glutamine and cytosine arabinoside; 2 μM). At 1-3 DIV, cultures were infected with ChR2H134R-mCherry and/or cre-mCherry containing viruses. Glial cultures were prepared from the neocortex of P0-P2 mouse pups and maintained in Neurobasal A containing 10% FBS and 50 $\mu\text{g}/\text{ml}$ penicillin, 50 U/ml streptomycin, Sigma) for 3-4 weeks (Viviani 2006).

Neurobasal A media was conditioned for 48 hour, collected and stored at 4°C for no more than one week prior to use.

Virus preparation

HEK293T cells at 90% confluency were transfected with Rev, RRE, VSVg and specific lenti-viral based construct (ChR2H134R-mcherry or cre-mCherry) using Lipofectamine 2000 (Invitrogen) according to the manufacturer's instructions. 12-18 hour after transfection, the cell culture media was replaced with Neurobasal A media with B27. Media (where viruses were secreted) were harvested 48-60 hour after transfection, and then filtered by a 0.45 µm filter. The virus-containing media will be stored at 4°C for up to one week if not used immediately.

RNA extraction and qPCR

At DIV14, dissociated cultures were subjected PPS as indicated in the text, and then RNA was extracted from treated dissociated cultures using TriZol reagent (Invitrogen), followed by purification using RNeasy micro columns (Qiagen). Equal amounts of RNA were prepared for reverse transcription reactions using the Superscript II reverse transcriptase enzyme (Invitrogen). The efficiency of each primer set used in real-time quantitative PCR experiments was first tested on 10-fold serial dilutions of hippocampal cDNA to ensure that the primers promoted specific, exponential amplification of the target cDNA. Optimal primer

sets for each gene were then used to assess the abundance of the reverse-transcribed mRNA in cDNA samples. PCR reactions were run in triplicate using iTaq universal SYBR green supermix. Each reaction was quantified using the $\Delta\Delta C_t$ method as previously described (Tsankova et al 2006). Expression for each gene was normalized to GAPDH expression.

Primers used were: *Gapdh* forward: 5'-AGG TCG GTG TGA ACG GAT TTG-3'; *Gapdh* reverse: 5'-TGT AGA CCA TGT AGT TGA GGT CA-3'; *Arc* forward: 5'-AGC AGC AGA CCT GAC ATC CT-3'; *Arc* reverse: 5'-GGC TTG TCT TCA CCT TCA GC-3'; *Mef2a* forward: 5'-AAC CGA CAG GTT ACT TTT AC-3'; *Mef2a* reverse: 5'-TCT TAA CGT CTC AAC GAT AT-3'.

Statistics

All electrophysiological data from paired recordings were analyzed by a paired t-test. For data sets not fitting a normal distribution, nonparametric analysis was applied. For analysis of electrophysiological data from different studies, ratio of response from transfected neuron over untransfected neuron for each recording pair was log transformed (termed “depression index”), followed by unpaired t-test. Grouped MRE-GFP induction data was analyzed by one-way ANOVA or two-way ANOVA followed by multiple comparison. Results from qPCR experiments were analyzed by one-way ANOVA test or two-way ANOVA followed by multiple comparison. (* p< 0.05; ** p<0.01; ***p<0.05, **** p< 0.001). All

grouped data was displayed as mean \pm standard error of the mean.

Results

Brief (1 hour) Postsynaptic Bursts of Action Potentials Activate MEF2A/D-mediated

Transcription

MEF2A/D-dependent transcription is induced in response to neuronal depolarization, with high KCl, but the physiological activity patterns that drive MEF2A/D or induce MEF2A/D-dependent synaptic plasticity are unknown. To address this question, I expressed ChR2-mCherry in a sparse population (< 0.5%) of CA1 neurons in organotypic hippocampal slice cultures and drove transfected CA1 neurons to fire in bursts of action potentials at 3 Hz with light (Fig. 1A). I chose this pattern because hippocampal CA1 neurons fire in bursts at 3-8 Hz *in vivo* during spatial exploration (Kandel & Spencer 1961) and chronic (24 hr) patterns of stimulation are reported to induce synapse elimination, and therefore may activate MEF2 (Goold & Nicoll 2010). To measure MEF2-regulated transcriptional activation in individual CA1 neurons, I used biolistics to cotransfect neurons with a MEF2 transcriptional reporter (MRE-GFP) and ChR2. Patterned photostimulation (PPS; 50ms pulses of blue light at 3 Hz) of slice cultures, 8-13 days posttransfection, caused transfected CA1 neurons to fire in a burst of 1-3 action potential spikes at 3 Hz with 2.34 spikes per burst, and the average inter-spike interval in bursts with 2 or more spikes was \sim 31 ms (Figure 2.1). In unstimulated

cultures without PPS, MRE-GFP levels were low or undetectable (Figure 2.2). This result suggests that the basal activity levels in the slice cultures are low, such that they are not driving MEF2-mediated transcription. However, PPS stimulation for 1-24 hrs robustly induced the MRE-GFP reporter (Figure 2.2). To determine if endogenous MEF2A/D mediated PPS-induced MRE-GFP, I cotransfected CA1 neurons in slice cultures prepared from wildtype (WT) mice or mice with floxed alleles of *Mef2a* and *Mef2d* (*Mef2a/d^{fl/fl}*) (Akhtar et al 2012, Lyons et al 1995) with Cre-mCherry, ChR2 and MRE-GFP. *Mef2a/d* deletion did not affect the low, basal levels of MRE-GFP, but did block MRE-GFP induction in response to both brief (1 hr) and chronic (24 hrs) PPS (Figure 2.3 A, B). *Mef2a/d* deletion did not affect ChR2 expression, as assessed by blue light-induced currents (Fig 2.4A; Table 2.1). These results indicate that physiological action potential patterns activate MEF2A/D-driven transcriptional activation.

Brief and Chronic Bursts of Postsynaptic Action Potentials Induce Depression of Excitatory Synaptic Transmission that Differentially Rely on MEF2A/D

Both brief and chronic PPS induce MEF2A/D-dependent transcriptional activity, and thus I hypothesized these activity patterns would elicit MEF2A/D-dependent synaptic plasticity, most likely synapse elimination (Flavell et al 2006, Pfeiffer et al 2010). Since a brief (1 hr) PPS was sufficient to activate MEF2A/D-dependent transcription, I first tested the effects of brief PPS on synaptic function. Slice cultures were biolistically transfected with

ChR2-mCherry and Cre-mCherry from WT mice, as described above. WT slice cultures were exposed to 1 hr (brief) PPS and at 24-30 hour after PPS, I performed dual, whole cell voltage clamp recordings from ChR2-transfected and neighboring untransfected neurons and measured evoked and spontaneous, miniature (m) EPSCs. Brief PPS resulted in a robust (~50%) depression of evoked EPSC amplitude in transfected neurons as well as depression of mEPSC frequency (Figure 2.5A). The amplitude of mEPSCs, a measure of the strength of individual synapses, was unchanged, as well as paired pulse facilitation of evoked EPSCs, a measure of presynaptic release probability (Table 2.1). As a control, transfection of ChR2, without PPS, had no effect on any measure of synaptic function (Figure 2.4B). Longer durations of PPS (6 or 24hr (chronic); recording at 24hr after PPS onset) also resulted in a depression of evoked EPSCs and mEPSC frequency (Fig. 2.6A), without changes in mEPSC amplitude or paired-pulse facilitation (Table 2.1). These results suggest that brief (1hr) periods of postsynaptic activity are sufficient to depress synaptic function and prolonging the stimulation does not result in greater levels of synaptic depression. Previous studies suggest both Chronic PPS and overexpression of constitutively active MEF2 in CA1 neurons causes a functional and structural elimination of synapses that is manifest functionally as a reduction in evoked EPSC amplitude and mEPSC frequency without changes in mEPSC amplitude or paired-pulse facilitation (Goold & Nicoll 2010, Pfeiffer et al 2010). Because brief PPS has similar effects on synaptic properties, it may also induce elimination of synapses.

Considering this data together with my findings that PPS activates MEF2/D-dependent transcriptional reporter expression, I hypothesized that different durations of PPS eliminate excitatory synapses through activation of MEF2A/D-driven transcription. To test this hypothesis, I deleted *Mef2a/d* in individual CA1 neurons by co-transfecting Cre-mCherry and ChR2-mCherry into slice cultures prepared from *Mef2a/d^{fl/fl}* mice. *Mef2a/d* deletion had no effect on evoked or mEPSCs (Figure 2.5C) in unstimulated cultures, but blocked the ability of brief PPS (1 hr) to depress EPSCs or mEPSC frequency (Figure 2.5B). These results, together with the results of the MRE-GFP reporter (Figure 2.3), indicate that basal activity levels in the slice cultures are insufficient to drive MEF2A/D transcriptional activity and synaptic depression, but elevations in postsynaptic activity can drive MEF2A/D transcriptional activity and suppress synaptic function. Surprisingly, *Mef2a/d* deletion did not block synaptic depression induced by chronic PPS. 6 hr of PPS in *Mef2a/d* deleted neurons induced only a trend towards a depressed EPSC (Figure 2.6B). Because *Mef2a/d* deletion was sufficient to block MRE-GFP expression with chronic PPS (Figure 2.3), these results suggest that other activity-dependent transcription mechanisms can mediate synaptic depression in response to chronic postsynaptic activity increases.

Brief Periods of Postsynaptic Bursting Functionally Silences Excitatory Synapses, whereas

Chronic Bursting Causes Synapse Elimination

Although brief and chronic PPS similarly depress excitatory synaptic function, they differentially require MEF2A/D. This result suggests that brief and chronic PPS may regulate distinct aspects of synapse structure or function. For example, chronic PPS eliminates functional and structural excitatory synapses in rat CA1 neurons. Brief PPS may not eliminate synapses structurally, but only “silence” them by selective depression of AMPA receptor (AMPA) mediated EPSCs (Atwood & Wojtowicz 1999). NMDA receptors colocalize with AMPARs at excitatory synapses and selective depression of AMPAR-mediated synaptic transmission can be detected by measuring the effects of PPS on evoked NMDA receptor (NMDAR) EPSCs and the ratio of AMPAR/NMDAR EPSCs. To do this, I performed paired recordings from ChR2-mCherry transfected and neighboring untransfected neurons 24 hr after the onset of PPS, measured evoked AMPAR EPSCs. In the same cell pairs I then measured pharmacologically isolates NMDAR EPSCs in the presence of the AMPAR blocker DNQX while voltage-clamping at +40mV (Figure 2.7A). Although brief PPS suppressed evoked AMPAR EPSCs, it had no effect on NMDAR EPSCs and thus resulted in a significantly decreased ratio of AMPAR/NMDAR EPSC amplitudes (Figure 2.7A). In contrast, chronic PPS similarly depressed both AMPAR and NMDAR-mediated EPSCs (Figure 2.7B) and did not alter the ratio of AMPAR/NMDAR EPSC. These results support the idea that brief PPS “silences” synapses by selectively suppressing AMPAR function, whereas chronic PPS depresses both AMPAR and NMDAR EPSCs consistent with the elimination of

excitatory synapses.

The differential effect of brief and chronic PPS on NMDAR EPSCs may represent progressive stages of activity-dependent excitatory synapse elimination. Brief PPS may selectively remove AMPARs and if PPS is continued, then the synapse is structurally disassembled. Alternatively, brief PPS may initially eliminate synapses, or at least suppress both AMPAR and NMDAR EPSCs, but NMDAR function recovers upon the cessation of postsynaptic bursting. To differentiate between these possibilities, I measured AMPAR and NMDAR EPSCs earlier, or 12 hrs, after the onset of a brief, 1 hour, PPS. Consistent with an initial silencing of AMPAR-function, brief PPS depressed AMPAR, but not NMDAR, EPSCs and decreased the ratio of AMPAR/NMDAR EPSC amplitudes measured 12 hr after brief PPS onset (Fig. 2.8). These results support the idea that brief PPS induces synapse silencing by selectively suppressing AMPAR function or number.

My measurements of synapse function suggest that chronic PPS eliminates structural synapses, whereas brief PPS only silences them functionally. To measure the effects of PPS on synapse structure, I co-expressed a myristoylated GFP (PA1-GFP) with ChR2-mCherry in CA1 neurons in slice culture to visualize dendritic spines, the structural correlate of excitatory synapses. Corresponding to my measurements of synapse function, chronic PPS reduced dendritic spine density on secondary apical dendrites, whereas brief PPS had no effect (Figure 2.9 A and B). As a control, chronic PPS of neurons transfected with GFP alone, without ChR2,

had no effect on dendritic spine number, indicating that the decreases in dendritic spine density were a result of Chr2-mediated activity increases (Figure 2.9C). Therefore, both structural and functional measures of excitatory synapses indicate that brief increases in postsynaptic firing initially silence excitatory synapses and if the activity increases persist, synapses are eliminated.

PPS-induced Synapse Silencing Requires Activation of L-type Voltage-Gated Ca²⁺ channels and *de novo* Transcription.

Brief PPS induces activation of the MEF2 transcriptional reporter and synapse silencing, which relies on MEF2A/D. These results suggest that postsynaptic bursting activates MEF2A/D which then stimulates transcription of specific targets which silence synapses. A major mechanism by which neuronal depolarization drives MEF2A/D-mediated transcriptional activation is by triggering Ca²⁺ influx through L-type voltage-gated Ca²⁺ channels (VGCC) (Flavell et al 2006). To determine if L-type VGCCs were required for MRE-GFP activation or synapse silencing in response to brief PPS, I treated slice cultures with nifedipine (20 μM) or vehicle before and during brief PPS. Under basal or unstimulated conditions, nifedipine had no effect on MRE-GFP expression in comparison to that observed in vehicle-treated sister cultures, but nifedipine prevented induction of MRE-GFP by brief PPS (Figure 5.10A and B). Importantly, nifedipine blocked depression of evoked EPSCs and mEPSC frequency in response to brief PPS without affecting expression of Chr2 (Figure

5.10C and D; Table 2.2). Together these results support a model where PPS-activates VGCCs and Ca^{2+} influx to stimulate MEF2A/D-dependent transcriptional activation and silence synapses.

To additionally test this model, I determined if *de novo* transcription during PPS is necessary for synapse silencing. Slice cultures were pretreated (1 hr) with one of two distinct inhibitors of transcription; actinomycin D (ActD; 1 μM) or 5,6-Dichloro-1-beta-D-ribofuranosylbenzimidazole (DRB; 160 μM). While vehicle-treated sister cultures displayed robust decreases in mEPSC frequency in response to brief PPS, this effect was blocked by DRB or ActD pretreatment (Fig. 5.11). mEPSC amplitudes were unchanged across all conditions. As expected, DRB also blocked MRE-GFP expression in response to brief PPS. These results indicate that *de novo* transcription is necessary for PPS-induced synapse silencing.

Brief Postsynaptic Burst Firing Selectively Activates MEF2-dependent *Arc* Transcription, which is Required for Synapse Silencing

My results indicate that MEF2A/D-regulated gene targets mediate activity-induced synapse silencing. To identify potential MEF2-regulated genes driven by brief PPS who may play a role in synapse silencing, I prepared primary dissociated hippocampal cultures from WT or *Mef2a/d^{fl/fl}* pups. To drive neurons with photostimulation, cultures were infected with lentivirus to express ChR2-YFP and Cre-mCherry. Sister control cultures expressed Cre.

Using this method, I was able to drive patterned firing of dissociated cultured neurons reliably with blue light using 3 Hz PPS. To assess potential MEF2A/D regulated genes that may play a role in synapse silencing, I harvested cultures (DIV14) at 1, 3, 6, or 12 hours after photostimulation onset and performed qPCR analysis (Figure 2.12).

I assayed potential MEF2A/D target genes, whose expression was shown to be induced by exogenous expression of a constitutively active MEF2 (MEF2-VP16) and/or tonic depolarization by high potassium (Flavell et al 2008): activity-regulated cytoskeletal-associated protein, or *Arc*, which is necessary for synapse elimination in response to MEF2VP16 (Wilkerson et al 2014) and stimulates AMPA receptor endocytosis (Chowdhury et al 2006, Shepherd et al 2006); Homer1a (*H1a*), which reduces AMPA/NMDA ratio when overexpressed and may play a role in AMPA receptor internalization (Rozov et al 2012); as well as Protocadherin 10 (*Pcdh10*), which is also necessary for MEF2-VP16 mediated synapse elimination and degradation of PSD-95 (Tsai et al 2012). As a control, I assayed Regulator of G-Protein Signaling 2 (*Rgs2*), a robust MEF2A/D driven target gene (Flavell et al 2008). Although these genes are strongly induced by either MEF2-VP16 or high KCl (Flavell et al 2008), only *Arc* was induced (~20 fold) by the patterned postsynaptic burst firing, observed at 3, 6 and 12 hr after PPS onset (Figure 2.12, n = 3-5 cultures). Although *H1a* level was elevated (~3-5 fold) at 3, 6 or 12 hr, this did not reach statistical significance (Figure 2.12A and C). To determine if PPS-induced *Arc* mRNA requires MEF2A/D, I

repeated experiments in *Mef2a/d^{fl/fl}* cultures. Lentivirus-mediated Cre-mCherry expression decreased *Mef2a/d* RNA levels by 99% at DIV14 (data not shown). *Mef2a/d* deletion abolished PPS-induced *Arc* expression at all time points assayed. Like WT neurons, PPS had no effect on *H1a* or *Rgs2* RNA levels in cultures with *Mef2a/d* deletion (Figure 2.12A). These results suggest physiological patterns of postsynaptic bursting, unlike MEF2-VP16 or tonic depolarization, selectively induce a subset of MEF2A/D target genes.

Since *Arc* is selectively induced by brief PPS, I hypothesized that *Arc* mediates PPS-induced synapse silencing. To test this idea, I examined synaptic depression in response to brief PPS in slice cultures prepared from *Arc* knockout mice. In support of my hypothesis, brief PPS failed to induce depression of AMPAR EPSCs or mEPSC frequency in *Arc* KO neurons in comparison to WT littermate controls (Figure 2.13A and B, Table S3). The deficit in activity-induced synapse silencing in *Arc* KO neurons could be due to a developmental or non-cell autonomous role for *Arc*. To determine if *Arc* plays an acute, cell autonomous and postsynaptic role in activity-dependent synapse silencing, I tested whether re-expression of *Arc* cDNA, together with ChR2, into *Arc* KO CA1 neurons rescued PPS-induced synaptic depression. *Arc* cDNA expression in unstimulated cultures, without PPS, had no effect on evoked EPSCs or mEPSCs (Figure 2.13C), indicating that expression of *Arc* alone is not sufficient to silence synapses. However, *Arc* cDNA expression in *Arc* KO neurons that received brief PPS rescued depression of evoked AMPAR EPSCs and mEPSC frequency

(Figure 2.13D). Together these results support a cell autonomous mechanism where postsynaptic bursts of activity activate a MEF2A/D-dependent induction of *Arc* which then functions to silence synapses onto that neuron.

Mef2a/d deletion blocks synaptic depression in response to brief, but not chronic (24 hr), PPS (Figure 2.5 and 2.6). Because MEF2A/D is necessary for PPS-induced *Arc* mRNA, this suggests that *Arc* may not be necessary for synaptic depression in response to chronic PPS. In support of this idea, chronic PPS induced depression of evoked EPSCs in *Arc* KO neurons, although the magnitude of the depression of EPSCs was less than observed in slice cultures from WT littermates (Figure 2.14A and C). However, chronic PPS failed to suppress mEPSC frequency in *Arc* KO neurons, indicating an essential role for *Arc* in suppression of mEPSCs in response to either brief or chronic PPS (Figure 2.14B). Thus, these suggest in response to chronic activity increases, there are MEF2A/D and *Arc*-independent mechanisms that can either compensate to mediate synapse elimination.

Discussion

From Indiscriminative Stimulation to Precise Cell Autonomous Stimulation

Earlier research on activity-dependent factors tended to use straightforward but overly strong approaches, like high potassium or glutamate to enhanced neuronal activity. However, these methods have disadvantages that limit their research potency. First, those methods strongly activate neurons, and it could activate multiple factors at the same time, including

factors that drive pathways lead to opposite phenotype, such that researchers might detect no net change in their interested phenotype. Second, these approaches globally affect the neuronal circuit, which might synchronize the whole circuit and compromise the competition between different synapse, which are critical in determining whether a synapse would persist or diminish (Wiegert & Oertner 2013, Winnubst et al 2015). On the contrary, in my study, I utilized optogenetics and biolistic method that overcomes some of these disadvantages. Optogenetics allows precise control of neuronal activity, and thus can address the concern raised by overactivation. Biolistic method transfects ChR2 and other desired constructs into a sparse population of neurons, and thus allows the study of cell autonomous effect without the concern of circuit global synchronization or synapse de-competition.

PPS-induced Physiologically Relevant Neuronal Activity

Despite optogenetics allows precise cell autonomous control of neuronal activity, there is another question to be answered: is the postsynaptic bursting firing introduced by PPS in my studies is really relevant to physiological activity? To address this question, the most direct strategy is to compare the postsynaptic burst firing induced by optogenetics and the postsynaptic burst firing observed *in vivo* or *ex vivo*.

Action potential firing is a feature that distinguishes neurons from many other cell types. Hippocampal neurons are commonly used to study synapse plasticity due to the

involvement of hippocampal neurons in critical neuronal functions that require prompt modification of synapses, such as spatial learning, memory and navigation (Bannerman et al 2014). Like other neurons, hippocampal pyramidal neurons fire. The firing property for hippocampal neurons has been addressed *in vivo* (Kandel & Spencer 1961); hippocampal pyramidal neurons can fire as single spikes or cluster of repetitive spikes (bursts).

The postsynaptic firing properties for developing hippocampal neurons have been characterized using two-photon imaging for calcium transients occurring in CA1 pyramidal neurons, and simultaneous current-clamp recording (Crepel et al 2007). At embryonic stage (E16 – 19), only a small portion (~20%) of neurons fired sporadic spikes with and little synchrony. At neonatal stage (p0 – p2), there were more neurons firing with sporadic and asynchronous spikes. Notably, around 20% of neurons fired with a persisting calcium plateau. Unlike neurons firing sporadic spikes, neurons firing persisting calcium plateau exhibited high synchrony between each other. At later postnatal stages (p6 – p10), a majority of neurons (65%) fired with bursts, and the timing between firing neurons were highly correlated.

The postsynaptic firing properties of pyramidal neurons during adulthood are somewhat different from what observed in the developing hippocampus. Adult hippocampal pyramidal neurons do not fire all the time. Instead, they are categorized into two populations: (1) place cells, neurons that fire when the animal steps in a specific direction within an environment, and (2) silent cells, neurons that only fire at low frequency no matter where the

animal goes within an environment (Ahmed & Mehta 2009). Notably, the discrepancy in firing rate between place cells and silent cells does not last forever, when the animal enters slow wave sleep, both place cells and silent cells behave similarly in terms of their firing rates (Thompson & Best 1989). Hence, whenever the animal switches from awake/rapid eye movement status to slow wave sleep, silent cells undergo an activity switch, and their neuronal firing rate increases from very low frequency to be equivalent with place cells (Thompson & Best 1989). Moreover, even during the awake state, silent cells can be transformed into place cells when the animal enters a novel environment (Epsztein et al 2011, Frank et al 2004). On the other hand, even if a neuron is a place cell, its firing rate is decreased in an environment without a place field, and increased drastically when the animal is in the place field (Thompson & Best 1989). Those electrophysiological features mark the capricious nature of hippocampal neuronal activity *in vivo*; hippocampal pyramidal can undergo natural changes in their firing frequency *in vivo*, and synapse plasticity mediated by increase or decrease in postsynaptic firing rate may take place here. In awake rat, CA1 and CA3 pyramidal neurons fire with bursts composed of multiple spikes (1 – 4 spikes for each burst) (Suzuki & Smith 1985), and electroencephalogram study show CA1 neurons fired at theta bursts (3-10 Hz) when the rat was exploring. (Lever et al 2010, Otto et al 1991).

In conclusion, PPS-induced postsynaptic burst firing resembles postsynaptic burst firing observed *in vivo* (Figure 2.15). Moreover, changes in postsynaptic burst firing

frequency also occurs *in vivo*, supporting the physiological relevance of PPS-induced postsynaptic burst firing utilized in my study.

Differential Activity Patterns Lead to Different Types of Synapse Depression

My research demonstrates that physiologically-relevant activity patterns by postsynaptic burst firing, drive synapse silencing or synapse elimination by selectively recruiting downstream factors such as L-type voltage gated calcium channels and MEF2A/D (Figure 2.16). Brief postsynaptic burst firing drives MEF2A/D-regulated gene expression, including *Arc*, which promotes synapse silencing; chronic postsynaptic burst firing fosters partially-*Arc* dependent synapse elimination that does not require MEF2A/D. Moreover, contrary to the gene expression profile induced by conventional neuronal activity-enhancing methods, such as tonic depolarization by high potassium or overexpression of constitutively active artificial transcription factors, physiologically-relevant neuronal postsynaptic burst firing selectively activates a subset of MEF2-regulated genes. Overall, I demonstrate that brief and chronic postsynaptic neuronal activity recruit distinct mechanisms to effect different forms of synapse depression.

Endogenous MEF2 and Activity-Driven Transcriptional Regulation

Brief postsynaptic burst firing drives MEF2-mediated synapse silencing, not elimination, which is unlike results from experiments using constitutively active MEF2-viral

activator fusion protein, MEF2-VP16 (Pfeiffer et al 2010, Tsai et al 2012, Wilkerson et al 2014). This phenotypic discrepancy indicates that endogenous MEF2 stimulated by physiological activity functions differently than the artificial MEF2-VP16 fusion protein. This may result from differences between endogenous MEF2 and MEF2-VP16. MEF2-VP16 was created by fusing the MADS/MEF2 domain from MEF2C gene with the viral transactivator VP16 (Black et al 1996); therefore, transactivation by MEF2-VP16 is achieved by VP16, rather than the natural transactivation domain from MEF2 genes. Differences in transactivation indicate recruitment of distinct co-factors, which might lead to differential transcriptional profiles that result in phenotypes not normally achieved by natural transcription factors.

Moreover, when endogenous MEF2 is activated by postsynaptic burst firing, the internal environment of the neuron is also altered by elevated activity, such that other events sensitive to electrophysiological change may also occur (e.g. the increased calcium influx can trigger calcium-mediated pathways) In contrast, MEF2-VP16-triggered gene transcription was studied when the neuron was still in under basal electrophysiological conditions. The difference in the cellular environment may thus contribute to differential transcriptional profiles and phenotypes. In fact, the transcriptional profile induced by PPS (Figure 2.12) is unlike the profile induced by MEF-VP16 expression or high extracellular potassium (Flavell et al 2008), further supporting the idea that endogenous MEF2 stimulated by physiological

activity results in transactivation that is different from that triggered by MEF2-VP16 or a less physiological activity condition.

Involvement of *Arc* in Brief PPS-Induced Synapse Silencing

Brain-wide *Arc* deletion blocked brief PPS-induced synapse depression, and this phenotype is rescued by cell autonomous expression of exogenous *Arc* (Figure 2.13), suggesting the postsynaptic role of *Arc* in mediating PPS-induced synapse depression. Interestingly, expression of *Arc* in *Arc* KO neurons did not affect basal transmission (Figure 2.13B), suggesting that *Arc* expression alone is not sufficient to induce synapse depression. And thus a question emerges: if *Arc* is actually the key factor that mediates PPS-induced synapse depression, why did *Arc* overexpression not affect synaptic transmission on its own?

One possible explanation is that despite *Arc*'s critical role in mediating synapse depression, it may require other activity-dependent effectors to work in synergy. PPS-induced MEF2 transactivation may also drive expression of other MEF2 transcripts, including targets associated with AMPA receptor trafficking, like *Syngap1* (Kim et al 2003). Moreover, PPS-induced postsynaptic burst firing may stimulate other activity-dependent effectors as well, such as CaMKs. Those MEF2 transcripts and effectors induced by PPS in parallel with *Arc* induction might be required to work together with *Arc* to achieve the synapse depression phenotype.

Another possibility is concerns the nature of the *Arc* expression plasmid I used. In the construct, *Arc* expression is driven by a CMV promoter with 4 copies of cAMP response elements in it regulatory. Evidence has shown that transcription activity driven by this kind of promoter can be further enhanced by depolarization in neurons (Wheeler & Cooper 2001). Hence, it is possible that the basal exogenous *Arc* expression level was insufficient to induce synapse depression, but with PPS, *Arc* expression was further enhanced to an extent that can elicit synapse depression. My findings raise another questions: why was the basal expression of exogenous *Arc* not sufficient to induce synapse depression? One reason could be because that the basal exogenous *Arc* expression level was simply not high enough to do so. However, it is also possible that exogenous *Arc* expression actually caused synapse depression in the first few days after transfection, but this acute effect was later compensated for by certain homeostatic mechanisms. Later, with application of PPS, the expression level of the exogenous *Arc* was further enhanced such that another round of synapse depression occurred and was observed in my experimental time window.

Implication of Partial *Arc*-Dependence in Chronic PPS-Induced Synapse Elimination

Arc deletion blocked chronic PPS-induced mEPSC frequency depression but only partially attenuated PPS-induced eEPSC amplitude depression (Figure 2.14). Supposedly, both eEPSC amplitude and mEPSC frequency are proportional to synapse number as long as

there is no difference in presynaptic release probability and individual synaptic strength; in this scenario, what accounts for the differential *Arc* dependence of mEPSC frequency and eEPSC amplitude?

When measuring mEPSCs, which represent the collection of all inputs onto the recorded neuron, I collected every signal received by the recorded neuron. In contrast, when recording eEPSCs, only a subset of synapses (approximately 6 – 10 synapses, based on the ratio of eEPSC amplitude over mEPSC amplitude, which represents the size of response caused by single synapse activation) (Table 2.1) were activated and their responses recorded. Thus eEPSCs represent responses elicited by a subset of inputs onto the recorded neuron. Moreover, during the eEPSC recording, stimulations were made within the range of 50 μ m from the neuronal soma, indicating that eEPSC recordings are a collection of more proximal inputs.

In other words, the differential *Arc* dependence of mEPSC frequency and eEPSC amplitude may imply a differential impact of *Arc* deletion on global synapses and proximal synapses. Proximal synapse depression might be less dependent on *Arc* such that chronic PPS-induced eEPSC amplitude depression was only blunted by *Arc* deletion, but globally, depression of most synapses still require *Arc* and thus PPS-induced mEPSC frequency depression was blocked by *Arc* deletion. What can explain the possible differential *Arc* dependence of proximal synapses and global synapses? I speculate it might be due to the

trafficking ability of *Arc*; *Arc* might be more readily trafficked to distal synapses and regulate their depression. Other synapse depression effectors with poorer trafficking ability may stay around the soma (calcineurin could be one of the candidates (Sun et al 2010)), and mediate proximal synapse depression without impacting distal synapses. Consequently, without *Arc*, proximal synapses might still utilize local depression machinery, while distal synapses would have difficulty accessing the depression machinery.

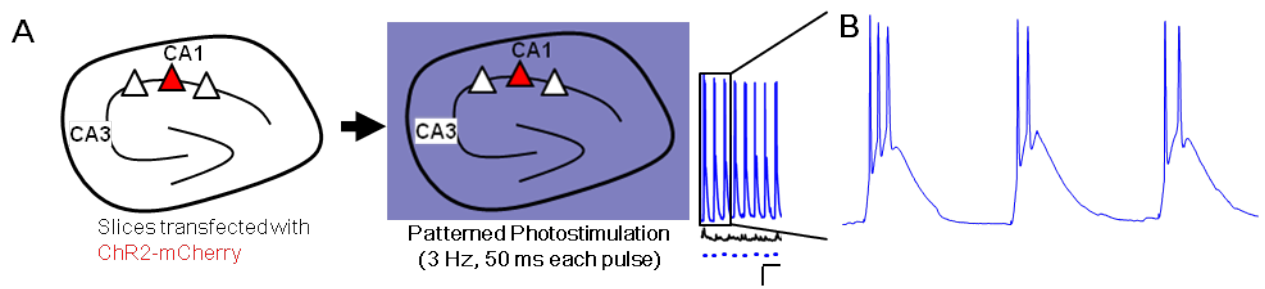


Figure 2. 1 PPS induced patterned firing activity on neurons transfected with Channelrhodopsin

A. Organotypic hippocampal slices were prepared from wild-type (WT) mice and biolistically transfected with ChR2H134R-mCherry. Blue trace represents response in a transfected neuron during PPS, and black trace represents simultaneous response in a neighboring untransfected neuron. Blue bars represent the 50 ms blue light pulses. Scale bar is 500 ms/ 10 mV. **B.** Zoomed-in view of the first 3 bursts (indicated by the black rectangle in A).

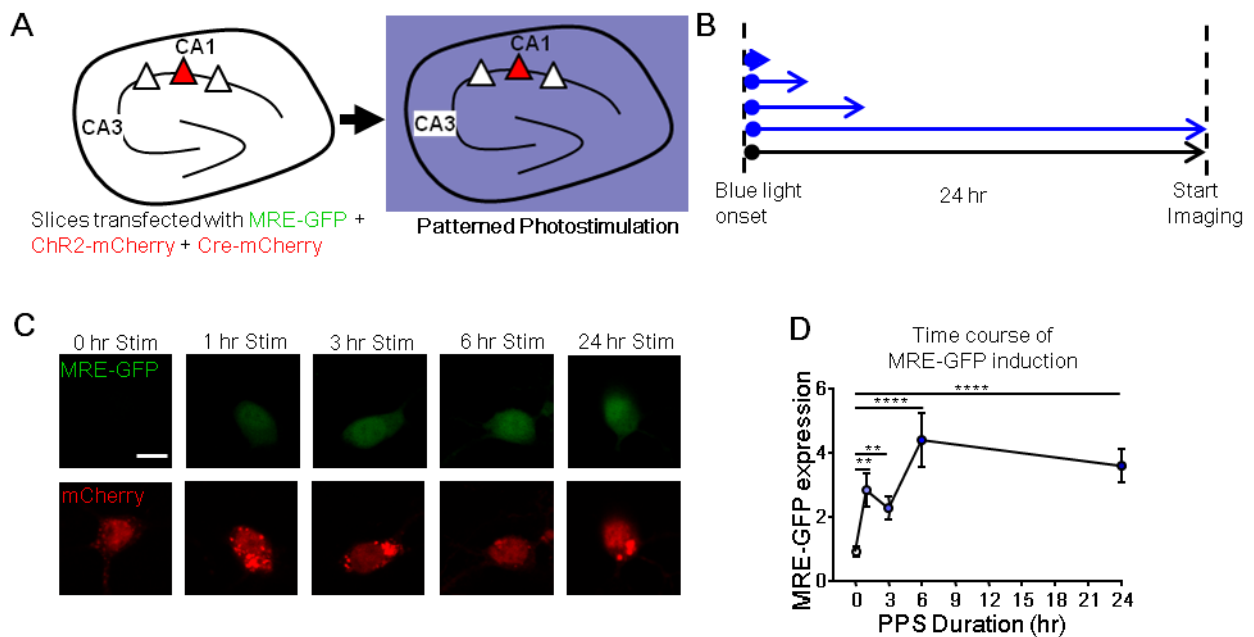


Figure 2. 2 Postsynaptic burst firing induces MEF2-dependent transcriptional activity

A. Experimental paradigm. Organotypic hippocampal slices were prepared from wild-type (WT) or *Mef2a^{fl/fl}/d^{fl/fl}* mice and biolistically transfected with MRE-GFP, ChR2H134R-mCherry and cre-mCherry. **B.** Illustration of time course of PPS, 0 hour, 1 hour, 3 hour, 6 hour, and 24 hour. Lengths of arrows represents the duration of blue light flashing; round heads represent the time point where blue light began to flash and arrow heads indicate the time point where blue light stopped flashing. WT slices were treated with PPS for indicated lengths followed by incubation without exposure to blue light until 24 hour has passed after blue light onset. **C.** Representative images of neurons from WT slices treated with PPS of conditions indicated in B. **D.** Group data of normalized MRE-GFP expression in C. Statistic: One-way ANOVA followed by multiple comparison between all groups using Dunn's test. N = 26 ~ 52 cells.

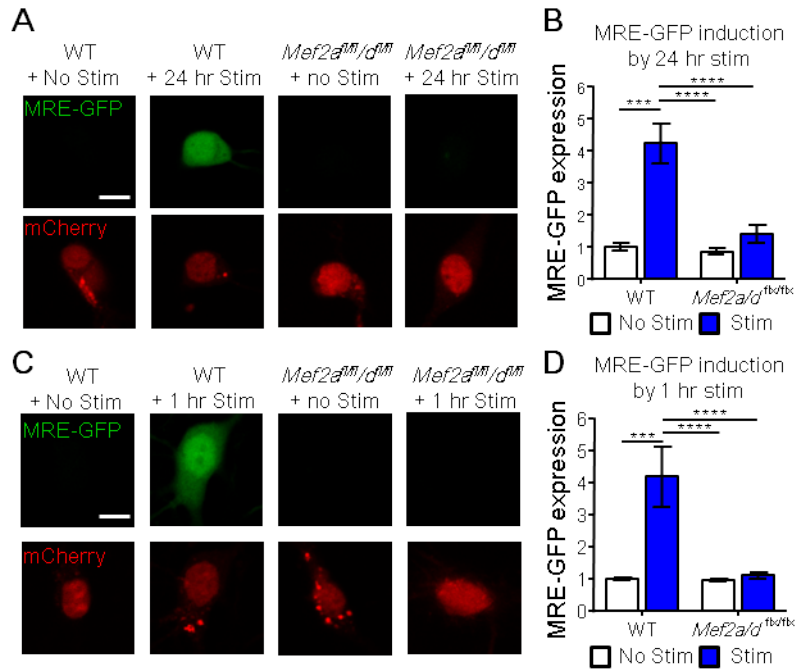


Figure 2. 3 Postsynaptic burst firing-induced MEF2-dependent transcription is blocked by cell autonomous *Mef2a/d* deletion

A. Representative images for MRE-GFP expression induced by 24 hour PPS in WT or *Mef2a^{fl/fl}/d^{fl/fl}* neurons. Scale bar is 10 μ m. **B.** Group data of normalized MRE-GFP expression in A. Statistic: two-way ANOVA followed by multiple comparisons between all groups using Tukey's test. N = 19 ~ 48 cells. **C.** Representative images for MRE-GFP expression induced by 1 hour PPS in WT or *MEF2A^{fl/fl}/D^{fl/fl}* neurons. Scale bar is 10 μ m. **D.** Group data of normalized MRE-GFP expression in A. Statistic: two-way ANOVA followed by multiple comparison between all groups using Tukey's test. N = 20 ~ 24 cells.

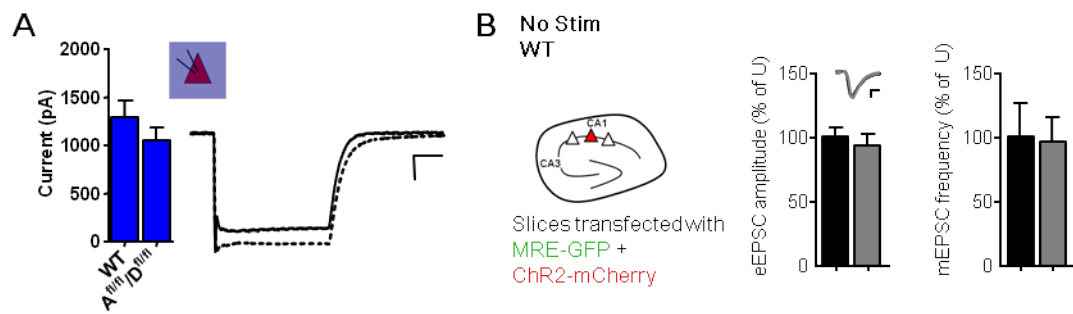


Figure 2. 4 ChR2H134R expression is not altered by the genotype of transfected cell and does not change basal neuronal transmission.

A. A single pulse of blue light (470 nm) was applied to a neuron transfected with ChR2H134R. Blue light-induced current was recorded in WT (solid trace) or *Mef2a^{fl/fl}/d^{fl/fl}* slices (dashed trace). Scale bar is 50 ms/ 200 pA. **B.** Left panel: experimental diagram. WT slices were biolistically transfected with ChR2H134R-mCherry and MRE-GFP, without photostimulation. Middle panel: eEPSC from neighboring untransfected (black bar) and transfected (grey bar) neurons via dual simultaneous whole-cell patch-clamp. Inset: Representative eEPSC from untransfected (black) and transfected (grey) neurons. Stimulation artifact was removed from the trace for clarity. Scale bar is 10 ms/20 pA. Right panel: mEPSC from neighboring untransfected and transfected neurons. Statistic for A: unpaired t-test, N = 15 ~ 16 cells. Statistic for B: paired t-test, N = 12 ~ 19 cell pairs.

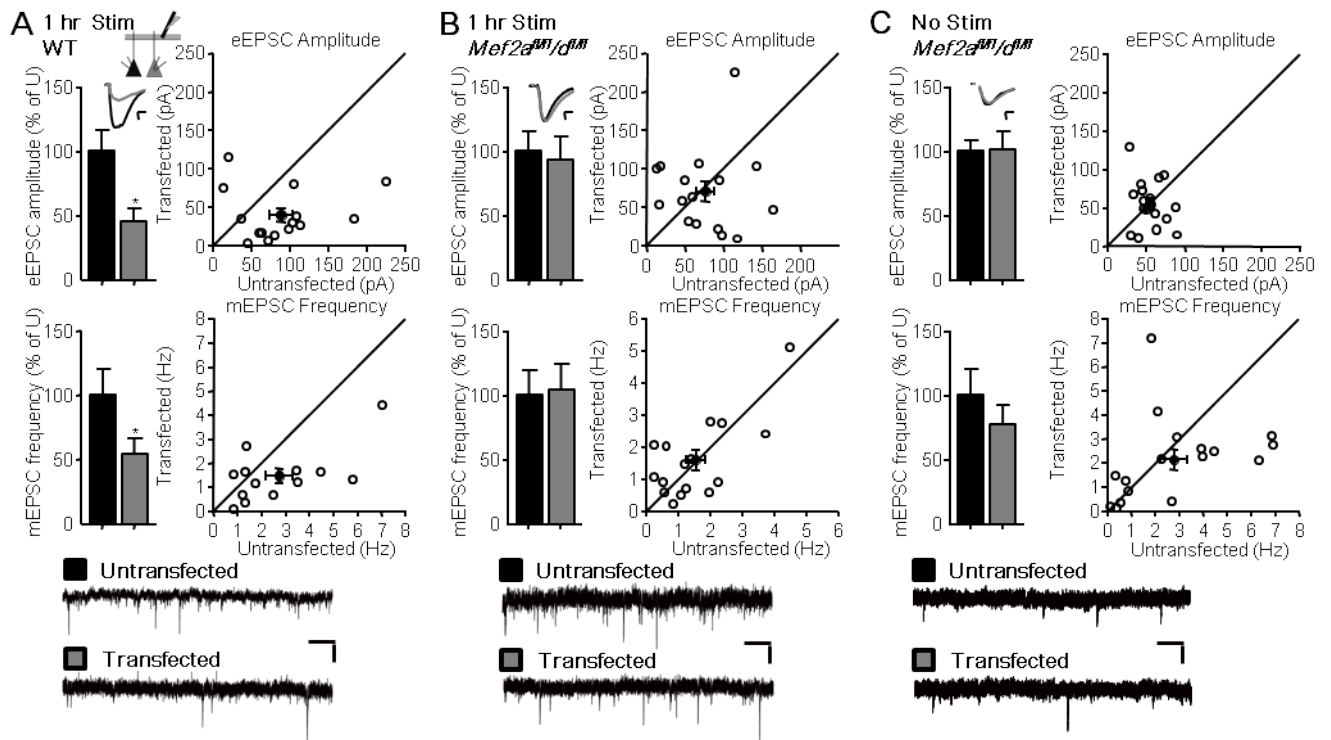


Figure 2. 5 Brief postsynaptic burst firing activates MEF2-dependent synapse depression

A. Electrophysiological recordings from WT slices biolistically transfected with Chr2H134R-mCherry, cre-mCherry, and MRE-GFP and treated with 1 hour PPS. eEPSCs and mEPSCs were obtained from neighboring untransfected (black bar) and transfected (grey bar) neurons via dual simultaneous whole-cell patch-clamp. Both eEPSC and mEPSC responses are presented as the percentage of average response in untransfected neurons (% of U). Scatter plot of all data pairs is shown in the right column. Inset: Representative eEPSCs from untransfected (black) and transfected (grey) neurons. Stimulation artifact was removed from the trace for clarity. Bottom: Representative mEPSCs. Scale bar for eEPSC is 10 ms/20 pA and for mEPSC is 500 ms/10 pA. **B.** The same as A, except recordings were acquired from *Mef2a^{fl/fl}* slices. **C.** The same as D, except no PPS was applied. Statistic: paired t-test. N =15 -19 cell pairs.

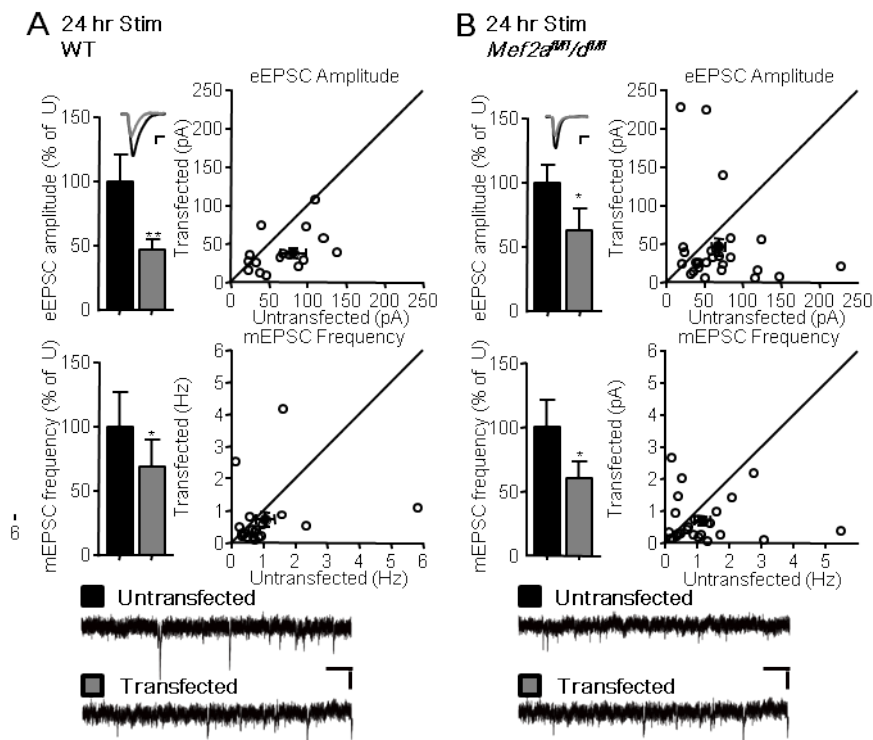


Figure 2. 6 Chronic postsynaptic burst firing induces synapse depression that does not rely on cell autonomous MEF2A and MEF2D

A. Electrophysiological recordings from WT slices biolistically transfected with ChR2H134R-mCherry, cre-mCherry, and MRE-GFP and treated with 24 hour PPS. eEPSCs and mEPSCs were obtained from neighboring untransfected (black bar) and transfected (grey bar) neurons via dual simultaneous whole-cell patch-clamp. Both eEPSC and mEPSC responses are presented as the percentage of average response in untransfected neurons (% of U). Scatter plot of all data pairs is shown in the right column. Inset: Representative eEPSCs from untransfected (black) and transfected (grey) neurons. Stimulation artifact was removed from the trace for clarity. Bottom: Representative mEPSCs. Scale bar for eEPSC is 10 ms/20 pA and for mEPSC is 500 ms/10 pA. **B.** The same as A, except recordings were acquired from *Mef2a^{fl/fl}/d^{fl/fl}* slices. Statistic: paired t-test. N =17 -24 cell pairs.

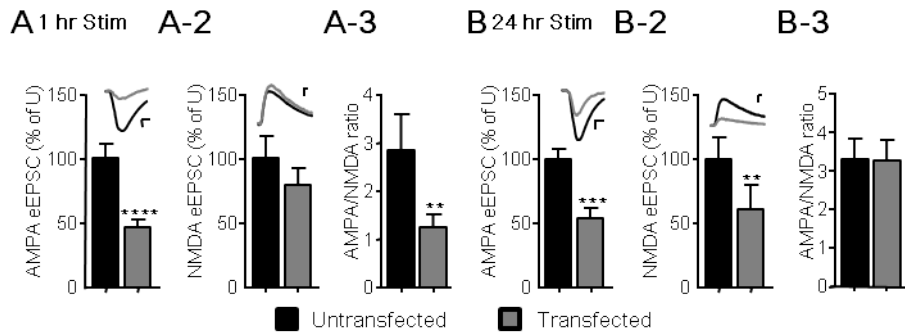


Figure 2. 7 Brief activity induce synapse silencing rather than synapse elimination

A. Electrophysiological recordings from WT slices treated with 1 hour PPS. AMPA eEPSCs were recorded at a holding potential of -60 mV. Responses are presented as the percentage of average response in untransfected neurons (% of U). Inset: Representative traces for AMPA eEPSCs. Scale bar is 10ms/ 20 pA. **A-2.** Pharmacologically isolated NMDA eEPSCs were recorded at holding potential of +40 mV in the presence of DNQX and glycine after the acquisition of AMPA eEPSCs in A. Inset: Representative traces for NMDA eEPSCs. Scale bar is 10ms/ 20 pA. **A-3.** The ratio of AMPA/NMDA eEPSC amplitude from A and A-2. **B, B-2, B-3.** The same as A and A-2, except 24 hour PPS was used to treat slices. Statistic: paired t-test. N = 13 ~ 30 cell pairs.

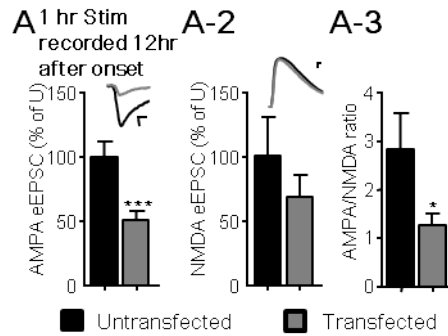


Figure 2. 8 Synapse depression generated by brief postsynaptic burst firing are caused by synapse silencing rather than partial recovery of eliminated synapses

A. Electrophysiological recordings from WT slices treated with 1 hour PPS. Recording was done 12-16 hour after the onset of photostimulation. AMPA eEPSCs were recorded at holding potential of -60 mV. Responses are presented as the percentage of average response in untransfected neurons (% of U). Inset: Representative traces for AMPA eEPSCs. Scale bar is 10ms/ 20 pA. **A-2.** Pharmacologically isolated NMDA eEPSCs were recorded at holding potential of +40 mV in the presence of DNQX and glycine after the acquisition of AMPA eEPSCs in A. Inset: Representative traces for NMDA eEPSCs. Scale bar is 10ms/ 20 pA. **A-3.** The ratio of AMPA/NMDA eEPSC amplitude from A and A-2. Statistic: paired t-test. N = 17 cell pairs.

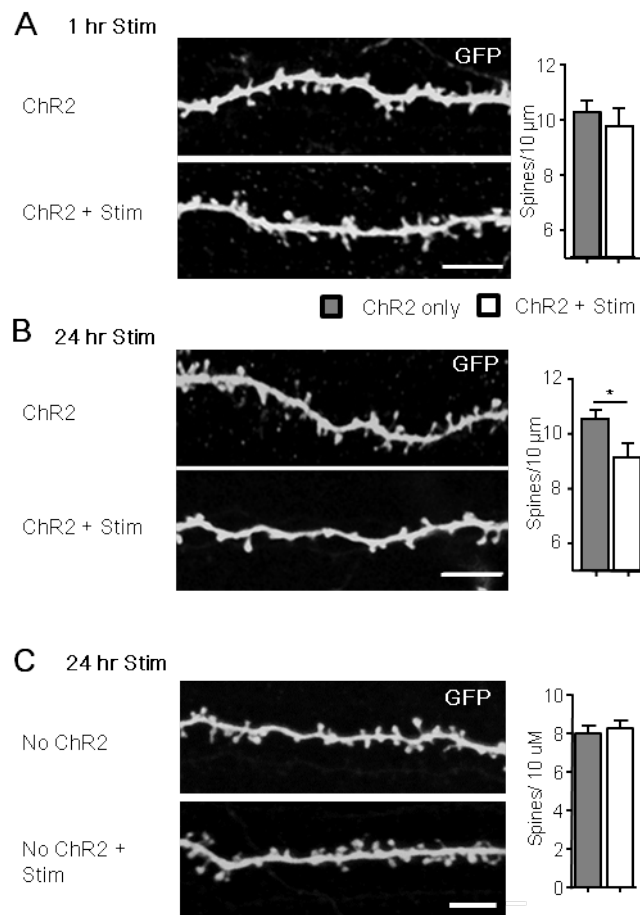


Figure 2.9 Dendritic spine elimination is observed in response to chronic, but not brief, postsynaptic burst firing

A. Slices were transfected with PA1-GFP in addition to ChR2H134R and treated with 1 hour PPS, followed by confocal imaging of secondary apical dendrites. Dendritic spine structure was analyzed and dendritic spine density was quantified. Grey bar: neurons without PPS. White bar: neurons with 1 hour PPS. Representative image for each condition are shown in left. Scale bar is 5 μ m. **B.** The same as D, except slices were treated with 24 hr PPS instead. **C.** Slices were transfected with PA1-GFP in the absence of ChR2H134R and treated with 24 hour PPS, followed by confocal imaging of secondary apical dendrites. Statistic: unpaired t-test. N = 13 ~ 20 cells.

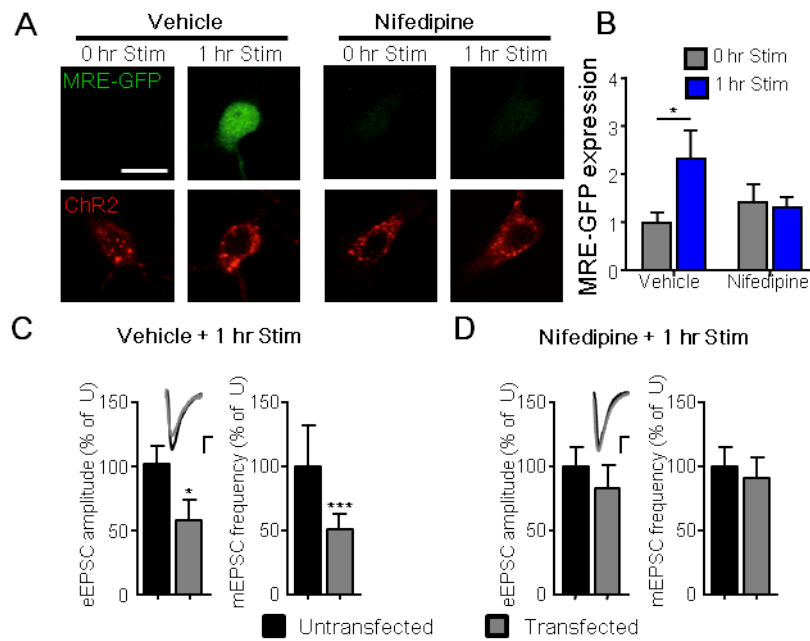


Figure 2. 10 Brief postsynaptic burst firing-induced activation of MEF2-dependent transcription and synapse depression require L-type voltage-gated calcium channel activity

A. Representative images of MRE-GFP expression induced by 1 hour PPS, in the presence of vehicle (0.1% DMSO) or L-type voltage-gated calcium channel antagonist, nifedipine (20 μ M). Scale bar is 10 μ m. **B.** Group data of **A**. Statistic: two-way ANOVA with Tukey's multiple comparisons. N = 15 ~ 27 cells. **C, D.** Electrophysiological recordings were obtained from WT slices transfected with ChR2H134R-mCherry as well as MRE-GFP, and treated with 1 hour PPS in the presence of **C.** vehicle (0.1% DMSO) or **D.** nifedipine (20 μ M). Statistic: paired t-test. N = 12 ~ 19 cell pairs.

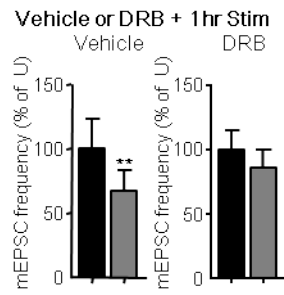


Figure 2. 11 Brief postsynaptic burst firing-induced synapse depression requires *de novo* transcription

Electrophysiological recordings were obtained from WT slices transfected with ChR2H134R-mCherry as well as MRE-GFP, and treated with 1 hour PPS in the presence of vehicle (0.2% DMSO) (left panel) or DRB (160 μ M) (right panel). Statistic: paired t-test. N = 14 ~ 16 cell pairs.

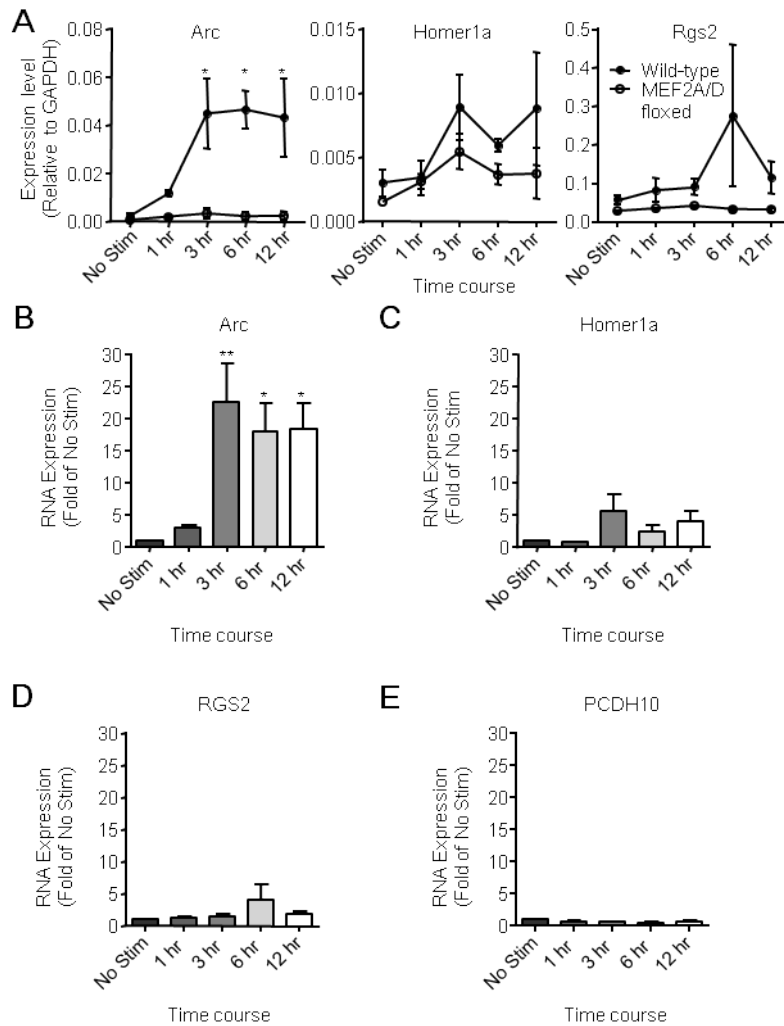


Figure 2. 12 Brief postsynaptic burst firing specifically activates MEF2-dependent *Arc* expression

A. Time course of qPCR results from extracts of dissociated primary cultures prepared from WT (closed circle) or *Mef2A^{fl/fl}/D^{fl/fl}* (open circle) neonatal mice. Cultures were transfected with cre and ChR2 using lentivirus method, and subjected to 1 hour PPS followed by incubation without exposure to blue light until 1, 3, 6, or 12 hour after stimulation onset. Expression profile for *Arc* (left panel), *Homer1a* (middle) and *RGS2* (right) are shown. Statistic: 2-way ANOVA followed by multiple comparison of RNA expression level between the two genotypes at each time point using Sidak's test. **B, C, D, E** Data is from A, but RNA expression for each gene from WT cultures only is plotted as fold of RNA expression level in each control group. The expression level of **B. Arc C. Homer1a D. RGS2 E. PCDH10** at each time course point was normalized to the group without PPS. Statistic: one-way ANOVA test followed by multiple comparison of the RNA expression level of each group undergoing photostimulation to the RNA expression level of the control group without photostimulation using Dunnett's test. N = 3 ~ 5 independent culture.

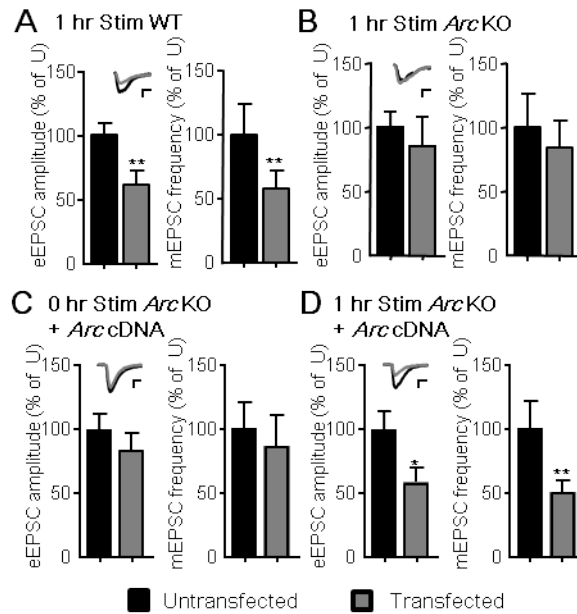


Figure 2. 13 Activity-driven expression of *Arc* is required for brief postsynaptic burst firing induced synapse depression

A, B. Slices were prepared from littermates of **A.** WT or **B.** *Arc* knockout mice, transfected with Chr2H134R-mCherry as well as *Arc* cDNA, and then subjected to 1 hour PPS, followed by electrophysiological assay. eEPSC and mEPSC responses are presented as the percentage of average response in untransfected neurons (% of U). **C.** The same as B, except *Arc* cDNA was included during transfection and no PPS was applied. **D.** The same as C, except 1 hour PPS was applied. Insets: Representative traces for eEPSC; scale bar = 10 ms/20 pA. Statistic: paired t-test. N = 11 ~ 16 cell pairs.

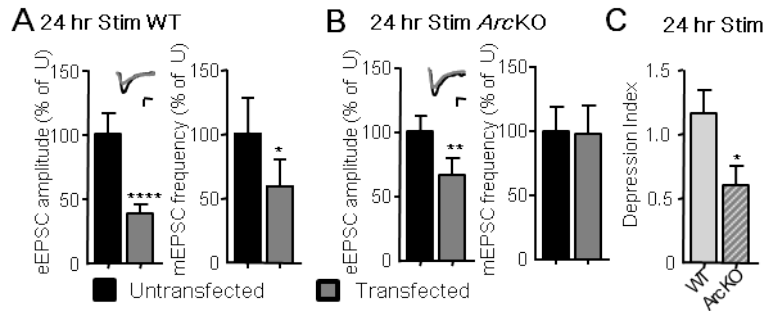


Figure 2. 14 Chronic postsynaptic burst firing-induced synapse depression exhibits partial *Arc* dependence

A, B. Slices were prepared from littermates of **A.** WT or **B.** *Arc* knockout mice, transfected with Chr2H134R-mCherry as well as *Arc* cDNA, and then subjected to 24 hour PPS, followed by electrophysiological assay. eEPSC and mEPSC responses are presented as the percentage of average response in untransfected neurons (% of U). Insets: Representative traces for eEPSC; scale bar = 10 ms/20 pA. Statistic: paired t-test. N = 13 ~ 22 cell pairs. **C.** Depression index of transfected neurons recorded in A and B. Statistic: unpaired t-test.

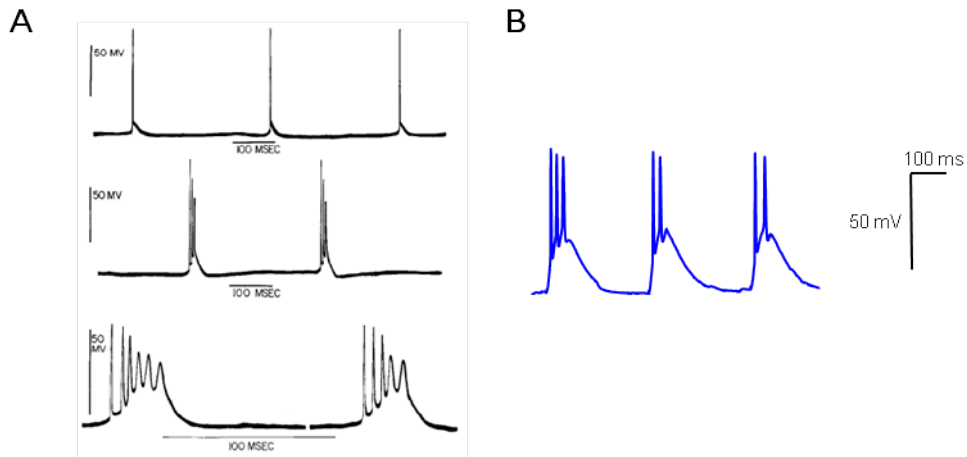


Figure 2. 15 Comparison of postsynaptic burst firing observed *in vivo* and induced *ex vivo* by PPS

A. Intracellular recording from cat hippocampal pyramidal neuron. Pictures are excerpted from Kandel et al's work (Kandel & Spencer 1961). **B.** Postsynaptic burst firing induced by PPS in organotypic hippocampal slice culture transfected with ChR2H134R-mCherry.

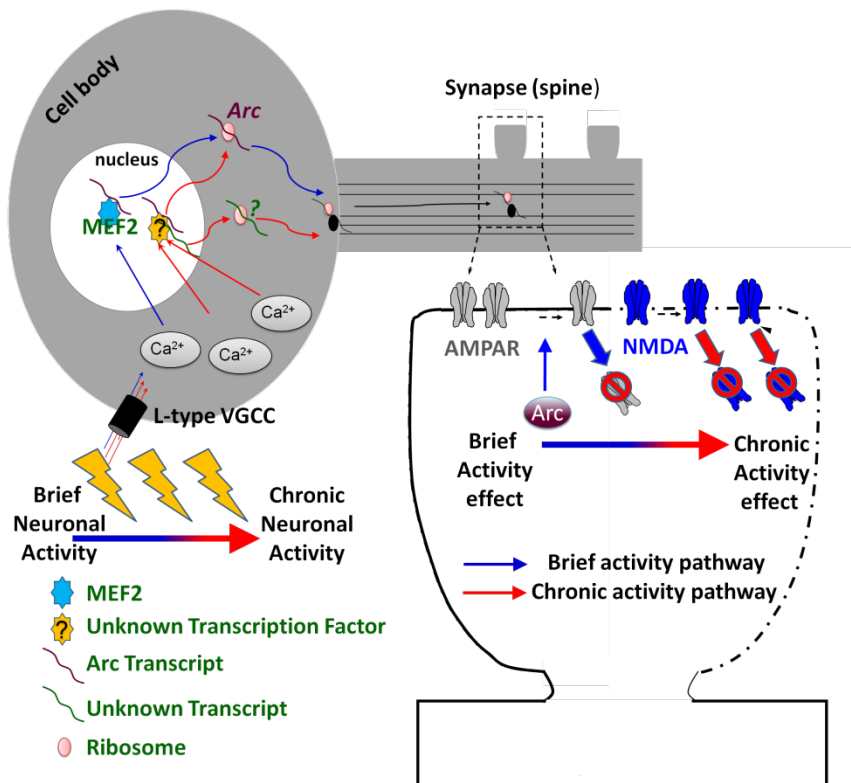


Figure 2. 16 Model of postsynaptic burst firing-induced synapse plasticity

Elevation of postsynaptic neuronal activity by PPS-induced postsynaptic burst firing promotes calcium influx via L-voltage-gated calcium channel. Accumulation of intracellular calcium activates calcium sensitive transcriptional factors, like MEF2, and with persistence calcium influx, more kinds of transcriptional factors will be activated. When the neuronal activity is briefly elevated, MEF2 transcriptional activity will be activated to induce AMPA receptor internalization-associated factors such as *Arc*, and in turn drive synapse silencing. When the neuronal activity is chronically elevated, other transcriptional factors will be recruited to activate more downstream factors, resulting in synapse elimination.

Table 2. 1 Raw electrophysiological measurements in untransfected (U) or transfected (T) hippocampal CA1 neurons in from WT and *Mef2a/d^{fl/fl}* mice

		Evoked EPSC (pA)	PPF (S2/S1)	mEPSC Amp (pA)	mEPSC Freq (Hz)	R _n (MΩ)	V _m [#] (mV)	I _{LED} (pA)
0 hr Stim								
<i>WT</i>	U	42±9 (12)	1.15±0.08 (12)	12±0.6 (19)	2.01±0.53 (19)	520±63 (19)	-61±0.9 (19)	
	T	40±4	1.22±0.08	13±0.8	1.92±0.38	409±46** ² p=0.0095	-58±1.3* ² p=0.0483	
<i>MEF2A/D flx/flx (no ChR2)</i>	U	55±5 (17)	1.49 ±0.10 (14)	12±0.6 (17)	2.8±0.6 (17)	417±29 (17)	-58±1.6 (17)	
	T	56±8	1.22±0.09* ¹ p=0.0125	12±0.9	2.2±0.4	342±30	-57±1.4	
1 hr Stim								
<i>WT</i>	U	88±15 (15)	1.46±0.14 (14)	15±1.3 (13)	2.72±0.56 (13)	160±23 (15)	-59±1.0 (15)	1300±173 (15)
	T	40±8* ¹ p=0.0121	1.22±0.09	13±1.0	1.48±0.31* ² p=0.0215	192±32	-54±1.8* ¹ p=0.0241	
<i>MEF2A/D flx/flx</i>	U	76±11 (16)	1.44 ±0.10 (13)	12±1.2 (16)	1.5±0.3 (16)	167±21 (16)	-59±1.0 (16)	1060±128 (16)
	T	71±13	1.31±0.06	12±0.9	1.6±0.3	148±20	-55±1.0 ¹ p=0.0061	
6 hr Stim								
<i>WT</i>	U	61±8 (18)	1.39±0.08 (17)	11±0.7 (18)	0.93±0.12 (18)	352±33 (18)	-58±1.1 (18)	
	T	40±5* ² p=0.0385	1.44±0.07	11±0.5	0.61±0.14** ² p=0.009	243±23* ¹ p=0.013	-54±1.4* ¹ p=0.0396	
<i>MEF2A/D flx/flx</i>	U	76±11 (20)	1.39 ±0.08 (19)	15±1.2 (19)	0.86±0.23 (19)	163±15 (23)	-60±1.3 (23)	
	T	48±10	1.31±0.08	14±1.6	0.93±0.24	196±16	-51±1.2** * ² p<0.0001	
24 hr Stim								
<i>WT</i>	U	82±17	1.39±0.12	14±1.1	1.07±0.29	209±14	-55±1.0	

		(17)	(16)	(19)	(19)	(17)	(17)	
	T	38±6**	1.37±0.08	13±1.1	0.73±0.23*	224±29	-54±1.6	
		² p=0.0032			² p=0.0446			
<i>MEF2A/D</i>	U	76±11	1.45 ±0.12	14±0.8	1.3±0.32	246±28	-57±1.4	
	<i>flx/flx</i>	(24)	(22)	(20)	(20)	(24)	(24)	
	T	48±12	1.32±0.11	12±0.8	0.81±0.19	240±28	-51±1.7	
					² p=0.0491		¹ p=0.0023	

#not corrected for junction potential; data are presented as mean±SEM; *p<0.05, **p<0.01,

***p<0.001, ¹paired t-test (Gaussian distribution) or ²Wilcoxon matched-pairs signed rank test (non

Gaussian distribution); number of cell pairs indicated in parentheses

Table 2. 2 Raw electrophysiological measurements in untransfected (U) or transfected (T) hippocampal CA1 neurons in OHSC treated with vehicle or nifedipine

	Evoked EPSC (pA)	PPF (S2/S1)	mEPSC Amp (pA)	mEPSC Freq (Hz)	R _n (MΩ)	V _m [#] (mV)	I _{LED} (pA)
Wildtype							
<i>1hr Stim-Nifedipine</i>							
Vehicle (DMSO)	U 49±8 (12)	1.2±0.2 (7)	15±0.7 (16)	1.4±0.5 (16)	183±13 (21)	-55±1 (21)	
	T 29±8* ² p=0.0342	1.3±0.2	12±0.4*** ¹ p=0.0005	0.73±0.2*** ² p=0.0002	171±11	-52±1	997±122 (21)
20μM Nifedipine	U 53±8 (14)	1.1 ±0.2 (12)	14±0.6 (19)	1.1±0.2 (19)	178±8 (23)	-53±1 (23)	
	T 44±9	0.99±0.1	12±0.4* ¹ p=0.0165	0.98±0.2	184±11	-51±0.9	910±46 (23)

[#]not corrected for junction potential; data are presented as mean±SEM; *p<0.05, **p<0.01, ***p<0.001, ¹paired t-test (Gaussian distribution) or ²Wilcoxon matched-pairs signed rank test (non Gaussian distribution); number of cell pairs indicated in parentheses

Table 2. 3 Raw electrophysiological measurements in untransfected (U) or transfected (T) hippocampal CA1 neurons from WT or *Arc* KO mice

	Evoked EPSC (pA)	PPF (S2/S1)	mEPSC Amp (pA)	mEPSC Freq (Hz)	R _n (MΩ)	V _m [#] (mV)	I _{LED} (pA)
1hr PPS							
WT	U 50±5 (17)	1.3±0.1 (15)	15±0.6 (16)	1.3±0.3 (16)	174±10 (25)	-55±1 (25)	
	T 31±5** ² p=0.0034	1.5±0.1	14±0.6	0.76±0.2** ² p=0.0027	187±10* ² p=0.0313	-52±1	789±110 (21)
<i>Arc</i> KO	U 38±5 (16)	1.5 ±0.2 (11)	15±0.6 (15)	1.2±0.3 (15)	181±11 (24)	-55±1 (24)	
	T 33±9	1.6±0.2	14±0.7	0.98±0.2	184±15	-53±1	748±119 (19)
24hr PPS							
WT	U 57±7 (23)	1.2 ±0.1 (13)	16±1 (18)	1.9±0.5 (17)	194±10 (34)	-56±0.8 (34)	
	T 22±10*** ² p<0.0001	1.2±0.2	14±0.8	1.1±0.4* ² p=0.0348	170±12	-54±1	674±82 (33)
<i>Arc</i> KO	U 51±6 (24)	1.4±0.1 (15)	15±0.6 (22)	0.99±0.2 (22)	183±9 (39)	-56±0.7 (39)	
	T 34±7** ² p=0.0039	1.4±0.2	14±0.7	0.97±0.2	193±8	-54±0.8	586±53 (37)

[#]not corrected for junction potential; data are presented as mean±SEM; *p<0.05, **p<0.01,

***p<0.001, ¹paired t-test (Gaussian distribution) or ²Wilcoxon matched-pairs signed rank test (non Gaussian distribution); number of cell pairs indicated in parentheses

CHAPTER THREE

***BRG1* IS INVOLVED IN FUNCTIONAL EXCITATORY SYNAPSE DEVELOPMENT**

Introduction

Myocyte enhancer factor 2 (MEF2) family activity-responsive transcription factors are implicated in ASD and reported being important for neural development and synaptogenesis. Deletion of MEF2 family members in mouse brains increases synapse numbers and dendritic spines in both cortical and hippocampal neurons (Flavell et al 2006, Harrington et al 2016), which may account for the learning and memory defects and autistic phenotypes observed. Conversely, expression of an MEF2-VP16 constitutively active protein causes synapse elimination. At the molecular level, MEF2 interacts with several transcription cofactors, and calcium signaling-induced switch of MEF2-associated cofactors from the corepressor complex to coactivator complex is crucial for MEF2 transcription activities. However, it is unclear how these cofactors coordinate with MEF2 to activate gene expression in response to neuronal activities.

Many autism risk genes encode transcription factors and epigenetic regulators, which likely function to regulate the expression of synaptic genes. A gene network analysis predicted the core subunit of a SWI/SNF-like BRG1-associated factor (BAF) ATP-dependent chromatin remodeling complex, Brg1/SmarcA4, as one of the key nodes in autism pathogenesis. BAF complexes containing the ATPase Brg1 or Brm use energy derived from ATP hydrolysis to modulate chromatin structures and regulate transcription. Mutations in

several BAF subunits are the genetic causes of Coffin-Siris syndrome and Nicolaides-Baraitser syndrome with autistic symptoms such as intellectual disability and delayed speech. In addition, de novo functional mutations of genes encoding several BAF subunits are identified repeatedly in autism patients. Mutations in a gene encoding the BAF-associated protein activity-dependent neuroprotective protein have been identified in 1.3% of autism patients, the most frequent of all autism risk-associated mutations identified so far. These data suggest that BAF complexes function in normal neural development and that mutations cause autistic disorders. Previously, I identified a neuron-specific BAF complex (nBAF) that regulates neuronal gene expression and is required for neural development. The BAF53b subunit of nBAF complexes is required for activity-dependent dendrite growth and learning and memory. However, the functions of nBAF complexes in synapse development and in ASD remain unknown. Neuronal activity regulates the expression of many ASD-associated genes and is critical in synapse maturation and plasticity. Neuronal activity, which triggers Ca²⁺ influx, initiates multiple signaling pathways that transduce the signals into the nucleus to affect gene transcription (Zhang et al 2016).

Brg1 is a chromatin remodeling factor implicated in several developmental neurological defects and autistic symptoms (De Rubeis et al 2014) and potentially associated with MEF2. My colleagues and I speculated that Brg1 may be a key regulator of synapse regulation. To address my speculation, I biolistically transfected cre into organotypic slices

prepared from mice with homozygous floxed *Brg1* allele (*Brg1^{fl/fl}*), and performed simultaneous dual whole cell recording of transfected and neighboring untransfected neurons. In recording miniature excitatory postsynaptic currents (mEPSCs) to examine whether cell-autonomous *Brg1* deletion has an impact on electrophysiological properties, I observed a reduction in mEPSC frequency in *Brg1*-deleted neurons, suggesting that Brg1 has a role in synapse formation or persistence.

Materials and methods

Animals

Mice with homozygous floxed *Brg1* allele (*Brg1^{fl/fl}*) were obtained from Dr. Jiang Wu's laboratory (Zhang et al 2016).

Hippocampal Slice Cultures and Transfection

Organotypic hippocampal slice cultures were prepared from postnatal day (P) 6-7 WT or *Brg1^{fl/fl}* mice. Cultures were biolistically transfected at 3 DIV with cre-mCherry. Biolistic transfection and gold bullet preparation were performed with the Helios Gene Gun system (BioRad) according to the manufacturer's protocols (McAllister, 2004). Slices were subjected to electrophysiology analysis 10-12 days after transfection.

Electrophysiology:

Simultaneous whole-cell recordings were obtained from CA1 pyramidal neurons in slice cultures visualized using IR-DIC and mCherry fluorescence to identify transfected and non-transfected neurons. Recordings were made at 32°C in a submersion chamber perfused with artificial cerebrospinal fluid (ACSF) containing (in mM): 119 NaCl, 2.5 KCl, 26 NaHCO₃, 1 NaH₂PO₄, 11 D-Glucose, 3 CaCl₂, 2 MgCl₂, 0.1 picrotoxin, 0.002 2-chloro-adenosine; 0.1% DMSO pH 7.28, 305 mOsm and saturated with 95% O₂/5%CO₂. Neurons were voltage clamped at -60 mV through whole cell recording pipettes (~4-6 MΩ) filled with an intracellular solution containing (in mM): 0.2 EGTA, 130 K-Gluconate, 6 KCl, 3 NaCl, 10 HEPES, 2 QX-314, 4 ATP-Mg, 0.4 GTP-Na, 14 phosphocreatine-Tris, pH7.2 adjusted by KOH, 285 mOsm.

For mEPSC measurements, the ACSF was supplemented with 1 μM TTX. Series and input resistance were measured in voltage clamp with a 400-ms, 10 mV step from a -60 mV holding potential (filtered at 30 kHz, sampled at 50 kHz). Cells were only used for analysis if the starting series resistance was less than 30 MΩ and was stable throughout the experiment. Input resistance ranged from 50-900 MΩ. Data were not corrected for junction potential. No significant difference was observed between transfected and untransfected neurons in resting membrane potential, indicating that overall neuronal health were unaffected by expression of Cre-mCherry.

Synaptic currents were filtered at 3 kHz, acquired and digitized at 10 kHz on a PC using custom software (Labview; National Instruments, Austin, TX). mEPSCs were filtered at 1k Hz and detected off-line using an automatic detection program (MiniAnalysis; Synaptosoft Inc, Decatur, Ga.) with a detection threshold set at a value greater than at least 5 fold of the root mean square noise levels, followed by a subsequent round of visual confirmation. Significance of differences between transfected and untransfected neurons was determined using a paired t-test.

Results and Discussion

***Brg1* deletion results in functional synapse loss**

To examine the role of *Brg1* in regulating functional synapses, I biolistically transfected cre-mCherry into organotypic slice cultures prepared from *Brg1^{ff}* mice followed by dual whole cell recording of transfected neurons and nearby untransfected neurons as the control. Cell autonomous deletion of *Brg1* results in a reduction of mEPSC frequency, suggesting a decrease in functional synapses (Figure 3.1A). There is no change in mEPSC amplitude, suggesting that the strength for each individual synapse is unaltered. However, I also observed a reduction in input resistance and an increase in capacitance of transfected neurons, indicating a diminishment of cell volume in neurons with *Brg1* deletion. Thus, it is possible that the decrease in functional synapses caused by *Brg1* cell autonomous deletion

might not be directly due to regulation of synapse formation, but rather a secondary effect due to the reduced volume; the smaller the cell volume, the less available space for synapses to occur. Moreover, a reduction in input resistance indicates diminished excitability, and since neuronal activity plays a critical role in synapse dynamics, this might also contribute to the decrease in functional synapses by changing the metaplasticity – the ability of a neuron to be induced plasticity - of neurons with *Brg1* deletion.

All effects observed in neurons with *Brg1* deletion were not due to cre expression, as cre expression in WT neurons did not elicit changes the in parameters I was measuring (Figure 3.1B).

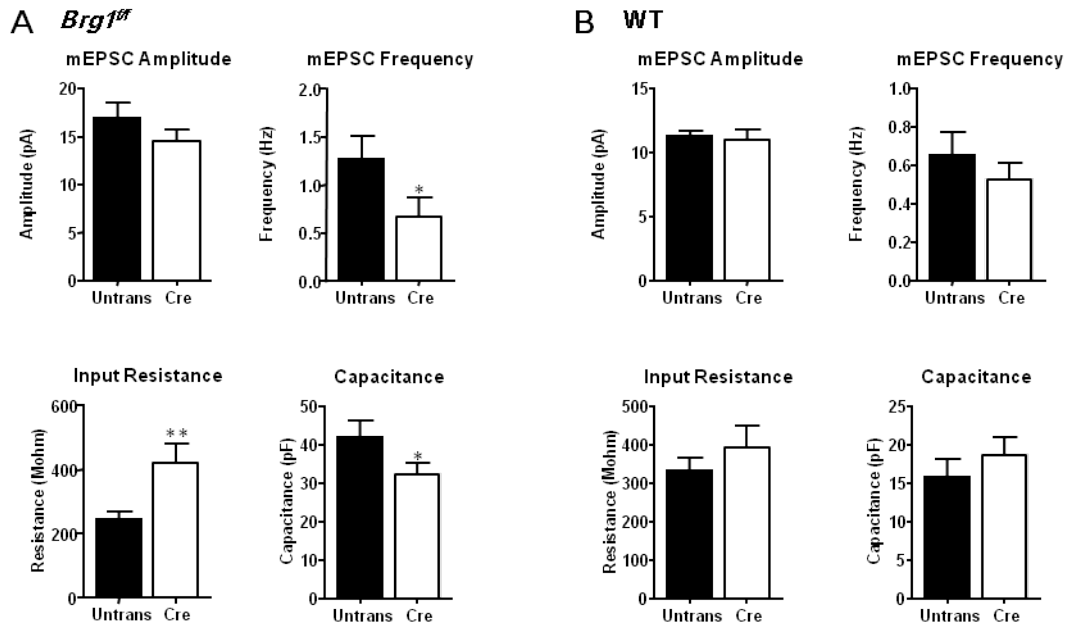


Figure 3. 1 *Brg1* deletion causes reduction of functional synapses

A. Electrophysiological recordings from *Brg1*^{Δf} slices biolistically transfected with cre-mCherry. Electrophysiological properties were obtained from neighboring untransfected (black bar) and transfected (white bar) neurons via dual simultaneous whole-cell patch-clamp.

B. The same as A, except recordings were performed on slices from WT mice. N = 21 cell pairs. Statistic: paired t-test.

CHAPTER FOUR

**PHOSPHOINOSITIDE-3-KINASE ENHANCER IS ASSOCIATED WITH
CORTICAL HYPEREXCITABILITY AND EPILEPSY IN FRAGILE X SYNDROME
MOUSE MODEL**

Introduction

Dysregulated phosphoinositide-3 kinase (PI3K)-mediated signaling pathway has been reported as a common pathological mechanism responsible for diverse brain disorders, such as epilepsy, schizophrenia, intellectual disability and autism. Receptor-mediated PI3K/mTOR signaling plays a crucial role in synaptic plasticity and neuronal function. Studying the neuronal functions of proteins that directly mediate receptor-induced activation of PI3K signaling is therefore of particular interest in order to understand how molecular defects could lead to mental diseases. The PI3K enhancer PIKE (gene name: *Centg1*, a.k.a. *Agap2*) is an important regulator of receptor-mediated PI3K activity. PIKE binds and activates PI3K and Akt and plays roles in many aspects of cellular function, such as apoptosis, migration, and receptor trafficking. In the brain, PIKE-mediated PI3K activity downstream of group 1 metabotropic glutamate receptors (mGluR1/5) is essential for neuronal survival. In the neocortex, *Centg1* deletion (*Centg1* KO) mice resulted in reduced neuronal density and decreased dendritic complexity (Chan et al 2011). However, the role of PIKE in mGlu1/5-dependent synaptic plasticity and possible implication for the etiology of mental disorders is unknown. The inherited intellectual disability and autism spectrum disorder

Fragile X syndrome (FXS) is characterized by increased and stimulus-insensitive signaling through mGlu1/5, but the underlying mechanisms are unclear. Recent phase-3 clinical trials in patients with FXS using mGluR5 negative modulators have been unsuccessful to improve the outcome measures in behavior, corroborating the critical need to better understand the mechanisms underlying dysregulated mGluR1/5 signaling in FXS. The detailed analysis of these mechanisms might reveal alternative therapeutic strategies in FXS (Gross et al 2015).

Elevated PI3K (phosphoinositide-3-kinase) activity is associated with hyperexcitability and epilepsy implicated in Fragile X syndrome (Gibson et al 2008, Gross et al 2010). However, since PI3K loss-of-function is lethal in the mouse model, I looked into the enhancer protein for PI3K, PIKE (phosphoinositide-3-kinase enhancer), which mediates the interaction between PI3K and metabotropic glutamate receptors (mGluRs) and is a putative target of Fragile X Mental Retardation Protein (FMRP) (Sharma et al 2010). mGluRs are also implicated in circuitry and behavioral deficits associated with Fragile X Syndrome (Ronesi et al 2012). To investigate the role of PIKE, I studied neocortical circuit function and epilepsy in *Fmr1* KO mice using transgenic mice that have a deletion of PIKE. I used electrophysiological recordings to measure the activity of populations of neocortical neurons in acute slices of somatosensory cortex, and performed audiogenic seizure experiments to assess the vulnerability of different transgenic mice toward epilepsy.

Materials and Methods

Animals

Mice were generated by crossing female Fragile X mental retardation protein gene (*Fmr1*) heterozygous knockout mice (The Jackson Laboratory) with male *Centg1* (the gene for PIKE) heterozygous knockout mice, and were genotyped by PCR. Both mouse lines were backcrossed into C57BL/6J background more than ten times. Male mice of all 4 genotypes (*Centg1* WT + *Fmr1* WT, *Centg1* WT + *Fmr1* KO, *Centg1* Het + *Fmr1*WT, *Centg1* Het + *Fmr1* KO) were used at postnatal day 21-22 for audiogenic seizure experiments and at postnatal day 18-23 for UP state analysis.

Slice preparation

Procedure was done as previously described (Hays et al 2011). Briefly Male mice at 3 weeks of age (P18-P24) were deeply anesthetized with Euthasol (pentobarbital sodium and phenytoin sodium solution) and decapitated. The brain was transferred into ice-cold dissection buffer containing (in mM): 87 NaCl, 3 KCl, 1.25 NaH₂PO₄, 26 NaHCO₃, 7 MgCl₂, 0.5 CaCl₂, 20 D-glucose, 75 sucrose and 1.3 ascorbic acid aerating with 95% O₂-5% CO₂. Thalamocortical slices 400 μm were made on an angled block using a vibratome (Vibratome 1000 Plus). Following cutting, slices were transected parallel to the pia mater to remove the thalamus and midbrain. This first transection was not used for the experiment. Slices were

immediately transferred to an interface recording chamber (Harvard Instruments) and allowed to recover for 1 hr in nominal ACSF at 32°C containing (in mM): 126 NaCl, 3 KCl, 1.25 NaH₂PO₄, 26 NaHCO₃, 2 MgCl₂, 2 CaCl₂, and 25 D-glucose. After this, slices were perfused with a modified ACSF that better mimics physiological ionic concentrations *in vivo* which contained (in mM): 126 NaCl, 5 KCl, 1.25 NaH₂PO₄, 26 NaHCO₃, 1 MgCl₂, 1 CaCl₂, and 25 D-glucose. For experiments using Wortmannin, 200 nM Wortmannin or vehicle were added into the modified ACSF. Slices remained in this modified ACSF for 45 minutes and then recordings were performed with the same modified ACSF.

UP-state recording

UP-state is a persistent activity state observed in cortex and is used as a measurement of cortical excitability. UP-state recording was performed as described in (Hays et al 2011). Spontaneously generated UP states *in vitro* were extracellularly recorded using 0.5 MΩ tungsten microelectrodes (FHC, Bowdoinham, ME) placed in layer 4 of primary somatosensory cortex. 10 min of spontaneous activity was collected from each slice. For drug wash-on experiments, data was collected for 70 min. Recordings were amplified 10,000-fold, sampled at 2.5 kHz, and filtered on-line between 500Hz and 3 kHz. All measurements were analyzed off-line using custom Labview software. For visualization and analysis of UP states, traces were offset to zero, rectified, and low-pass filtered with a 0.2 Hz cutoff frequency.

Using these processed traces, the threshold for detection was set at 4× the RMS (root mean square) noise, and an event was defined as an UP state if its amplitude remained above the threshold for at least 200 ms. The end of the UP state was determined when the amplitude decreased below threshold for >600 ms. Two events occurring within 600ms of one another were grouped as a single UP state.

Audiogenic Seizure test

Mice were placed in a plastic chamber covered with a Styrofoam lid containing a 120-dB (based on product description) personal security alarm. The alarm was set active after the mice were placed into the chamber 5 min. Mice were observed or video-taped during the entire procedure, and the result was scored based their phenotype; specifically, for death at the end of experiments, the score is 3; for full tonic-clonic seizure, the score is 2; for wild running, the score is 1; if none of the phenotypes described, the score is 0.

Results and Discussion

PIKE functional knockdown rescues prolonged UP-states in Fragile X syndrome mouse model

To address the role of PIKE in *Fmr1* deficiency-associated hyper excitability, I crossed *Centg1* Het to *Fmr1* Het mice to generate litters with 4 possible genotypes: *Centg1* WT + *Fmr1* WT, *Centg1* WT + *Fmr1* KO, *Centg1* Het + *Fmr1* WT, *Centg1* Het + *Fmr1* KO.

Slices isolated from all 4 genotypes were subjected to UP-state analysis.

Centg1 WT + *Fmr1* WT show normal duration of UP-states (Figure 4.1). *Centg1* Het + *Fmr1* WT also exhibited normal UP-state duration, suggesting that the reduction in PIKE function does not cause alteration in cortical excitability. As expected, *Centg1* WT + *Fmr1* KO show prolonged UP-state, corresponding to an earlier finding that deficiency in Fragile X mental retardation protein in mice causes cortical hyperexcitability (Hays et al 2011). PIKE functional knockdown does not change basal excitability, since *Centg1* Het + *Fmr1* WT did not show changed UP-dated compared to *Centg1* WT + *Fmr1* WT. But the *Fmr1* KO-associated hyperexcitability was rescued when PIKE function was sapped (*Centg1* Het + *Fmr1* KO), suggesting the involvement of PI3 kinase signaling cascades in *Fmr1* deficiency-associated hyperexcitability.

Since PIKE function is involved in *Fmr1* deficiency-associated hyperexcitability, I expected PI3K function to be involved as well. To test my hypothesis, slices prepared from WT or *Fmr1* KO mice were subjected to UP-states analysis, and vehicle or 200 nM Wortmannin, a PI3K inhibitor, were added to the modified ACSF. However, acute inhibition of PI3K by Wortmannin treatment did not attenuate the prolonged UP-states in slices isolated from *Fmr1* KO mice (Figure 4.2). Wortmannin treatment did not affect UP-state in WT slices, suggesting acute PI3K inhibition does not cause changes in basal excitability. These results indicates that the PI3K/PIKE signaling cascade likely has a developmental/chronic role in

cortical hyperexcitability, since embryonic knockdown of PI3K/PIKE signal cascade blocked cortical hyperexcitability but acute PI3K/PIKE signal inhibition failed to do so.

PIKE functional knockdown attenuates epileptic behavior associated with *Fmr1* deficiency

Cortical hyperexcitability is hypothesized to contribute to epilepsy and seizures and is a characteristic of *Fmr1* deficiency (Hays et al 2011). Since PIKE functional knockdown mitigates cortical hyperexcitability as assessed by UP-states (Figure 2.1), my colleagues and I hypothesized that PIKE may also rescue seizure behavior in the *Fmr1* KO mouse model. To verify this hypothesis, I subjected litters from mouse colonies used in UP-state experiments (Figure 4.1) to an audiogenic seizure assay. Based on the performance of the experimental animal during the audiogenic seizure test, the result for each experimental animal was scored using the following criteria: (1) if the animal was dead at the end of the experiment, it was scored 3 points; (2) if the animal exhibited tonic-clonic seizure but survived the experiment, it was scored 2 points; (3) if the animal performed wild running but did have further seizure behavior, it was scored 1 point; (4) if the animal did not display any of the seizure behavior described above, it got 0 points. Animals that were dead or showed tonic clonic seizures were considered to be suffering seizures, and animals that showed wild running behavior only or were devoid of any behaviors described above were considered to be not suffering seizures.

Although the audiogenic seizure test persists for 5 minutes, if an animal exhibited

seizure behavior, it was always observed in the first 2 minutes. Animals that were dead or entered a tonic clonic seizure state usually displayed wild running behavior beforehand, but there were cases of mice that died or entered a tonic clonic seizure state without performing obvious wild running.

While *Fmr1* WT groups have an extremely low seizure rate, the *Centg1* WT + *Fmr1* KO group show over 60% seizure rate and a significantly higher seizure score (Figure 4.3, Table 4.1). Interesting, the *Centg1* Het + *Fmr1* KO group show a significantly attenuated seizure score when compared with *Centg1* WT + *Fmr1* KO group, and its seizure rate was also significantly reduced, to around 1/3 of the *Centg1* WT + *Fmr1* KO group (table 4.2), suggesting that PIKE functional knockdown mitigated *Fmr1* deficiency-associated seizures. However, the *Centg1* Het + *Fmr1* KO group still had a non-significant trend towards an increased seizure score, and it still had a seizure rate of ~20%, indicating that even if PIKE functional knockdown rescues cortical hyperexcitability and attenuates audiogenic seizure behavior in the *Fmr1* KO mouse model, it is not sufficient to completely rescue the seizure phenotype associated with *Fmr1* deficiency.

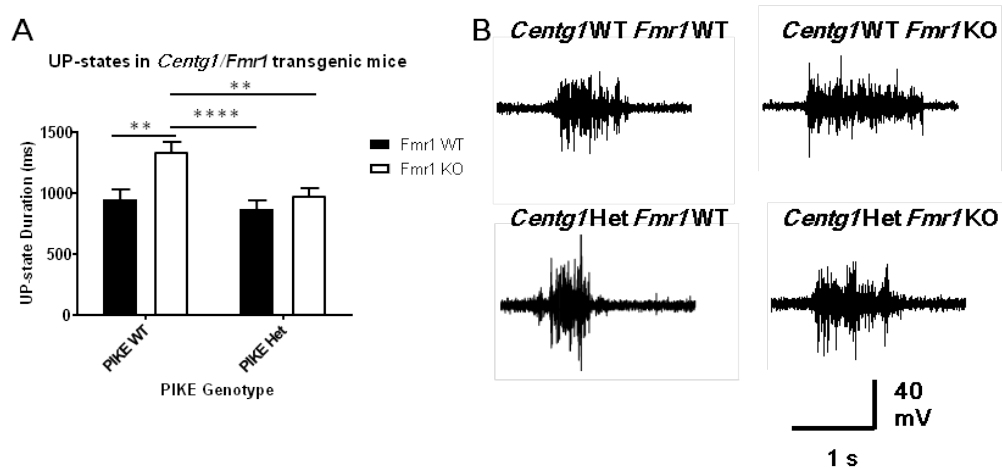


Figure 4. 1 PIKE functional knockdown rescues cortical hyperexcitability in *Fmr1* KO mice
A. UP-state duration recorded in slices isolated from littermates with genotypes of : *Centg1* WT + *Fmr1* WT, *Centg1* WT + *Fmr1* KO, *Centg1* Het + *Fmr1* WT, *Centg1* Het + *Fmr1* KO. Statistic: Two-way ANOVA with multiple comparisons using Bonferroni's test by comparing all groups. **B.** Representative traces from each group. N = 34 – 44 slices, 7-8 mice.

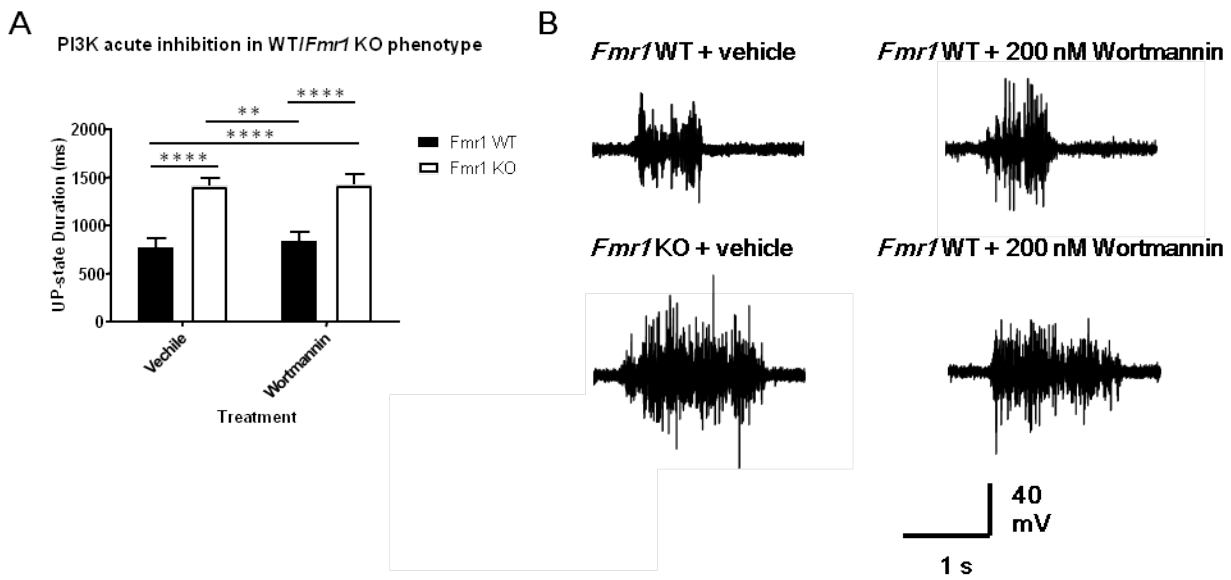


Figure 4. 2 Acute inhibition of PI3K does not mitigate prolonged UP-states in *Fmr1* KO mice
A. UP-state duration recorded in slices isolated from WT or *Fmr1* KO mice. Vehicle or 200 nM Wortmannin was added to the modified ACSF. Statistic: Two-way ANOVA with multiple comparisons using Bonferroni's test by comparing all groups. **B.** Representative traces from each group. N = 14 – 18 slices, 4 – 5 mice.

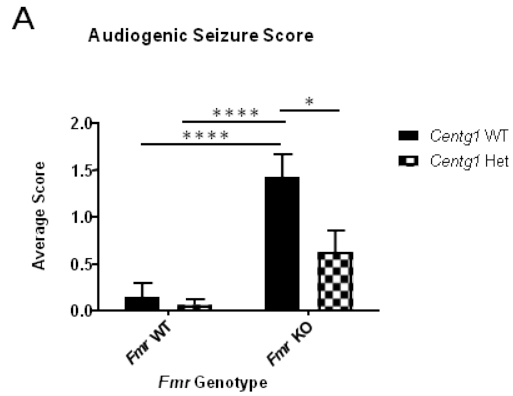


Figure 4. 3 PIKE functional knockdown attenuates seizure behavior in *Fmr1* KO mice

A. Audiogenic seizure score acquired from audiogenic seizure test on littermates with genotypes of : *Centg1* WT + *Fmr1* WT, *Centg1* WT + *Fmr1* KO, *Centg1* Het + *Fmr1* WT, *Centg1* Het + *Fmr1* KO. Score earned: Death – 3, Tonic clonic seizure – 2, Wild running only - 1, No above seizure behavior – 0. N = 13 – 26 animals. Statistic: 2-way ANOVA with multiple comparisons using Bonferroni’s test.

Genotype	Total Number of Pups	Nothing	Wild Run	Seizure	Dead	Total Score	% Seized
<i>Centg1</i> WT, <i>Fmr1</i> WT	20	19	0	0	1	3	5
<i>Centg1</i> WT, <i>Fmr1</i> KO	21	7	1	10	3	30	61.90
<i>Centg1</i> Het, <i>Fmr1</i> WT	33	32	0	1	0	2	3.03
<i>Centg1</i> Het, <i>Fmr1</i> KO	27	20	1	2	4	17	22.22

Table 4. 1 Animal performance in audiogenic seizure

Littermates with genotypes of *Centg1* WT + *Fmr1* WT, *Centg1* WT + *Fmr1* KO, *Centg1* Het + *Fmr1* WT, *Centg1* Het + *Fmr1* KO were subjected to audiogenic seizure test, and their performance were recorded and scored. Score criteria: Score earned: Death – 3, Tonic clonic seizure – 2, Wild running only - 1, No above seizure behavior – 0.

Fisher's Test	Comparison	p-value
<i>Centg1</i> WT <i>Fmr1</i> WT V.S <i>Centg1</i> Het <i>Fmr1</i> WT	Seizure or not	1
<i>Centg1</i> WT <i>Fmr1</i> KO V.S <i>Centg1</i> Het <i>Fmr1</i> KO	Seizure or not	0.0078

Table 4. 2 Fisher's exact test of seizure behavior

Animals from experiments done in figure 2-3 and table 2-1 were divided into two populations for each group, based on their performance in the audiogenic seizure test: animal that was dead or entered tonic clonic seizure was considered suffering seizure, and animal that exhibited wild running only or seizure behavior described above was considered not suffering seizure. Then Fisher's exact test was done in between groups of *Centg1* WT + *Fmr1* WT and *Centg1* Het + *Fmr1* WT as well as between groups of *Centg1* WT + *Fmr1* KO and PIKE *Centg1* Het + *Fmr1* KO to determine if there was difference in the percentage of seizure population between those groups.

CHAPTER FIVE

ADDITIONAL STUDIES OF ACTIVITY-DEPENDENT SYNAPTIC DEPRESSION

Summary

This section comprises data obtained during work on the project described in Chapter Two. These data were not integrated into the chapter either because the results were negative, or the results opened more possibilities that require additional experiments to find a solid answer. Despite their incompleteness, the information these data carry may be helpful for researchers who study or continue my work.

Materials and methods

Most materials and methods used in this section have been described in Chapter Two. The only method not previously described is in the following paragraph.

Dendritic Spine Imaging by Cell Filling

Organotypic slice cultures were prepared as described earlier. During patching, 100 μ M AlexaFluor488 dye and 2 mg/mL biocytin (Life Technologies, Inc.) were added into the internal solution. The AlexaFluor488 dye was included for real-time visualization of how well the patched cell had been filled. Neurons were filled for 20 minutes, and then the pipette was retracted to obtain an outside-out patch to reseal the cell membrane. Filled slices were kept in the recording Warner chamber immersed in recording ACSF for at least another 30

minutes for recovering. Slices were fixed in 4% sucrose/2.5% paraformaldehyde and stained with Alexa488-conjugated streptavidin (Life Technologies, Inc.) and mounted on glass slides. 1-3 images of dendritic spines were acquired from CA1 secondary apical dendrites. All images (1024 × 2048 pixel resolution, 2.5x digital zoom) were acquired using an oil-immersion 40x objective on a Zeiss LSM 780 microscope equipped with a Chameleon-Ti: sapphire standard laser at an excitation wavelength of 920 nm. Images were analyzed with Neuron Studio.

Results & Discussion

Calcineurin inhibition exhibits trends of attenuating chronic postsynaptic burst firing induced MEF2-dependent transcription

In the early stages of my project, I proposed that chronic postsynaptic burst firing-induced synapse elimination is a MEF2-dependent process, since postsynaptic burst firing- and MEF2VP16-induced synapse elimination have shared features. Specifically, both are activity-dependent and also require the activation of L-type voltage gated calcium channels (Flavell et al 2006, Goold & Nicoll 2010). However, an inconsistency existed between the two processes: postsynaptic burst firing-induced synapse elimination is insensitive to Calcineurin inhibition, while MEF2-VP16-mediated synapse elimination still persist even when calcineurin was blocked (Goold & Nicoll 2010). Hence, I hypothesized that

MEF2-dependent transcription induced by chronic postsynaptic burst firing might not be blocked by calcineurin inhibition.

Slices prepared from WT mice were transfected with MRE-GFP and ChR2H134-mCherry, and subjected to chronic PPS 4-10 days after transfection. The calcineurin inhibitors FK-506 (1 μ M) + cyclosporine (1 μ M) or vehicle were added to the media 1 hr prior to the onset of PPS, and slices were imaged for MRE-GFP expression. Although only vehicle-treated groups showed a significant difference in MRE-GFP expression between groups with PPS or not, there is a strong trend suggesting that chronic activity-induced MRE-GFP expression was reduced in the presence of calcineurin inhibitors (Figure 5.1). If an unpaired t-test was used instead of two-way ANOVA to analyze the difference between any two groups, MRE-GFP expression in the drug-treated group with photostimulation would be significantly lower than the vehicle-treated group with photostimulation. This data suggest that inhibition of calcineurin may attenuate chronic postsynaptic burst firing-induced MRE-GFP expression.

Nevertheless, my other data demonstrate that chronic postsynaptic burst firing-induced synapse depression does not rely on MEF2 (Figure 2.4). Therefore, it is not surprising that chronic activity can induce synapse depression without the need for calcineurin activity.

CaMKK is not required for chronic postsynaptic burst firing-induced MEF2-dependent transcription.

Another difference between chronic postsynaptic burst firing-induced synapse elimination and MEF2-VP16-mediated synapse elimination is that chronic postsynaptic burst firing-induced synapse elimination was reported to require CaMKK activity (Goold & Nicoll 2010), but there was no report regarding the involvement of CaMKK in MEF2-VP16-mediated synapse pruning. Based on my initial hypothesis that chronic postsynaptic burst firing-induced synapse elimination is a MEF2-dependent process, I hypothesized that CaMKK is involved in chronic activity-induced MEF2-dependent transcription.

Slices prepared from WT mice were transfected with MRE-GFP and ChR2H134-mCherry, and subjected to chronic PPS 4-10 days after transfection. The CaMKK inhibitor STO-609 (3 μ M) or vehicle was added to the media 1 hr prior to the onset of PPS, and slices were imaged for MRE-GFP expression. 24 hour PPS induced significant MRE-GFP expression in both vehicle and STO-609-treated group (Figure 5.2), and there was no difference in groups subjected to PPS between vehicle and STO-609-treated groups, suggesting that CaMKK is not involved in chronic postsynaptic burst firing-induced MEF2-dependent transcription.

Analysis of dendritic spine density in neurons subjected to PPS with biocytin filling

I observed that brief postsynaptic burst firing induced a reduction in AMPA/NMDA eEPSC amplitude ratio, but detected no difference following chronic postsynaptic burst firing (Figure 2.8), I therefore hypothesized that brief postsynaptic burst firing promotes synapse silencing while chronic postsynaptic burst firing promotes synapse elimination. I initially sought to validate my hypothesis by examining the effect of postsynaptic burst firing on dendritic spine density by patching and filling transfected neurons with biocytin.

Slices from WT mice were prepared and transfected with MRE-GFP and ChR2H134-mCherry. At 8-13 days after transfection, the slices were subjected to 0 hour, 1 hour or 24 hours PPS, and transfected neurons were patched and filled with biocytin. During biocytin filling I acquired mEPSC data, and following completion of filling, the neuron was fixed and treated with Alexa488-conjugated streptavidin for visualization. Surprisingly, I did not observe any change in either dendritic spine density (Figure 5.3A) or mEPSC frequency (Figure 5.3B), even in the 24-hour photostimulation-treated group. Considering the length time required to troubleshoot this experiment, I switched to a biolistic method with PA1-GFP included in the bullets for visualization of dendritic spines (Figure 2.10).

Chronic (24 hour) neuronal activity stimulates transcription of the MRE-GFP reporter, and is blocked by embryonic MEF2A/D deletion

After confirming that patterned photostimulation can reliably introduce elevated activity by triggering patterned postsynaptic firing (Figure 3.1), I wanted to validate whether

patterned photostimulation induces MEF2-dependent transcription, and furthermore whether *Mef2* deletion abolishes patterned photostimulation-induced synapse depression. My first attempt to accomplish this task was to utilize transgenic mice with embryonic *Mef2a/d* deletion.

I crossed mice with floxed *Mef2a* and *Mef2d* genes to an *Emx1-cre* mouse line to generate *Emx1-cre Mef2a^{flx/flx}Mef2d^{flx/flx}* mice, in which *Mef2a* and *Mef2d* would be knocked out in cortical and hippocampal excitatory neurons by E12.5 (Gorski et al 2002). Slices prepared from *Mef2a^{flx/flx}Mef2d^{flx/flx}* or *Emx1-cre Mef2a^{flx/flx}Mef2d^{flx/flx}* mice were transfected with MRE-GFP and ChR2H134-mCherry, and subjected to chronic patterned photostimulation 4-10 days after transfection. Slices were then imaged for MRE-GFP expression.

While chronic patterned photostimulation significantly induced MRE-GFP expression in *Mef2a^{flx/flx}Mef2d^{flx/flx}* neurons (effectively WT neurons), MRE-GFP expression was blocked in *Emx1-cre Mef2a^{flx/flx}Mef2d^{flx/flx}* neurons (effectively *Mef2a/d* knockout neurons) (Figure 5.4). These results not only suggest that postsynaptic burst firing introduced by patterned photostimulation is able activate MEF2-dependent transcription, but also validate the specificity of MRE-GFP as a MEF2-dependent transcriptional activity reporter.

Chronic postsynaptic burst firing induces synapse depression, which is blocked by embryonic MEF2 deletion

Since chronic postsynaptic burst firing activated MEF2-regulated transcription, I proposed it would induce MEF2-dependent synapse depression. Slices prepared from *Mef2a^{flx/flx}Mef2d^{flx/flx}* or Emx1-cre *Mef2a^{flx/flx}Mef2d^{flx/flx}* mice were transfected with MRE-GFP and Chr2H134-mCherry followed by chronic patterned photostimulation, and slices were then analyzed by dual whole cell recording (Figure 5.5A). Chronic photostimulation induced synapse depression in WT neurons as assessed by a reduction in evoked excitatory postsynaptic current (eEPSC) amplitude and miniature excitatory postsynaptic (mEPSC) current frequency (Figure 5.5B). No change in paired pulse ratio was observed (Table 2.1), indicating the absence of a presynaptic effect induced by chronic postsynaptic burst firing. On the other hand, chronic postsynaptic burst firing-induced synapse depression was blocked in Emx1-cre *Mef2a^{flx/flx}Mef2d^{flx/flx}* slices, indicating the involvement of MEF2A and MEF2D in synapse depression.

Although the actual reason is still unclear why embryonic brain-wide deletion of *Mef2a/d* blocked chronic postsynaptic burst firing-induced synapse depression, which was not blocked by cell autonomous *Mef2a/d* deletion, I speculate it may be because MEF2 plays a role in synaptogenesis during early developmental stages, such that embryonic *Mef2a/d* deletion might result in deficits in the generation of synapses/spines that is sensitive to postsynaptic burst firing-mediated synapse depression. In fact, it has been reported MEF2 can

regulate dendrite outgrowth via mediating the transcription of microRNAs in dissociate rat hippocampal cultures at the developmental stage roughly equivalent to the first postnatal week (Fiore et al 2009). Hence, since the loss of function of MEF2 during early postnatal days could cause deficits in dendrite/spine formation, and if the resultant dendrites/spines had deficiency that those spines were insensitive to activity-drive depression, it could explain why embryonic deletion of *Mef2a/d* blocked chronic postsynaptic burst firing-induced synapse depression

FMRP is not implicated in postsynaptic burst firing-induced synapse depression

FMRP/*Fmr1* has been reported to be essential for MEF2-VP16-mediated synapse depression (Pfeiffer et al 2010), and since brief postsynaptic burst firing-induced synapse depression is a MEF2-dependent process, I hypothesized that *Fmr1* is also necessary for brief postsynaptic burst firing-induced synapse depression. To determine the role of *Fmr1* in brief postsynaptic burst firing-induced synapse depression, slices were prepared from *Fmr1* KO mice, transfected with MRE-GFP and ChR2, and then subjected to either chronic or brief PPS. Surprisingly, in slices prepared from *Fmr1* KO mice, both chronic (Figure 5.6A) and brief PPS (Figure 5.6B) caused functional synapse depression, suggesting that *Fmr1* is not required for postsynaptic burst firing-induced synapse depression regardless of activity conditions.

The relationship between FMRP, MEF2 and activity-dependent synapse depression

will be discussed in detail in chapter six. Brief, it might be because the postsynaptic bursting can activate other pathways in addition to activating MEF2 transcriptional activity, and those pathways that are activated in parallel with MEF2 might contribute to bypassing the requirement of FMRP in activity-dependent MEF2-mediated synapse depression.

The involvement of mGluR5 in brief activity-induced synapse depression

Because previous reports demonstrate that mGluR5 regulates local dendritic translation of *Arc* (Wilkerson et al 2014), I hypothesized that mGluR5 activity is required for brief PPS-induced synapse depression. Treatment with MTEP (1 μ M), an mGluR5 inhibitor, blocked brief PPS-induced MEF2 transcriptional activity (Figure 3.16A), although I observed a trend for higher MEF2-transcriptional activity in MTEP-treated neurons with photostimulation compared to MTEP-treated neurons without photostimulation. Moreover, MTEP treatment blocked brief PPS-induced depression of mEPSC frequency but not eEPSC amplitude (Figure 3.16B, 3.16C), and the depression of eEPSC was not blunted at all in MTEP-treated transfected neurons (Figure 3.16D). These results indicate that mGluR5 may partially account for synapse plasticity in response to brief elevation of activity.

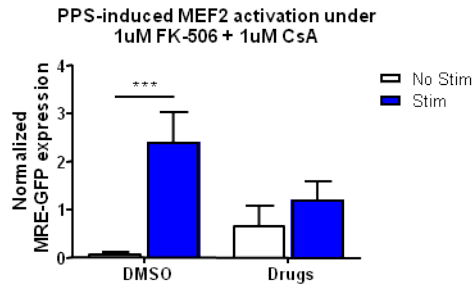


Figure 5. 1 Calcineurin inhibition may attenuate chronic postsynaptic burst firing induced MEF2-dependent transcription

Grouped data of normalized (to mCherry expression level) MRE-GFP expression in WT slices subjected to 24 hour pattern photostimulation with 1 μ M FK-506 + 1 μ M cyclosporin or vehicle. Statistic: Two-way ANOVA with multiple comparisons using Tukey's test and comparing all groups. N = 14 - 31 cells.

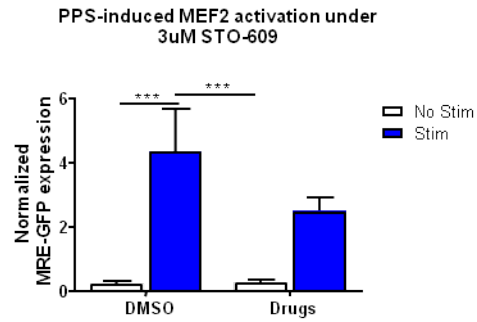


Figure 5. 2 CaMKK inhibition does not significantly affect chronic postsynaptic burst firing induced MEF2-dependent transcription

Grouped data of normalized (to mCherry expression level) MRE-GFP expression in WT slices subjected to 24 hour pattern photostimulation with 3 μ M STO-609 or vehicle. Statistic: Two-way ANOVA with multiple comparisons using Turkey's test by comparing all groups. N = 35 - 46 cells.

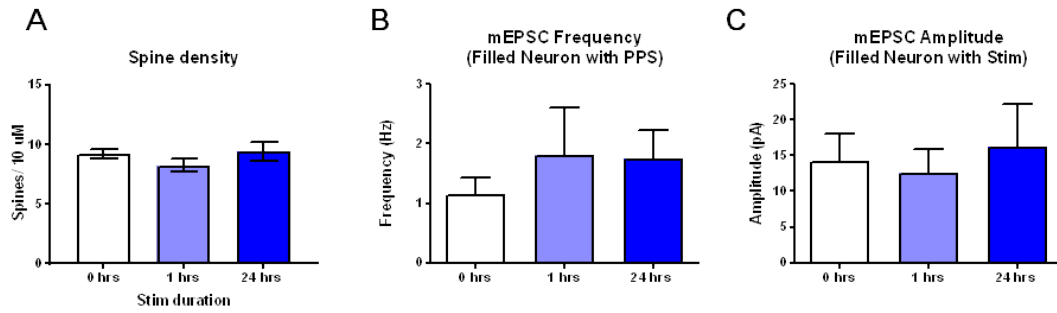


Figure 5.3 Dendritic spine density and mEPSC acquired from neurons subjected to PPS and filled with biocytin

Neurons from WT slices were transfected with Chr2H134R + MRE-GFP and subjected to 0 hour, 1 hour and 24 hour PPS. Then the transfected neurons were filled biocytin and then stained with Alexa488-conjugated streptavidin for visualization of dendritic spines and **A.** analysis of dendritic spine density. During the course of biocytin filling, **B.** mEPSC was acquired from the filled neuron. Statistic: Kruskal Wallis test with multiple comparisons using Dunn's test by comparing all groups. N = 10 cells for each group.

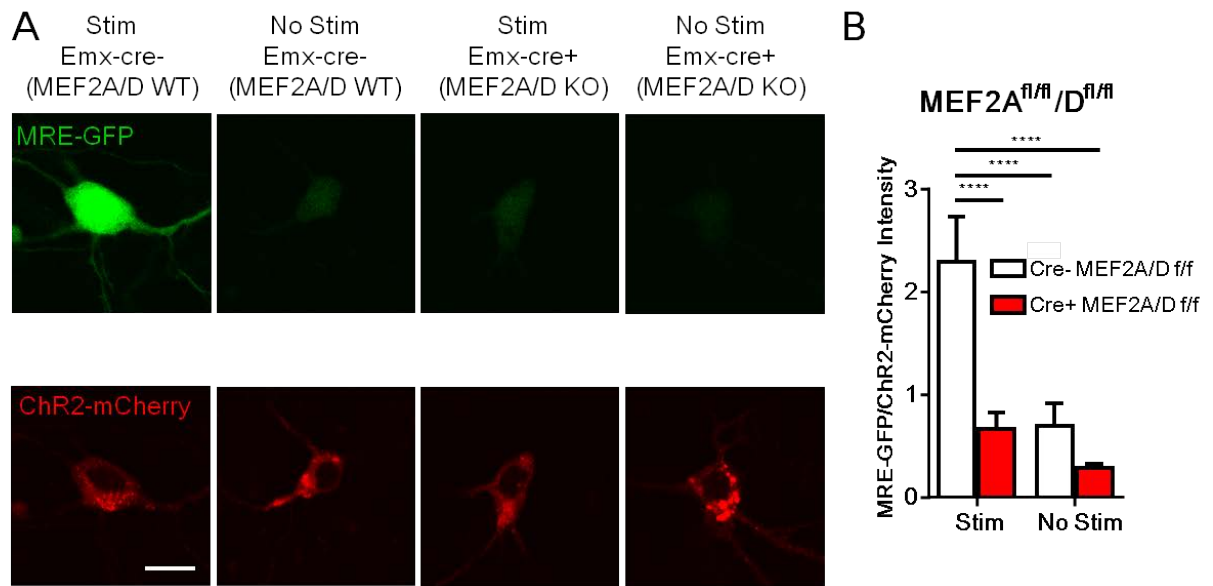


Figure 5. 4 Chronic (24 hour) PPS activates MEF2-dependent transcriptional activity

A. Representative images of MRE-GFP (uper row) and ChR2-mCherry (bottom row) expression from slices prepared from MEF2A^{fl/fl}/D^{fl/fl} Emx1-Cre or MEF2A^{fl/fl}/D^{fl/fl} mice, which have undergone PPS (Stim) or not (No Stim). Scale bar: 10 μ m. **B** Grouped data of the intensity ratio of MRE-GFP over mCherry. Statistic: Two-way ANOVA with multiple comparisons using Bonferroni's test by comparing all groups. N = 28 -39 cells.

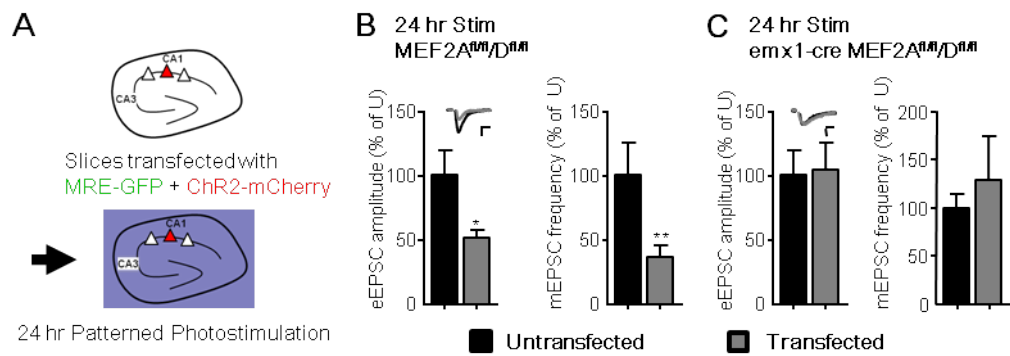


Figure 5.5 Chronic postsynaptic burst firing-induced synapse depression is blocked by embryonic knockout of MEF2A and MEF2D

A. Experimental diagram: MEF2A^{fl/fl}/D^{fl/fl} slices were biolistically transfected with ChR2H134R-mCherry and MRE-GFP and treated with 24 hour PPS. **B.** Electrophysiological recordings were obtained from neighboring untransfected (black bar) and transfected (grey bar) neurons via dual simultaneous whole-cell patch-clamp. Both eEPSC and mEPSC responses are presented as the percentage of average response in untransfected neurons (% of U). Inset: Representative eEPSC from untransfected (black) and transfected (grey) neurons. Stimulation artifact was removed from the trace for clarity. Scale bar for eEPSC is 10 ms/20 pA. **C.** The same as A, except recordings were done in emx1-cre MEF2A^{fl/fl}/D^{fl/fl} slices. Statistic: paired t-test. N = 13 ~ 22 cell pairs.

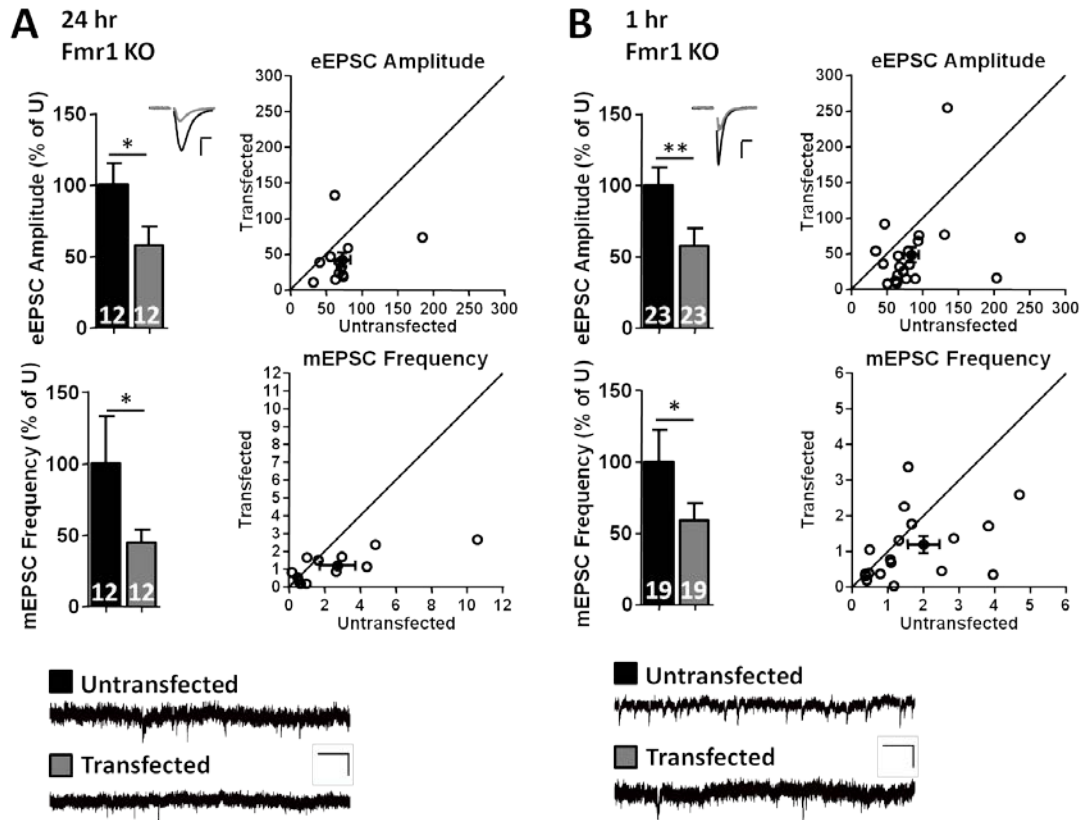


Figure 5. 6 FMRP is not required for postsynaptic burst firing induced synapse depression

A. Electrophysiological recordings from *Fmr1* KO slices treated with 24 hour PPS. eEPSCs and mEPSCs obtained from untransfected (black bar) and transfected (grey bar) neurons. Inset: Representative eEPSC. Scale bar is 10 ms/20 pA. Bottom: Representative mEPSCs. Scale bar is 500 ms/10 pA. **B.** The same as A, except recordings were acquired from *Fmr1* KO slices treated with 1 hour patterned photostimulation.

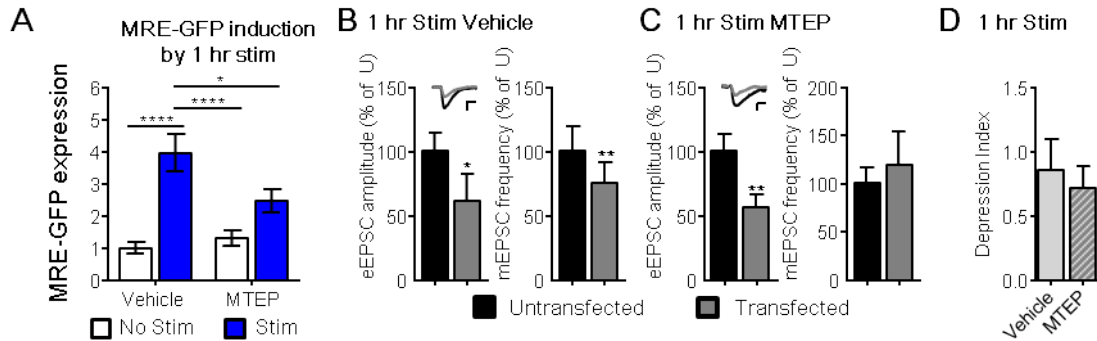


Figure 5.7 mGluR5 is partially involved in brief postsynaptic burst firing induced-synapse plasticity

A. Grouped data of MRE-GFP expression in neurons transfected with MRE-GFP + Chr2H134R from WT slices treated with vehicle or MTEP as well as 1 hour PPS or not. Statistic: two-way ANOVA followed by multiple comparisons between all groups using Tukey's test. N = 20 - 53 cells. **B, C.** Simultaneous dual whole-cell recordings acquired from transfected (grey) and nearby untransfected (black) in neurons from WT slices treated with 1 hour PPS and B. vehicle (ddH₂O) or C. MTEP. Recordings were performed 24 - 30 hour after photostimulation onset. Inset: representative eEPSC traces. Scale bar: 20 pA/10 ms. Statistic: paired t-test. N = 14 - 18 cell pairs. **D.** Comparison of depression index (refer the statistic part of materials and methods section of chapter two) of transfected neurons in B and C. Statistic: unpaired t-test.

CHAPTER SIX

DISCUSSION AND IMPLICATION

Transcription Regulation in Chronic Postsynaptic Burst Firing-induced Synapse

Depression

Chronic postsynaptic burst firing drives synapse elimination independently of MEF2, suggesting that other transcription factors may mediate this synapse pruning event. However, this process still partially requires *Arc*, implying that other transcription factors involved in *Arc* regulation might contribute to the elimination of synapses in response to chronic postsynaptic burst firing. In addition to MEF2, serum response factor (SRF) and cAMP response element binding protein (CREB) are both known to regulate *Arc* transcription (Rodriguez-Tornos et al 2013). This raises the possibility that SRF and CREB could mediate chronic postsynaptic burst firing-induced synapse pruning. One hypothesis is that MEF2 is dispensable for the synaptic effects in response to chronic stimulation due to compensation by SRF and CREB. However, SRF and CREB might be less or slowly responsive to postsynaptic burst firing, and therefore do not have roles in the observed synaptic effects following brief stimulation. If SRF and/or CREB are involved in mediating the chronic event, it would indicate that MEF2, SRF, CREB might act as separate sensors that respond to differential activity environments to mediate processes that adapt the cellular environment.

Brief and chronic postsynaptic burst firing induce synapse silencing and synapse elimination, respectively, suggesting that these activity paradigms may achieve their effects

through differential regulation of responding factors. The key difference between synapse silencing and synapse elimination is the removal of NMDA receptors and synapse structure. The depression of NMDAR-mediated transmission can be achieved solely by NMDA receptor activation (Selig et al 1995) regardless of AMPAR-mediated transmission. This implies a possible mechanism in which chronic postsynaptic burst firing might promote synapse elimination by continual activation of postsynaptic NMDA receptors. However, chronic postsynaptic burst firing can induce synapse elimination even in the absence of NMDAR activity (Goold & Nicoll 2010), suggesting there might be alternative mechanisms for removal of the synapse structure.

Evidence also suggests that synapse elimination is associated with microglial activation (Kettenmann et al 2013) and autophagy (Tang et al 2014). Glutamate treatment induces neuronal process extension and increases microglia-neuron contact time in a NMDAR-dependent manner (Eyo et al 2014), indicating another path by which chronic postsynaptic burst firing could lead to synapse elimination. In an ASD mouse model with impaired dendritic spine pruning and autistic-like behavior, activation of the macroautophagy pathway was able to rescue these phenotypes, suggesting a role of autophagy in synapse elimination (Tang et al 2014). Moreover, it has been shown that voltage-gated calcium channels in *Drosophila* play a role in the regulation of lysosomal fusion with autophagic vacuoles (Tian et al 2015), suggesting a possible activity-dependent mechanism of autophagy

activation, which might mediate subsequent synapse elimination.

Another interesting candidate is nerve growth factor receptor 1 (Nr4a1/NUR77), a nuclear receptor that acts as a transcriptional factor (Hanna et al 2011). Nr4a1 overexpression causes spine elimination without affecting excitatory transmission while preserving PSD structure in dendritic shaft (Chen et al 2014); in other words, Nr4a1 is an effector that can mediate structural elimination without functional depression. Moreover, Nr4a1 is a transactivation target of MEF2 and CREB (Flavell et al 2008), making it an intriguing candidate to consider as an effector involved in chronic postsynaptic burst firing-induced synapse elimination. With brief/mild enhanced postsynaptic activity, immediate early genes with high sensitivity that is sensitive to activity elevation, like Arc, would be preferentially activated in this stage to mediate synapse silencing; with prolonged enhanced postsynaptic activity, activity-driven genes with less sensitivity toward activity, like Nr4a1, will be activated as well, which in turn mediate synapse elimination.

Study of Nr4a1 suggests the possibility that functional synaptic depression, PSD removal and structural elimination can be uncoupled. Because PSD-95 degradation occurs in MEF2-VP16-induced synapse elimination (Tsai et al 2012), it would also be interesting to investigate whether PSD-95 degradation is involved in brief/chronic postsynaptic burst firing-induced synapse silencing/elimination. It is known PSD-95 ubiquitination and its subsequent degradation by proteasome facilitates AMPA receptor endocytosis (Colledge et al

2003), but it is still unclear PSD-95 ubiquitination and degradation is mandatory for AMPA receptor internalization. But we may get more hints about the relationship between AMPA receptor trafficking and PSD-95 turnover by studying the involvement of PSD-95 turn in brief/chronic postsynaptic bursts firing-induced synapse depression.

And here is another interesting topic to consider: is synapse silencing (removal of AMPA receptors) a prelude for synapse elimination? Brief postsynaptic bursts causes synapse silencing, and chronic postsynaptic bursts causes synapses elimination; from these scenarios, it seems with extended activity synapse silencing can progress into synapse elimination. It has been reported LTD, which involves the generation of silent synapses (Sanderson et al 2011, Selig et al 1995, Wan et al 2011), could facilitate synapse elimination (Wiegert & Oertner 2013), but there are studies reporting that NMDA receptor endocytosis as well as synapse structure can occur without prerequisite of AMPA receptor depression to occur. Hence, it seems synapses synapse silencing might not be the prelude for synapse elimination; synapse silencing and synapse elimination might be rather two biological processes with differential sensitivity toward neuronal activity change, such that these two processes can take action accordingly in response to a given electrophysiological environment. And the process which cuts in first might assist the initiation of the process with higher latency; there could be certain synergies between them, but not mandatorily required for each other.

Determinants that Decide which Synapses to be Silenced/Eliminated

What is the electrophysiological machinery underlying postsynaptic burst firing-driven synapse silencing/elimination? Additionally, how does a neuron determine which synapses will be eliminated during postsynaptic burst firing? Based on dogma for neuronal circuit refinement, which is, neurons that “fire together, wire together”, one plausible explanation is that when activity in the postsynaptic neuron increases, synaptic sites whose presynaptic firing cannot synchronize with elevated firing in the postsynaptic neuron would be silenced/eliminated. Synapse synchrony is crucial for synapse persistence (Huupponen et al 2013, Winnubst et al 2015), and it is reasonable that during postsynaptic neuronal postsynaptic burst firing, synapses that cannot keep synchrony would be degraded, whereas synapses that can maintain their coordination would be strengthened. In other words, if both the postsynaptic neuron and its presynaptic inputs exhibit coordinated burst firing, it is possible that postsynaptic burst firing-induced synapse elimination would be blocked.

A practical approach to test this hypothesis is to transfect CA1 and CA3 respectively with engineered channelrhodopsins that respond to different light spectrums. By altering the pattern/duration/timing of burst firing in presynaptic and postsynaptic sites using optogenetics, the synchrony between presynaptic (CA3) and postsynaptic (CA1) neurons could be manipulated to shed light on the mechanisms of postsynaptic burst firing-induced synapse depression.

However, chronic PPS can induce synapse elimination when AMPAR and NMDAR-mediated transmission were absent during the PPS session (Goold & Nicoll 2010), suggesting the real-time synchrony is not required to determine which synapses to be depressed. In other words, probably there other factor that may play the role of decision-maker to decide which synapse should persist and which synapses should perish. But what could be the decision-maker? One possible candidate is the previous activity history of the neuron, which has been reported to participate in regulation of synapse plasticity (Dvorkin & Ziv 2016). Some synapses may be “tagged” by previous activity, such that those tagged synapses would be more prone to be silenced/eliminated.

Then here comes the question, which factors could as the “tag”? Generally, GluA2 and GluA1 are two most probable candidate that may act as the tag for further activity-driven synapse silencing/elimination. It has been shown chronic postsynaptic burst firing requires the presence of GluA2 to induced synapse depression, supporting the hypothesis that GluA2 might also have a role in brief postsynaptic burst firing-induced synapse depression. GluA2 is also required for Arc-mediated AMPAR receptor internalization in organotypic hippocampal slice culture (Rial Verde et al 2006), and GluA2 is required for mGluR-dependent LTD (Zhou et al 2011). Moreover, the phosphorylation status regulated by activity of GluA2 is crucial for AMPA receptor internalization (Henley & Wilkinson 2013, Isaac et al 2007). These evidence suggest GluA2 has many features to be a tag that could be marked by activity history: it is

involved in AMPA-receptor endocytosis, and its capacity to mediate AMPA receptor internalization is regulated by activity.

GluA1 is another interesting candidate to be the tag. Recent evidence showed GluA1 underwent activity-dependent ubiquitination (Schwarz et al 2010), which facilitates AMPA receptor endocytosis. GluA1 was also shown to be involved in Arc-mediated endocytosis (Chowdhury et al 2006, Shepherd et al 2006). And the phosphorylation status of GluA1 also affects its ability in regulating plasticity (Lee et al 2010); thus, GluA1 also has the features to act as a good tag. Although GluA1 is not crucial in chronic postsynaptic bursting firing-induced synapse depression, it is still possible for GluA1 to have a role in the brief postsynaptic bursting firing-induced synapse depression.

To test these hypotheses, the role of activity history needs to be clarified first. Cultures could be incubated with TTX for a prolonged time prior to PPS experiment to clear all possible “tag” made by previous activity history, and then test if the clearance of activity history would have impact on postsynaptic bursting firing-induced synapse depression. The role of GluA1/GluA2 could be examined by genetic or molecular biology tools.

Biological Roles of Postsynaptic Burst Firing-induced Synapse silencing/Elimination

It has been reported that MEF2 transcription factors mediate AMPA receptor expression without affecting dendritic spine density in developing cortical neurons (Elmer et

al 2013). This is consistent with my observation that brief postsynaptic burst firing drives MEF2-dependent removal of AMPA receptors from the synapse, and supports a role of MEF2-mediated synapse silencing during development. Moreover, silent synapse formation (Arendt et al 2013, Kerchner & Nicoll 2009, Phan et al 2015) is implicated in LTP, along with learning and memory, thus relaying the importance of brief postsynaptic burst firing-induced synapse silencing to learning and memory.

Is there any biological process that may be directly linked with the differential postsynaptic burst firing-induced synapse depression? One interesting application would involve hippocampal place cells. In the CA1 region, pyramidal neurons can be categorized into two populations: (1) place cells, which fire when the animal steps in a specific direction within an environment, and (2) silent cells, which fire at low frequency no matter where the animal goes within an environment (Ahmed & Mehta 2009). Notably, the discrepancy in firing rate between place cells and silent cells is not permanent, during slow wave sleep both place cells and silent cells show similar firing rates (Thompson & Best 1989). Whenever the animal switches from an awake/rapid eye movement sleep status to slow wave sleep, silent cells undergo a “postsynaptic burst firing” event; their neuronal firing rate increases from very low frequency to the equivalent of place cells (Thompson & Best 1989). Considering the role of slow wave sleep in memory consolidation (Tamminen et al 2013), it is reasonable to assume postsynaptic burst firing might have a role in memory consolidation during slow wave

sleep..

Moreover, even during awake periods, silent cells can be transformed into place cells when the animal enters a novel environment (Epsztein et al 2011, Frank et al 2004). On the other hand, place cell firing rates decrease in an environment without place field and increase drastically when the animal is on the place field (Thompson & Best 1989). Thus, all CA1 pyramidal cells, whether place cells or silent cells, can undergo plastic changes when the animal is moving on/off the place field or between environments; in this situation postsynaptic burst firing in a given pyramidal neuron could be a common event. Hippocampal plasticity is crucial for spatial memory storage (Hebert & Dash 2004), and these features support a role of postsynaptic burst firing-induced plasticity in hippocampal memory processing.

As the role of silent synapses was mostly studied in the developmental brain, whereas the involvement of silent synapses in adult brain was mostly done in the field of addiction (Hanse et al 2013), it would be very interesting if silent synapses also played a role in the mapping of place cells. It is important to note that the brief postsynaptic burst firing-induced synapse silencing reported in my studies was observed in organotypic slice cultures at an equivalent *in vivo* age of postnatal 2-3 weeks, still within the developmental period. Thus, any synapse plasticity caused by postsynaptic burst firing in adult brain (place cell mapping) may be different from that observed in developing brain tissue.

Nevertheless, since the role of silent synapses was mostly studied in developmental brain, while the involvement of silent synapses in adult brain was mostly done in the field of addiction (Hanse et al 2013), it would very appealing if silent synapses also played a role in the mapping of place cells. Note that, since the brief postsynaptic burst firing-induced synapse silencing reported from my study was actually done in organotypic slices with equivalent *in vivo* age of postnatal 2-3 weeks, still within the developmental period, it would be reasonable if the synapse plasticity caused by postsynaptic burst firing in adult brain (place cell mapping) was different from in developmental brain.

Our laboratory has demonstrated that *Arc* expression and translation can be induced in CA1pyramidal neurons when mice were exposed to novelty (Jakkamsetti et al 2013). CA1 pyramidal neurons with induced *Arc* expression are prone to LTD induced by mGluR activation or repeated novelty experience. This phenomenon may be an *in vivo* example how enhanced postsynaptic bursting firing-induced synapse silencing play a role in adult hippocampus. Novelty experience enhance the neuronal activity in a subpopulation of CA1 hippocampal neuron, and then the neurons with enhanced activity starts to express *Arc* and is primed for the expression of mGluR or repeated novelty experience-driven LTD, which involve synapse silencing (Sanderson et al 2011, Selig et al 1995, Wan et al 2011). Novelty-induced LTD was reported to be crucial for memory enhancement (Dong et al 2012).

Postsynaptic bursting firing-induced synapse depression may have a role during

development. In rodent hippocampus, spine formation rate prevails over spine pruning rate during the first three postnatal weeks, and then spine pruning rate gradually exceeds spine formation rate starting from the fourth postnatal week (Papa et al 1995, Zhao et al 2013). The trend of the hippocampal spine dynamic indicates a possible way how postsynaptic bursting firing-induced synapse depression is involved: during early postnatal days, there are fewer connections and the expression of GluRs is low, such that the excitability in CA1 neuron is low and the machinery of postsynaptic bursting firing-induced synapse depression is inactive. Throughout the first three postnatal weeks, along with the continuous connection outgrowth as well as increasing GluR expression (Pickard et al 2000), the excitability of CA1 neuron also keeps increasing across the development (Blair et al 2013). At the fourth postnatal week, excitability of CA1 neuron may have grown to the extent such that its own spontaneous burst firing is sufficient to turn the machinery of postsynaptic bursting firing-induced synapse depression active to prune unwanted connections. Moreover, the expression GluA2, one of the possible “tag” molecule for synapse depression as discussed earlier, also increases during the developmental stage (Henley & Wilkinson 2016), and the expression profile of GluA2 might serve as a milestone for the onset of machinery of postsynaptic bursting firing-induced synapse depression.

Fmr1 and MEF2-dependent Synapse Elimination

It seems paradoxical that *Fmr1* is required for MEF2VP16-mediated synapse depression (Pfeiffer et al 2010), but not brief PPS-induced MEF2-dependent synapse depression. However, MEFVP16 expression was in the absence of elevated neuronal activity, such that Channelrhodopsin-mediated postsynaptic burst firing may account for the difference. The elevated neuronal activity introduced by PPS may trigger other parallel activity-driven pathways to overcome the absence of *Fmr1*. *Fmr1* deletion increases elongation factor 1-alpha (EF1 α) expression, which can bind to and hinder the translocation of mouse double minute 2 homolog (mdm2). Mdm2 is an E3 ubiquitin-protein ligase that ubiquitinates its target proteins, such as PSD-95, to facilitate their subsequent degradation, a process mediated by PCDH10 and components of the proteasome (Tsai et al 2012). If the postsynaptic burst firing introduced by PPS promotes the dissociation of Mdm2 from EF1 α , bypassing *Fmr1*, this could help explain brief postsynaptic burst firing-induced functional synapse depression.

If the EF1 α -hyperexpression-associated mdm2 nuclear retention caused by *Fmr1* deletion underlies *Fmr1*-independence in postsynaptic burst firing-induced synapse depression, it would imply PSD-95 degradation mediated by PCDH10 and proteasome is also involved in postsynaptic burst firing-induced synapse depression. However, the role of PSD-95 degradation and the involvement of Mdm2 and PCDH10 in this form of plasticity is unclear and further investigation is warranted.

BIBLIOGRAPHY

- Abrahamsson T, Gustafsson B, Hanse E. 2007. Reversible synaptic depression in developing rat CA3 CA1 synapses explained by a novel cycle of AMPA silencing-unsilencing. *Journal of neurophysiology* 98: 2604-11
- Ahmed OJ, Mehta MR. 2009. The hippocampal rate code: anatomy, physiology and theory. *Trends in neurosciences* 32: 329-38
- Akhtar MW, Kim MS, Adachi M, Morris MJ, Qi X, et al. 2012. In vivo analysis of MEF2 transcription factors in synapse regulation and neuronal survival. *PLoS one* 7: e34863
- Anderson JP, Dodou E, Heidt AB, De Val SJ, Jaehnig EJ, et al. 2004. HRC is a direct transcriptional target of MEF2 during cardiac, skeletal, and arterial smooth muscle development in vivo. *Mol Cell Biol* 24: 3757-68
- Antar LN, Afroz R, Dichtenberg JB, Carroll RC, Bassell GJ. 2004. Metabotropic glutamate receptor activation regulates fragile x mental retardation protein and FMR1 mRNA localization differentially in dendrites and at synapses. *J Neurosci* 24: 2648-55
- Antonini A, Stryker MP. 1993. Rapid remodeling of axonal arbors in the visual cortex. *Science* 260: 1819-21
- Arendt KL, Sarti F, Chen L. 2013. Chronic Inactivation of a Neural Circuit Enhances LTP by Inducing Silent Synapse Formation. *J Neurosci* 33: 2087-96
- Ashby MC, Isaac JT. 2011. Maturation of a recurrent excitatory neocortical circuit by experience-dependent unsilencing of newly formed dendritic spines. *Neuron* 70: 510-21
- Atwood HL, Wojtowicz JM. 1999. Silent synapses in neural plasticity: Current evidence. *Learn Memory* 6: 542-71
- Balice-Gordon RJ, Chua CK, Nelson CC, Lichtman JW. 1993. Gradual loss of synaptic cartels precedes axon withdrawal at developing neuromuscular junctions. *Neuron* 11: 801-15
- Balice-Gordon RJ, Lichtman JW. 1993. In vivo observations of pre- and postsynaptic changes during the transition from multiple to single innervation at developing neuromuscular junctions. *J Neurosci* 13: 834-55
- Balice-Gordon RJ, Lichtman JW. 1994. Long-term synapse loss induced by focal blockade of postsynaptic receptors. *Nature* 372: 519-24
- Bannerman DM, Sprengel R, Sanderson DJ, McHugh SB, Rawlins JN, et al. 2014. Hippocampal synaptic plasticity, spatial memory and anxiety. *Nat Rev Neurosci* 15: 181-92
- Barbosa AC, Kim MS, Ertunc M, Adachi M, Nelson ED, et al. 2008. MEF2C, a transcription factor that facilitates learning and memory by negative regulation

- of synapse numbers and function. *Proceedings of the National Academy of Sciences of the United States of America* 105: 9391-96
- Beique JC, Lin DT, Kang MG, Aizawa H, Takamiya K, Huganir RL. 2006. Synapse-specific regulation of AMPA receptor function by PSD-95. *Proceedings of the National Academy of Sciences of the United States of America* 103: 19535-40
- Bennett MR, Pettigrew AG. 1975. The formation of synapses in amphibian striated muscle during development. *The Journal of physiology* 252: 203-39
- Black BL, Ligon KL, Zhang Y, Olson EN. 1996. Cooperative transcriptional activation by the neurogenic basic helix-loop-helix protein MASH1 and members of the myocyte enhancer factor-2 (MEF2) family. *Journal of Biological Chemistry* 271: 26659-63
- Black BL, Olson EN. 1998. Transcriptional control of muscle development by myocyte enhancer factor-2 (MEF2) proteins. *Annu Rev Cell Dev Bi* 14: 167-96
- Blair MG, Nguyen NN, Albani SH, L'Etoile MM, Andrawis MM, et al. 2013. Developmental changes in structural and functional properties of hippocampal AMPARs parallels the emergence of deliberative spatial navigation in juvenile rats. *J Neurosci* 33: 12218-28
- Brown TE, Lee BR, Mu P, Ferguson D, Dietz D, et al. 2011. A silent synapse-based mechanism for cocaine-induced locomotor sensitization. *J Neurosci* 31: 8163-74
- Cabezas C, Buno W. 2011. BDNF is required for the induction of a presynaptic component of the functional conversion of silent synapses. *Hippocampus* 21: 374-85
- Chan CB, Liu X, Pradoldej S, Hao C, An J, et al. 2011. Phosphoinositide 3-kinase enhancer regulates neuronal dendritogenesis and survival in neocortex. *J Neurosci* 31: 8083-92
- Chancey JH, Adlaf EW, Sapp MC, Pugh PC, Wadiche JI, Overstreet-Wadiche LS. 2013. GABA depolarization is required for experience-dependent synapse unsilencing in adult-born neurons. *J Neurosci* 33: 6614-22
- Chen C, Regehr WG. 2000. Developmental remodeling of the retinogeniculate synapse. *Neuron* 28: 955-66
- Chen Y, Wang Y, Erturk A, Kallop D, Jiang Z, et al. 2014. Activity-induced Nr4a1 regulates spine density and distribution pattern of excitatory synapses in pyramidal neurons. *Neuron* 83: 431-43
- Cheng C, Trzcinski O, Doering LC. 2014. Fluorescent labeling of dendritic spines in cell cultures with the carbocyanine dye "DiI". *Frontiers in neuroanatomy* 8: 30
- Choi S, Klingauf J, Tsien RW. 2000. Postfusional regulation of cleft glutamate

- concentration during LTP at 'silent synapses'. *Nature neuroscience* 3: 330-6
- Chowdhury S, Shepherd JD, Okuno H, Lyford G, Petralia RS, et al. 2006. Arc/Arg3.1 interacts with the endocytic machinery to regulate AMPA receptor trafficking. *Neuron* 52: 445-59
- Cole CJ, Mercaldo V, Restivo L, Yiu AP, Sekeres MJ, et al. 2012. MEF2 negatively regulates learning-induced structural plasticity and memory formation. *Nature neuroscience* 15: 1255-U121
- Colledge M, Snyder EM, Crozier RA, Soderling JA, Jin Y, et al. 2003. Ubiquitination regulates PSD-95 degradation and AMPA receptor surface expression. *Neuron* 40: 595-607
- Crepel F, Delhaye-Bouchaud N, Dupont JL, Sotelo C. 1980. Dendritic and axonic fields of Purkinje cells in developing and x-irradiated rat cerebellum. A comparative study using intracellular staining with horseradish peroxidase. *Neuroscience* 5: 333-47
- Crepel V, Aronov D, Jorquera I, Represa A, Ben-Ari Y, Cossart R. 2007. A parturition-associated nonsynaptic coherent activity pattern in the developing hippocampus. *Neuron* 54: 105-20
- De Rubeis S, He X, Goldberg AP, Poultney CS, Samocha K, et al. 2014. Synaptic, transcriptional and chromatin genes disrupted in autism. *Nature* 515: 209-15
- Dietrich JB. 2013. The MEF2 family and the brain: from molecules to memory. *Cell Tissue Res* 352: 179-90
- Dong Z, Gong B, Li H, Bai Y, Wu X, et al. 2012. Mechanisms of hippocampal long-term depression are required for memory enhancement by novelty exploration. *J Neurosci* 32: 11980-90
- Dvorkin R, Ziv NE. 2016. Relative Contributions of Specific Activity Histories and Spontaneous Processes to Size Remodeling of Glutamatergic Synapses. *PLoS biology* 14: e1002572
- Elmer BM, Estes ML, Barrow SL, McAllister AK. 2013. MHCII Requires MEF2 Transcription Factors to Negatively Regulate Synapse Density during Development and in Disease. *J Neurosci* 33: 13791-804
- Epsztein J, Brecht M, Lee AK. 2011. Intracellular Determinants of Hippocampal CA1 Place and Silent Cell Activity in a Novel Environment. *Neuron* 70: 109-20
- Eyo UB, Peng J, Swiatkowski P, Mukherjee A, Bispo A, Wu LJ. 2014. Neuronal hyperactivity recruits microglial processes via neuronal NMDA receptors and microglial P2Y12 receptors after status epilepticus. *J Neurosci* 34: 10528-40
- Faber DS, Korn H. 1991. Applicability of the coefficient of variation method for analyzing synaptic plasticity. *Biophysical journal* 60: 1288-94
- Fiore R, Khudayberdiev S, Christensen M, Siegel G, Flavell SW, et al. 2009.

- Mef2-mediated transcription of the miR379-410 cluster regulates activity-dependent dendritogenesis by fine-tuning Pumilio2 protein levels. *Embo J* 28: 697-710
- Flavell SW, Cowan CW, Kim TK, Greer PL, Lin Y, et al. 2006. Activity-dependent regulation of MEF2 transcription factors suppresses excitatory synapse number. *Science* 311: 1008-12
- Flavell SW, Kim TK, Gray JM, Harmin DA, Hemberg M, et al. 2008. Genome-Wide Analysis of MEF2 Transcriptional Program Reveals Synaptic Target Genes and Neuronal Activity-Dependent Polyadenylation Site Selection. *Neuron* 60: 1022-38
- Frank LM, Stanley GB, Brown EN. 2004. Hippocampal plasticity across multiple days of exposure to novel environments. *J Neurosci* 24: 7681-89
- Fu M, Zuo Y. 2011. Experience-dependent structural plasticity in the cortex. *Trends in neurosciences* 34: 177-87
- Funahashi R, Maruyama T, Yoshimura Y, Komatsu Y. 2013. Silent synapses persist into adulthood in layer 2/3 pyramidal neurons of visual cortex in dark-reared mice. *Journal of neurophysiology* 109: 2064-76
- Galvez R, Greenough WT. 2005. Sequence of abnormal dendritic spine development in primary somatosensory cortex of a mouse model of the fragile X mental retardation syndrome. *American journal of medical genetics. Part A* 135: 155-60
- Gibson JR, Bartley AF, Hays SA, Huber KM. 2008. Imbalance of neocortical excitation and inhibition and altered UP states reflect network hyperexcitability in the mouse model of fragile X syndrome. *Journal of neurophysiology* 100: 2615-26
- Gomperts SN, Rao A, Craig AM, Malenka RC, Nicoll RA. 1998. Postsynaptically silent synapses in single neuron cultures. *Neuron* 21: 1443-51
- Goold CP, Nicoll RA. 2010. Single-cell optogenetic excitation drives homeostatic synaptic depression. *Neuron* 68: 512-28
- Gorski JA, Talley T, Qiu M, Puellas L, Rubenstein JL, Jones KR. 2002. Cortical excitatory neurons and glia, but not GABAergic neurons, are produced in the Emx1-expressing lineage. *J Neurosci* 22: 6309-14
- Gossett LA, Kelvin DJ, Sternberg EA, Olson EN. 1989. A new myocyte-specific enhancer-binding factor that recognizes a conserved element associated with multiple muscle-specific genes. *Mol Cell Biol* 9: 5022-33
- Gregoire S, Yang XJ. 2005. Association with class IIa histone deacetylases upregulates the sumoylation of MEF2 transcription factors. *Mol Cell Biol* 25: 2273-87

- Gross C, Chang CW, Kelly SM, Bhattacharya A, McBride SM, et al. 2015. Increased expression of the PI3K enhancer PIKE mediates deficits in synaptic plasticity and behavior in fragile X syndrome. *Cell reports* 11: 727-36
- Gross C, Nakamoto M, Yao X, Chan CB, Yim SY, et al. 2010. Excess phosphoinositide 3-kinase subunit synthesis and activity as a novel therapeutic target in fragile X syndrome. *J Neurosci* 30: 10624-38
- Grossman AW, Elisseou NM, McKinney BC, Greenough WT. 2006. Hippocampal pyramidal cells in adult Fmr1 knockout mice exhibit an immature-appearing profile of dendritic spines. *Brain research* 1084: 158-64
- Guo W, Molinaro G, Collins KA, Hays SA, Paylor R, et al. 2016. Selective Disruption of Metabotropic Glutamate Receptor 5-Homer Interactions Mimics Phenotypes of Fragile X Syndrome in Mice. *J Neurosci* 36: 2131-47
- Hagerman RJ, Ono MY, Hagerman PJ. 2005. Recent advances in fragile X: a model for autism and neurodegeneration. *Current opinion in psychiatry* 18: 490-6
- Hanna RN, Carlin LM, Hubbeling HG, Nackiewicz D, Green AM, et al. 2011. The transcription factor NR4A1 (Nur77) controls bone marrow differentiation and the survival of Ly6C- monocytes. *Nature immunology* 12: 778-85
- Hanse E, Seth H, Riebe I. 2013. AMPA-silent synapses in brain development and pathology. *Nat Rev Neurosci* 14: 839-50
- Harrington AJ, Raissi A, Rajkovich K, Berto S, Kumar J, et al. 2016. MEF2C regulates cortical inhibitory and excitatory synapses and behaviors relevant to neurodevelopmental disorders. *eLife* 5
- Haruta M, Hata Y. 2007. Experience-driven axon retraction without binocular imbalance in developing visual cortex. *Current biology : CB* 17: 37-42
- Hashimoto K, Kano M. 2003. Functional differentiation of multiple climbing fiber inputs during synapse elimination in the developing cerebellum. *Neuron* 38: 785-96
- Hays SA, Huber KM, Gibson JR. 2011. Altered neocortical rhythmic activity states in Fmr1 KO mice are due to enhanced mGluR5 signaling and involve changes in excitatory circuitry. *J Neurosci* 31: 14223-34
- Hebert AE, Dash PK. 2004. Nonredundant roles for hippocampal and entorhinal cortical plasticity in spatial memory storage. *Pharmacol Biochem Be* 79: 143-53
- Henley JM, Wilkinson KA. 2013. AMPA receptor trafficking and the mechanisms underlying synaptic plasticity and cognitive aging. *Dialogues in clinical neuroscience* 15: 11-27
- Henley JM, Wilkinson KA. 2016. Synaptic AMPA receptor composition in development, plasticity and disease. *Nat Rev Neurosci* 17: 337-50

- Hering H, Sheng M. 2001. Dendritic spines: structure, dynamics and regulation. *Nat Rev Neurosci* 2: 880-8
- Hinton VJ, Brown WT, Wisniewski K, Rudelli RD. 1991. Analysis of neocortex in three males with the fragile X syndrome. *American journal of medical genetics* 41: 289-94
- Hua JY, Smith SJ. 2004. Neural activity and the dynamics of central nervous system development. *Nature neuroscience* 7: 327-32
- Huang YH, Lin Y, Mu P, Lee BR, Brown TE, et al. 2009. In vivo cocaine experience generates silent synapses. *Neuron* 63: 40-7
- Huttenlocher PR. 1979. Synaptic density in human frontal cortex - developmental changes and effects of aging. *Brain research* 163: 195-205
- Huttenlocher PR, de Courten C, Garey LJ, Van der Loos H. 1982. Synaptogenesis in human visual cortex--evidence for synapse elimination during normal development. *Neuroscience letters* 33: 247-52
- Huupponen J, Molchanova SM, Lauri SE, Taira T. 2013. Ongoing Intrinsic Synchronous Activity is Required for the Functional Maturation of CA3-CA1 Glutamatergic Synapses. *Cerebral cortex* 23: 2754-64
- Isaac JT, Ashby MC, McBain CJ. 2007. The role of the GluR2 subunit in AMPA receptor function and synaptic plasticity. *Neuron* 54: 859-71
- Isaac JT, Nicoll RA, Malenka RC. 1995. Evidence for silent synapses: implications for the expression of LTP. *Neuron* 15: 427-34
- Jakkamsetti V, Tsai NP, Gross C, Molinaro G, Collins KA, et al. 2013. Experience-induced Arc/Arg3.1 primes CA1 pyramidal neurons for metabotropic glutamate receptor-dependent long-term synaptic depression. *Neuron* 80: 72-9
- Kamme F, Salunga R, Yu J, Tran DT, Zhu J, et al. 2003. Single-cell microarray analysis in hippocampus CA1: demonstration and validation of cellular heterogeneity. *J Neurosci* 23: 3607-15
- Kanai Y, Dohmae N, Hirokawa N. 2004. Kinesin transports RNA: isolation and characterization of an RNA-transporting granule. *Neuron* 43: 513-25
- Kandel ER, Spencer WA. 1961. Electrophysiology of hippocampal neurons. II. After-potentials and repetitive firing. *Journal of neurophysiology* 24: 243-59
- Kang J, Gocke CB, Yu H. 2006. Phosphorylation-facilitated sumoylation of MEF2C negatively regulates its transcriptional activity. *BMC biochemistry* 7: 5
- Kerchner GA, Nicoll RA. 2009. Silent synapses and the emergence of a postsynaptic mechanism for LTP (vol 9, pg 813, 2008). *Nat Rev Neurosci* 10
- Kettenmann H, Kirchhoff F, Verkhratsky A. 2013. Microglia: new roles for the synaptic stripper. *Neuron* 77: 10-8

- Kim JH, Lee HK, Takamiya K, Huganir RL. 2003. The role of synaptic GTPase-activating protein in neuronal development and synaptic plasticity. *J Neurosci* 23: 1119-24
- Kullmann DM. 1994. Amplitude fluctuations of dual-component EPSCs in hippocampal pyramidal cells: implications for long-term potentiation. *Neuron* 12: 1111-20
- Lee HK, Takamiya K, He K, Song L, Huganir RL. 2010. Specific roles of AMPA receptor subunit GluR1 (GluA1) phosphorylation sites in regulating synaptic plasticity in the CA1 region of hippocampus. *Journal of neurophysiology* 103: 479-89
- Lever C, Burton S, Jeewajee A, Wills TJ, Cacucci F, et al. 2010. Environmental novelty elicits a later theta phase of firing in CA1 but not subiculum. *Hippocampus* 20: 229-34
- Liao D, Hessler NA, Malinow R. 1995. Activation of postsynaptically silent synapses during pairing-induced LTP in CA1 region of hippocampal slice. *Nature* 375: 400-4
- Lichtman JW, Colman H. 2000. Synapse elimination and indelible memory. *Neuron* 25: 269-78
- Lin JY. 2011. A user's guide to channelrhodopsin variants: features, limitations and future developments. *Experimental physiology* 96: 19-25
- Lu H, Liu B, Zhang FJ, Zhang J, Dong R, et al. 2014. The E3 ligase APC/C-Cdh1 regulates MEF2A-dependent transcription by targeting SUMO-specific protease 2 for ubiquitination and degradation. *Cell cycle* 13: 3892-902
- Lugenbeel KA, Peier AM, Carson NL, Chudley AE, Nelson DL. 1995. Intragenic loss of function mutations demonstrate the primary role of FMR1 in fragile X syndrome. *Nature genetics* 10: 483-5
- Lyons GE, Micales BK, Schwarz J, Martin JF, Olson EN. 1995. Expression of Mef2 Genes in the Mouse Central-Nervous-System Suggests a Role in Neuronal Maturation. *J Neurosci* 15: 5727-38
- Ma YY, Wang X, Huang Y, Marie H, Nestler EJ, et al. 2016. Re-silencing of silent synapses unmasks anti-relapse effects of environmental enrichment. *Proceedings of the National Academy of Sciences of the United States of America* 113: 5089-94
- Marie H, Morishita W, Yu X, Calakos N, Malenka RC. 2005. Generation of silent synapses by acute in vivo expression of CaMKIV and CREB. *Neuron* 45: 741-52
- McKinney BC, Grossman AW, Elisseou NM, Greenough WT. 2005. Dendritic spine abnormalities in the occipital cortex of C57BL/6 Fmr1 knockout mice.

American journal of medical genetics. Part B, Neuropsychiatric genetics : the official publication of the International Society of Psychiatric Genetics 136B: 98-102

- McKinsey TA, Zhang CL, Olson EN. 2002a. MEF2: a calcium-dependent regulator of cell division, differentiation and death. *Trends Biochem Sci* 27: 40-47
- McKinsey TA, Zhang CL, Olson EN. 2002b. MEF2: a calcium-dependent regulator of cell division, differentiation and death (vol 27, pg 40, 2002). *Trends Biochem Sci* 27: 271-71
- Merrill EG, Wall PD. 1972. Factors forming the edge of a receptive field: the presence of relatively ineffective afferent terminals. *The Journal of physiology* 226: 825-46
- Morishita W, Marie H, Malenka RC. 2005. Distinct triggering and expression mechanisms underlie LTD of AMPA and NMDA synaptic responses. *Nature neuroscience* 8: 1043-50
- Nakashiba T, Young JZ, McHugh TJ, Buhl DL, Tonegawa S. 2008. Transgenic inhibition of synaptic transmission reveals role of CA3 output in hippocampal learning. *Science* 319: 1260-64
- Okabe S, Kim HD, Miwa A, Kuriu T, Okado H. 1999. Continual remodeling of postsynaptic density and its regulation by synaptic activity. *Nature neuroscience* 2: 804-11
- Otto T, Eichenbaum H, Wiener SI, Wible CG. 1991. Learning-related patterns of CA1 spike trains parallel stimulation parameters optimal for inducing hippocampal long-term potentiation. *Hippocampus* 1: 181-92
- Pan F, Aldridge GM, Greenough WT, Gan WB. 2010. Dendritic spine instability and insensitivity to modulation by sensory experience in a mouse model of fragile X syndrome. *Proceedings of the National Academy of Sciences of the United States of America* 107: 17768-73
- Papa M, Bundman MC, Greenberger V, Segal M. 1995. Morphological analysis of dendritic spine development in primary cultures of hippocampal neurons. *J Neurosci* 15: 1-11
- Patel AB, Loerwald KW, Huber KM, Gibson JR. 2014. Postsynaptic FMRP promotes the pruning of cell-to-cell connections among pyramidal neurons in the L5A neocortical network. *J Neurosci* 34: 3413-8
- Petralia RS, Esteban JA, Wang YX, Partridge JG, Zhao HM, et al. 1999. Selective acquisition of AMPA receptors over postnatal development suggests a molecular basis for silent synapses. *Nature neuroscience* 2: 31-6
- Pfeiffer BE, Huber KM. 2007. Fragile X mental retardation protein induces synapse loss through acute postsynaptic translational regulation. *J Neurosci* 27:

- Pfeiffer BE, Huber KM. 2009. The state of synapses in fragile X syndrome. *The Neuroscientist : a review journal bringing neurobiology, neurology and psychiatry* 15: 549-67
- Pfeiffer BE, Zang T, Wilkerson JR, Taniguchi M, Maksimova MA, et al. 2010. Fragile X mental retardation protein is required for synapse elimination by the activity-dependent transcription factor MEF2. *Neuron* 66: 191-7
- Phan A, Suschkov S, Molinaro L, Reynolds K, Lymer JM, et al. 2015. Rapid increases in immature synapses parallel estrogen-induced hippocampal learning enhancements. *Proceedings of the National Academy of Sciences of the United States of America* 112: 16018-23
- Pickard L, Noel J, Henley JM, Collingridge GL, Molnar E. 2000. Developmental changes in synaptic AMPA and NMDA receptor distribution and AMPA receptor subunit composition in living hippocampal neurons. *J Neurosci* 20: 7922-31
- Potthoff MJ, Olson EN. 2007. MEF2: a central regulator of diverse developmental programs. *Development* 134: 4131-40
- Pulipparacharuvil S, Renthal W, Hale CF, Taniguchi M, Xiao GH, et al. 2008. Cocaine regulates MEF2 to control synaptic and behavioral plasticity. *Neuron* 59: 621-33
- Rakic P, Bourgeois JP, Eckenhoff MF, Zecevic N, Goldman-Rakic PS. 1986. Concurrent overproduction of synapses in diverse regions of the primate cerebral cortex. *Science* 232: 232-5
- Ramirez S, Liu X, Lin PA, Suh J, Pignatelli M, et al. 2013. Creating a false memory in the hippocampus. *Science* 341: 387-91
- Rashid AJ, Cole CJ, Josselyn SA. 2014. Emerging roles for MEF2 transcription factors in memory. *Genes Brain Behav* 13: 118-25
- Renger JJ, Egles C, Liu G. 2001. A developmental switch in neurotransmitter flux enhances synaptic efficacy by affecting AMPA receptor activation. *Neuron* 29: 469-84
- Rial Verde EM, Lee-Osbourne J, Worley PF, Malinow R, Cline HT. 2006. Increased expression of the immediate-early gene *arc/arg3.1* reduces AMPA receptor-mediated synaptic transmission. *Neuron* 52: 461-74
- Riquelme C, Barthel KK, Liu X. 2006. SUMO-1 modification of MEF2A regulates its transcriptional activity. *Journal of cellular and molecular medicine* 10: 132-44
- Rodriguez-Tornos FM, San Aniceto I, Cubelos B, Nieto M. 2013. Enrichment of Conserved Synaptic Activity-Responsive Element in Neuronal Genes Predicts a Coordinated Response of MEF2, CREB and SRF. *PLoS one* 8

- Ronesi JA, Collins KA, Hays SA, Tsai NP, Guo W, et al. 2012. Disrupted Homer scaffolds mediate abnormal mGluR5 function in a mouse model of fragile X syndrome. *Nature neuroscience* 15: 431-40, S1
- Rozov A, Zivkovic AR, Schwarz MK. 2012. Homer1 gene products orchestrate Ca(2+)-permeable AMPA receptor distribution and LTP expression. *Frontiers in synaptic neuroscience* 4: 4
- Rudelli RD, Brown WT, Wisniewski K, Jenkins EC, Laure-Kamionowska M, et al. 1985. Adult fragile X syndrome. Clinico-neuropathologic findings. *Acta neuropathologica* 67: 289-95
- Rumpel S, Kattenstroth G, Gottmann K. 2004. Silent synapses in the immature visual cortex: layer-specific developmental regulation. *Journal of neurophysiology* 91: 1097-101
- Sanderson TM, Collingridge GL, Fitzjohn SM. 2011. Differential trafficking of AMPA receptors following activation of NMDA receptors and mGluRs. *Molecular brain* 4: 30
- Schwarz LA, Hall BJ, Patrick GN. 2010. Activity-dependent ubiquitination of GluA1 mediates a distinct AMPA receptor endocytosis and sorting pathway. *J Neurosci* 30: 16718-29
- Selig DK, Hjelmstad GO, Herron C, Nicoll RA, Malenka RC. 1995. Independent mechanisms for long-term depression of AMPA and NMDA responses. *Neuron* 15: 417-26
- Shalizi AK, Bonni A. 2005. brawn for brains: the role of MEF2 proteins in the developing nervous system. *Current topics in developmental biology* 69: 239-66
- Sharma A, Hoeffler CA, Takayasu Y, Miyawaki T, McBride SM, et al. 2010. Dysregulation of mTOR signaling in fragile X syndrome. *J Neurosci* 30: 694-702
- Shepherd JD, Rumbaugh G, Wu J, Chowdhury S, Plath N, et al. 2006. Arc/Arg3.1 mediates homeostatic synaptic scaling of AMPA receptors. *Neuron* 52: 475-84
- Speliotes EK, Kowall NW, Shanti BF, Kosofsky B, Finklestein SP, Leifer D. 1996. Myocyte-specific enhancer binding factor 2C expression in gerbil brain following global cerebral ischemia. *Neuroscience* 70: 67-77
- Stoppini L, Buchs PA, Muller D. 1991. A Simple Method for Organotypic Cultures of Nervous-Tissue. *J Neurosci Meth* 37: 173-82
- Sun T, Wu XS, Xu J, McNeil BD, Pang ZP, et al. 2010. The role of calcium/calmodulin-activated calcineurin in rapid and slow endocytosis at central synapses. *J Neurosci* 30: 11838-47
- Suzuki SS, Smith GK. 1985. Burst characteristics of hippocampal complex spike cells

- in the awake rat. *Experimental neurology* 89: 90-5
- Tamminen J, Ralph MAL, Lewis PA. 2013. The Role of Sleep Spindles and Slow-Wave Activity in Integrating New Information in Semantic Memory. *J Neurosci* 33: 15376-81
- Tang G, Gudsnuk K, Kuo SH, Cotrina ML, Rosoklija G, et al. 2014. Loss of mTOR-dependent macroautophagy causes autistic-like synaptic pruning deficits. *Neuron* 83: 1131-43
- Tavazoie SF, Reid RC. 2000. Diverse receptive fields in the lateral geniculate nucleus during thalamocortical development. *Nature neuroscience* 3: 608-16
- Thompson LT, Best PJ. 1989. Place Cells and Silent Cells in the Hippocampus of Freely-Behaving Rats. *J Neurosci* 9: 2382-90
- Tian X, Gala U, Zhang Y, Shang W, Nagarkar Jaiswal S, et al. 2015. A voltage-gated calcium channel regulates lysosomal fusion with endosomes and autophagosomes and is required for neuronal homeostasis. *PLoS biology* 13: e1002103
- Tian XY, Kai L, Hockberger PE, Wokosin DL, Surmeier DJ. 2010. MEF-2 regulates activity-dependent spine loss in striatopallidal medium spiny neurons. *Mol Cell Neurosci* 44: 94-108
- Tsai NP, Wilkerson JR, Guo W, Maksimova MA, DeMartino GN, et al. 2012. Multiple autism-linked genes mediate synapse elimination via proteasomal degradation of a synaptic scaffold PSD-95. *Cell* 151: 1581-94
- Tsankova NM, Berton O, Renthal W, Kumar A, Neve RL, Nestler EJ. 2006. Sustained hippocampal chromatin regulation in a mouse model of depression and antidepressant action. *Nature neuroscience* 9: 519-25
- Viviani B. 2006. Preparation and coculture of neurons and glial cells. *Current protocols in cell biology / editorial board, Juan S. Bonifacino ... [et al.]* Chapter 2: Unit 2 7
- Wall PD. 1977. The presence of ineffective synapses and the circumstances which unmask them. *Philosophical transactions of the Royal Society of London. Series B, Biological sciences* 278: 361-72
- Wan Y, Feng G, Calakos N. 2011. Sapap3 deletion causes mGluR5-dependent silencing of AMPAR synapses. *J Neurosci* 31: 16685-91
- Wasling P, Strandberg J, Hanse E. 2012. AMPA receptor activation causes silencing of AMPA receptor-mediated synaptic transmission in the developing hippocampus. *PloS one* 7: e34474
- Waung MW, Pfeiffer BE, Nosyreva ED, Ronesi JA, Huber KM. 2008. Rapid translation of Arc/Arg3.1 selectively mediates mGluR-dependent LTD through persistent increases in AMPAR endocytosis rate. *Neuron* 59: 84-97

- Welch JM, Wang D, Feng G. 2004. Differential mRNA expression and protein localization of the SAP90/PSD-95-associated proteins (SAPAPs) in the nervous system of the mouse. *The Journal of comparative neurology* 472: 24-39
- Wheeler DG, Cooper E. 2001. Depolarization strongly induces human cytomegalovirus major immediate-early promoter/enhancer activity in neurons. *Journal of Biological Chemistry* 276: 31978-85
- Wiegert JS, Oertner TG. 2013. Long-term depression triggers the selective elimination of weakly integrated synapses. *Proceedings of the National Academy of Sciences of the United States of America* 110: E4510-E19
- Wilkerson JR, Tsai NP, Maksimova MA, Wu H, Cabalo NP, et al. 2014. A role for dendritic mGluR5-mediated local translation of Arc/Arg3.1 in MEF2-dependent synapse elimination. *Cell reports* 7: 1589-600
- Williams AL, Reese BE, Jeffery G. 2002. Role of retinal afferents in regulating growth and shape of the lateral geniculate nucleus. *The Journal of comparative neurology* 445: 269-77
- Winnubst J, Cheyne JE, Niculescu D, Lohmann C. 2015. Spontaneous Activity Drives Local Synaptic Plasticity In Vivo. *Neuron* 87: 399-410
- Wu TJ, Monokian G, Mark DF, Wobbe CR. 1994. Transcriptional activation by herpes simplex virus type 1 VP16 in vitro and its inhibition by oligopeptides. *Mol Cell Biol* 14: 3484-93
- Xiao MY, Wasling P, Hanse E, Gustafsson B. 2004. Creation of AMPA-silent synapses in the neonatal hippocampus. *Nature neuroscience* 7: 236-43
- Yamamoto M, Wada N, Kitabatake Y, Watanabe D, Anzai M, et al. 2003. Reversible suppression of glutamatergic neurotransmission of cerebellar granule cells in vivo by genetically manipulated expression of tetanus neurotoxin light chain. *J Neurosci* 23: 6759-67
- Yasuda M, Johnson-Venkatesh EM, Zhang H, Parent JM, Sutton MA, Umemori H. 2011. Multiple forms of activity-dependent competition refine hippocampal circuits in vivo. *Neuron* 70: 1128-42
- Zhang Z, Cao M, Chang CW, Wang C, Shi X, et al. 2016. Autism-Associated Chromatin Regulator Brg1/Smarca4 Is Required for Synapse Development and Myocyte Enhancer Factor 2-Mediated Synapse Remodeling. *Mol Cell Biol* 36: 70-83
- Zhao YD, Ou S, Cheng SY, Xiao Z, He WJ, et al. 2013. Dendritic development of hippocampal CA1 pyramidal cells in a neonatal hypoxia-ischemia injury model. *Journal of neuroscience research* 91: 1165-73
- Zheng CY, Petralia RS, Wang YX, Kachar B, Wenthold RJ. 2010. SAP102 is a highly

- mobile MAGUK in spines. *J Neurosci* 30: 4757-66
- Zhou Z, Hu J, Passafaro M, Xie W, Jia Z. 2011. GluA2 (GluR2) regulates metabotropic glutamate receptor-dependent long-term depression through N-cadherin-dependent and cofilin-mediated actin reorganization. *J Neurosci* 31: 819-33
- Ziff EB. 1997. Enlightening the postsynaptic density. *Neuron* 19: 1163-74
- Zuo Y, Lin A, Chang P, Gan WB. 2005a. Development of long-term dendritic spine stability in diverse regions of cerebral cortex. *Neuron* 46: 181-9
- Zuo Y, Yang G, Kwon E, Gan WB. 2005b. Long-term sensory deprivation prevents dendritic spine loss in primary somatosensory cortex. *Nature* 436: 261-5